GALAXY PROPERTIES ACROSS DIVERSE HALO ENVIRONMENTS

GALAXY PROPERTIES ACROSS DIVERSE HALO ENVIRONMENTS

By

Ian D. Roberts, B.Sc.

A Thesis

Submitted to the School of Graduate Studies

in Partial Fulfilment of the Requirements

for the Degree

Master of Science

McMaster University

Master of Science (2016) McMaster University

(Physics and Astronomy) Hamilton, Ontario

TITLE: Galaxy Properties Across Diverse Halo Environments

AUTHOR: Ian Roberts, B.Sc. (Mount Allison University)

SUPERVISOR: Laura Parker

NUMBER OF PAGES: ix, 140

Abstract

Correlations between galaxy properties and environment have been observed in many environments, showing that red, quiescent, early-type galaxies are found preferentially in dense regimes. This thesis uses a large sample of SDSS group galaxies to further probe these environmental dependences, with a focus on determining the properties of galaxies across different halo environments. We first investigate the mass segregation of galaxies in haloes of groups covering a wide range of masses. We find significant mass segregation in low-mass groups with the strength of mass segregation decreasing with increasing halo mass – to the point where high-mass clusters show no detectable mass segregation. We also find that mass segregation trends are more prominent when including lower mass galaxies. Similar trends are observed when considering the fraction of massive galaxies as a function of radius as opposed to mean galaxy mass. Secondly, we study the star formation and morphology of satellite galaxies in different halo environments. Specifically, we probe beyond the well established correlations with stellar and halo mass and investigate the dependence of star-forming and disc fractions on group X-ray luminosity. We show that galaxies in X-ray underluminous groups have enhanced star-forming and disc fractions, for a given stellar and halo mass. These observations contribute to the understanding and interpretation of the environmental dependence of galaxy properties by providing a framework with which the lack of consensus regarding the presence of mass segregation in groups and clusters can potentially be reconciled, as well as quantifying new correlations with X-ray luminosity beyond the established dependences on halo mass.

Acknowledgements

First and foremost, I would like to thank my supervisor Dr. Laura Parker. Your guidance and assistance has helped to make the past two years not only productive, but incredibly enjoyable as well. Your helpful comments along the way (both scientific and not) have without question improved this thesis significantly. I look forward to four more years to come! I would also like to thank the members of my committee, Dr. William Harris and Dr. James Wadsley.

Thank you to all of my professors and classmates, past and present, for continuing to make this adventure both interesting and fun over the years – academically and otherwise. I would also give a special thanks to Dr. Bob Hawkes for starting me down this road on such a positive note.

Last, but of course not least, thank you to my parents and family for always supporting me and also for always being willing to politely feign interest in the subtleties of secondary environmental dependences of galaxy properties.

Table of Contents

List of Figures

Chapter 1

Introduction

1.1 Galaxy evolution

In the first half of the 20th century the "Great Debate" regarding the nature of "spiral nebulae" was beginning to be settled, as distance measurements to M31 proved it to be a distinct galaxy far beyond the reaches of the Milky Way (Opik, 1922; Hubble, 1925). Further distance measurements to more of these "spiral nebulae" revealed a Universe populated with many similarly distinct galaxies (Hubble, 1926). This opened the door to studying the diverse population of observed galaxies in the Universe, thus beginning the field of galaxy evolution studies.

A subsequent breakthrough came with the discovery of the expanding Universe through the measurement of the velocity-distance relation for a sample of galaxies (Hubble, 1929; Hubble & Humason, 1931). Using relatively accurate distance measurements along with observed radial velocities (Slipher, 1917), Hubble (1929) showed that the recessional velocities of galaxies increased with distance, indicative of an expanding Universe. The rate of expansion is pa-

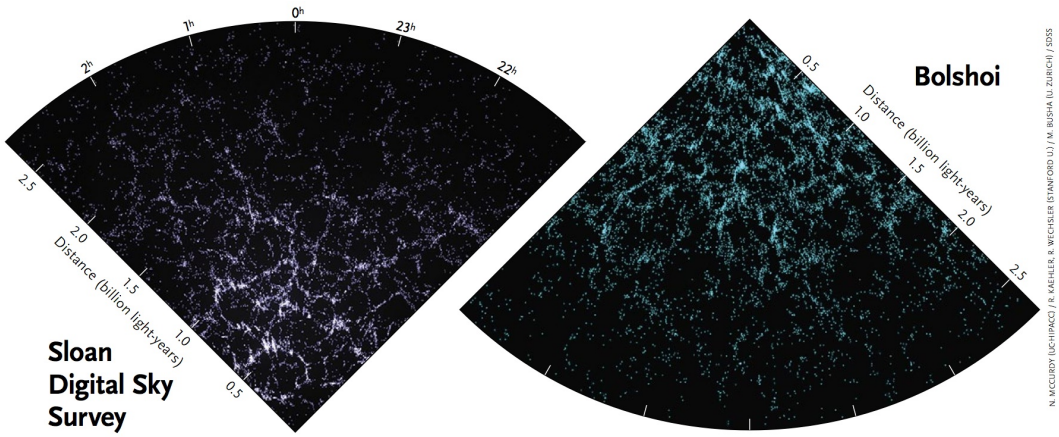

Figure 1.1: Large scale distribution of galaxies from the Sloan Digital Sky Survey and galaxy analogues from the Bolshoi simulation. Image credit: N. McCurdy (UC-HIPACC) / R. Kaehler, R. Wechsler (Stanford U.) / M. Busha (U. Zurich) / SDSS

rameterized by the so-called Hubble constant, H_0, where velocity and distance are related by $v = H_0\, d$. Hubble initially overestimated the numerical value to be $H_0 = 500\,\mathrm{km\,s^{-1}\,Mpc^{-1}}$ (Hubble, 1929) whereas modern observations have used similar methods to constrain H_0 to be $72\,\mathrm{km\,s^{-1}\,Mpc^{-1}}$ (Freedman et al., 2001). The discovery of Universal expansion showed the Universe to be a dynamic and evolving arena allowing the field of cosmology to probe the initial conditions and subsequent evolution.

With the discovery of the cosmic microwave background radiation (CMB; Penzias & Wilson 1965) and the subsequent measurement of the detailed power spectrum (COBE: Mather et al. 1990, WMAP: Hinshaw et al. 2003, Planck: Planck Collaboration et al. 2014) the era of precision cosmology was initiated. The emergent picture is one where primordial density fluctuations imprinted on the CMB provide the seeds from which structure, and eventually galaxies, grow. The growth of the initial overdensities are well described by a Gaus-

sian random field which grow according to linear theory below some critical overdensity, δ_c. The successful Press-Schechter formalism (Press & Schechter, 1974) then posits that regions where the overdensity is above the critical value ($\delta > \delta_c$) will collapse non-linearly and form virialized haloes. Structure in the Universe is then built up in a "bottom-up" fashion, where small galaxies collapse first and are then able to merge and coalesce to form larger galaxies, galaxy groups, and clusters. Insight into the structure of the Universe on the largest scales has been ascertained from N-body, dark matter only simulations (e.g. Springel et al., 2005; Klypin et al., 2011). These simulations have shown that the structure of the Universe on large scales is one of filaments and voids. Galaxies tend to distribute along large filaments, and galaxy clusters and superclusters are found where filaments intersect. This filamentary structure is clear in Fig. 1.1 which shows the distribution of galaxies on large scales both observationally from the Sloan Digital Sky Survey (York et al., 2000), as well as from the Bolshoi simulation (Klypin et al., 2011).

With large redshift surveys of galaxies, such as the 2dF Galaxy Redshift Survey (Colless et al., 2001) and the Sloan Digital Sky Survey (York et al., 2000) in the local Universe as well as the COSMOS (Scoville et al., 2007) and DEEP2 survey (Newman et al., 2013) at higher redshift, the evolution of galaxy properties across different environments as well as cosmic time can now be probed. Seminal papers from the past 40 years have shown that the population of red, passive, early-type galaxies has increased substantially over the past ~ 5 billion years (Butcher & Oemler, 1978), and additionally that these "red and dead" galaxies are preferentially found in dense environments as opposed to the more isolated field (Dressler, 1980). These observed trends have

been confirmed by many more recent studies (Dressler et al., 1997; Ellingson et al., 2001; Postman et al., 2005; Loh et al., 2008; Urquhart et al., 2010; Fasano et al., 2015), however the balance between different mechanisms driving these trends in different environments is still not well understood. Section 1.4 & 1.5 will provide more detailed discussions of different mechanisms capable of driving galaxy transformations.

1.2 Galaxy properties

Galaxies can be classified according to various properties. Colour, star formation, and morphology are three key properties (though this is certainly not an exhaustive list) which have been explored extensively in galaxy evolution studies across cosmic time. This section will describe these three properties, with a focus on how they are measured as well as how they depend on galaxy mass and redshift.

1.2.1 Colour

Colour is one of the simplest direct observables of galaxy properties. The colour of a galaxy is defined as the difference between the magnitudes of a galaxy in two different bands. As an example, the $g - r$ colour for a SDSS galaxy would be the difference between the galaxy's g-band magnitude (centred on 477.0 nm) and r-band magnitude (centred on 623.1 nm). Many studies have shown the colour distributions of galaxy populations to be well fit by a double-Gaussian across many environments (Balogh et al., 2004; Baldry et al., 2006).

The two components of the double-Gaussian fit are referred to as the 'red sequence' and the 'blue cloud'. In Fig. 1.2, I show the $g-r$ colour distribution for a sample of low-redshift ($z < 0.05$) SDSS group galaxies, with a double-Gaussian fit[†] (black) as well as the two components corresponding to the blue cloud and the red sequence overlaid. The red sequence peaks at red colours and has a relatively small dispersion, whereas the blue cloud is a bluer and broader sub-population.

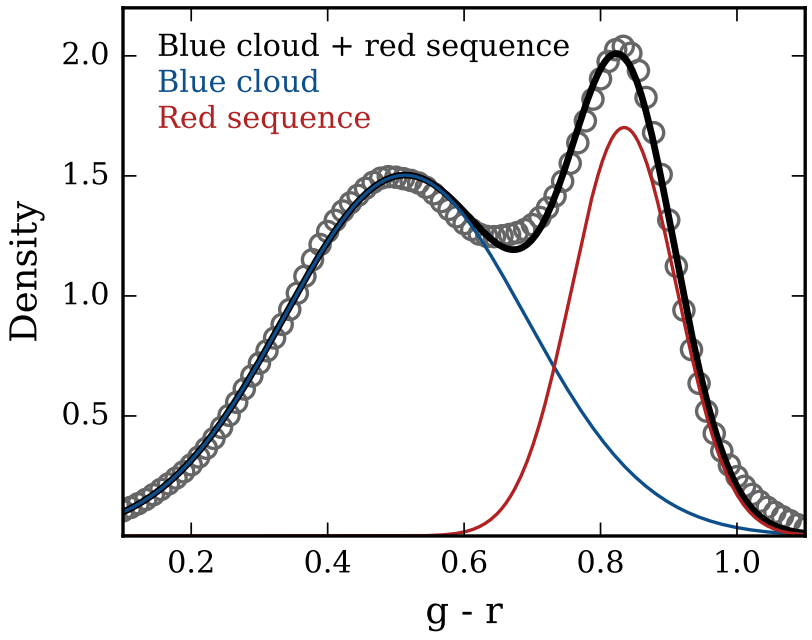

Figure 1.2: $g-r$ colour distribution for low-redshift galaxies in SDSS groups. Circles correspond to the smoothed density distribution of the data, the black line shows a double-Gaussian fit, and the red and blue lines show the components of the double-Gaussian fit corresponding to the red sequence and the blue cloud.

[†]The data was fit with the sum of two Gaussian functions using the `Python` non-linear least-squares fitting function `scipy.optimize.curve_fit`

The overlap region between the red sequence and the blue cloud is known as the "green valley" and is thought to be a transition region. It has been hypothesized that galaxies evolve from the blue cloud, through the green valley, onto the red sequence over time (e.g. Trayford et al., 2016). Though the physical mechanism driving galaxies through the green valley may differ for galaxies of different morphologies (Schawinski et al., 2014). The notion that galaxies evolve in colour through time is supported by the so-called Butcher-Oemler (BO) effect. The BO effect is an observed positive correlation between the fraction of blue galaxies and redshift within galaxy clusters, first observed by Butcher & Oemler (1978) and subsequently confirmed by many more recent studies (e.g. Butcher & Oemler, 1984; Ellingson et al., 2001; Loh et al., 2008; Urquhart et al., 2010). Therefore it seems that at early times populations of galaxies in clusters were bluer than they are at present day.

In addition to redshift correlations, galaxy colours also depend strongly on stellar mass. Both the fraction of red galaxies (Baldry et al., 2006; Bamford et al., 2009; Kimm et al., 2009; Prescott et al., 2011) as well as the average colour of galaxies (Cooper et al., 2008; van den Bosch et al., 2008) increase significantly toward high stellar masses. These stellar mass trends are in place both in the local Universe as well as at high redshift (Grützbauch et al., 2011).

1.2.2 Morphology

The first systematic classification scheme for the shapes of galaxies was laid out by Hubble (1926). This classification scheme (see Fig. 1.3), which has since become known colloquially as Hubble's tuning fork diagram, broadly divides

the galaxy population into elliptical and spiral galaxies. The class of ellipticals is further sub-divided by ellipticity, $e = 0, 1, 2, ..., 7$, where $e = 10 \times (a - b)/a$, with a and b denoting the major and minor axis of the ellipse, respectively. Ellipticals can then be classified as Ee, where E0 would be perfectly round (in projection) and E7 would be a highly elongated ellipse. Spiral galaxies are sub-classified by the brightness of the central region as well as how tightly coiled their spiral arms are. Spirals denoted as Sa are galaxies with bright central bulges and tightly wound spiral arms, galaxies denoted as Sc are galaxies with weak bulges and loosely wound spiral arms, and Sb spirals represent an intermediate class between the two. Spirals are also divided by the presence of a bar, or lackthereof, with barred spirals being denoted as SB galaxies. S0 or lenticular galaxies appear to have structure intermediate between ellipticals and spirals and are characterized by a strong bulge region, as well as the presence of a disc devoid of spiral arms. Following the nomenclature used by Hubble, it is commonplace to refer to elliptical and S0 galaxies as "early-types" and spiral galaxies as "late-types", due to their positions on the tuning fork diagram. It is however important to note that this nomenclature refers solely to the position on the diagram and is agnostic to evolutionary theories.

The first technique used to determine galaxy morphologies was visual classifications (Hubble 1926; more recently, Nair & Abraham 2010). Visual classifications are able to broadly divide galaxy samples into spirals, ellipticals, or S0's, however the time consuming nature of this practice has historically made it difficult to apply to large data sets. That being said, the onset of citizen science programs such as the Galaxy Zoo[†] (Lintott et al., 2008) have made

[†]https://www.galaxyzoo.org

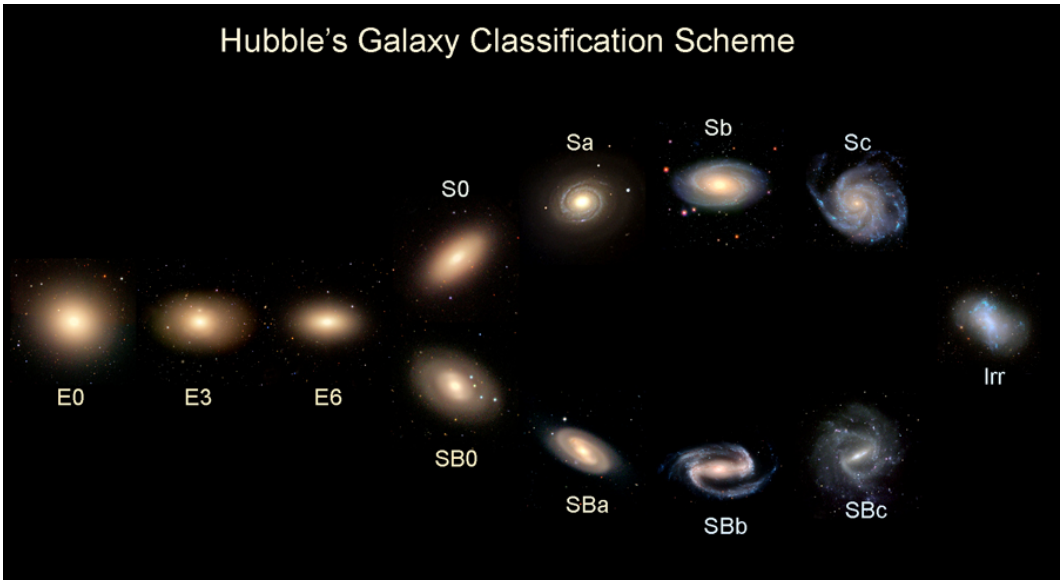

Figure 1.3: The Hubble tuning fork classification diagram. Image credit: Galaxy Zoo.

the application of visual classifications to large data sets increasingly feasible. As an alternative to visual classifications, modern automated techniques often rely on photometric measurements of light profiles of galaxies to classify morphology. In particular, two main measures known as the single Sérsic index (n) and the bulge-to-total ratio (B/T) are commonly used to quantitatively determine the morphology of a galaxy.

The Sérsic index, n, is a free parameter of the so-called Sérsic profile (Sersic, 1968) which is often fit to galaxy intensity profiles. Using the Sérsic profile, the intensity of a galaxy as a function of radius is given by

$$I(r) = I_e \exp\{-k[(r/r_e)^{1/n} - 1]\}, \tag{1.1}$$

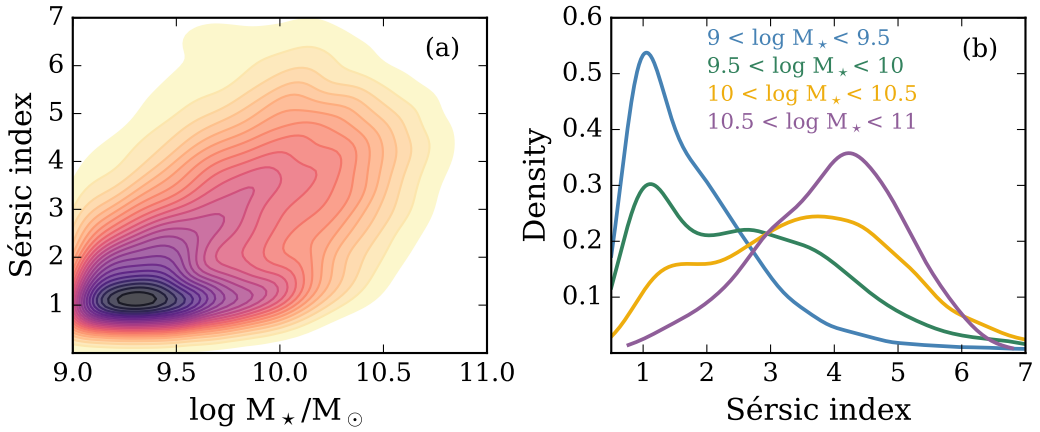

Figure 1.4: Left: Sérsic index versus stellar mass for a sample of low-redshift SDSS group galaxies. Right: Sérsic index density distribution for low-redshift SDSS group galaxies, divided into bins of stellar mass.

where r_e is the effective radius which encloses half of the total light, I_e is the intensity at the effective radius, and k is a normalization factor which depends on the Sérsic index, n. In general, the Sérsic index runs between $1 \lesssim n \lesssim 8$. Disc dominated, spiral galaxies have light profiles which are well fit by a Sérsic index of $n \lesssim 2$, with $n = 1$ corresponding to a purely exponential disc. Elliptical galaxies have more centrally concentrated light profiles, and are well fit by larger Sérsic indices, $n \gtrsim 2$. A commonly used empirical law to describe the brightness profiles of elliptical galaxies is de Vaucouleurs' law which states that the intensity of an elliptical galaxies goes as $\log I(r) \propto r^{1/4}$, this is also just a special case of the Sérsic profile with $n = 4$.

Instead of modelling galaxy light profiles as a single component, bulge + disc decompositions are used as another method of classifying the morphology of galaxies. The light profile of the bulge and disc are modelled separately, often with an $n = 4$ bulge and an $n = 1$ disc (e.g. Simard et al., 2002), the

sum of these two components is then the model for the galaxy as a whole. The fraction of the total light produced in the bulge component is the bulge-to-total ratio (B/T) which is used as a morphological discriminator for galaxies. Pure elliptical galaxies will have $B/T \to 1$, and pure disc galaxies will have $B/T \to 0$.

Galaxy morphology is also strongly correlated with stellar mass, with high-mass galaxies showing earlier type morphologies. This trend can be seen in Fig. 1.4 and has also been confirmed using different probes of morphology, such as Sérsic index (van der Wel, 2008), bulge-to-total ratio (Bluck et al., 2014), as well as visual morphological classifications (Bamford et al., 2009).

1.2.3 Star formation rates

The star formation rate (SFR) of a galaxy is defined as the rate at which a galaxy generates new mass in the form of stars, measured in units of solar-masses per year ($\mathrm{M}_\odot\,\mathrm{yr}^{-1}$). Being able to accurately determine the SFRs of galaxies is crucial for the study of galaxy evolution, as many of the evolutionary effects felt by galaxies (both environmental and secular) will influence star formation. Currently there are multiple methods used to derive SFRs for galaxies, which rely on emission across a wide range of wavelengths.

Two of the most common methods are to derive SFRs from UV or IR continuum emission. UV continuum emission directly probes light emitted from young stars and therefore is an indicator of a galaxies recent SFR. The largest shortcoming of UV as a SFR indicator is interstellar dust which causes galaxies to be relatively opaque to UV photons. In fact, approximately half the

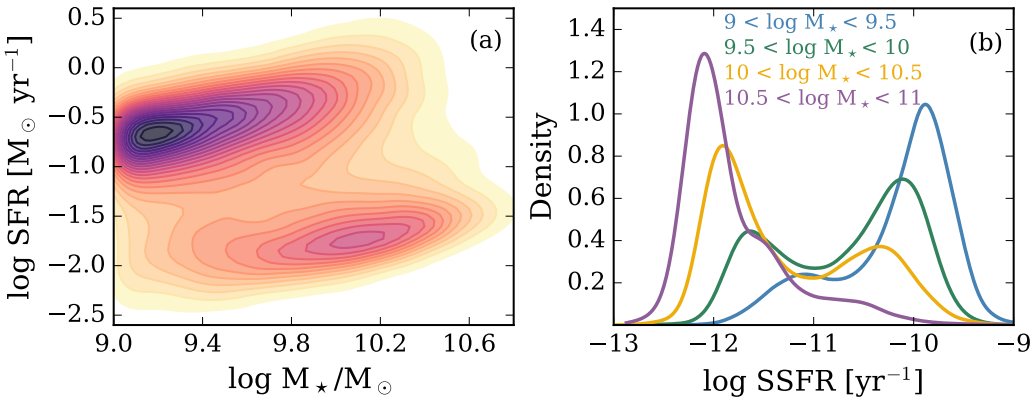

Figure 1.5: Left: Star formation rate versus stellar mass for a sample of low-redshift SDSS group galaxies. Right: Star formation rate per unit mass (specific star formation rate; SSFR) density distribution for low-redshift SDSS group galaxies, divided into bins of stellar mass.

emission from stars in the Universe is absorbed and re-emitted by dust in the infrared (Kennicutt & Evans, 2012). This leads to IR continuum emission from dust being a useful probe of galaxy SFRs. As mentioned previously, both UV and IR continuum luminosities can be converted to SFRs using wavelength-dependent relationships, and often UV and IR observations will be used in tandem to account for both obscured and unobscured star formation.

In addition to continuum emission, emission line strengths can also be used as star formation indicators, with the Hα line being the most commonly used emission line SFR indicator for galaxies in the local Universe. At higher redshift the Hα line is redshifted out of the optical window and the [OII] doublet is often used instead. Similar to the UV continuum, the largest shortcoming of this method is dust attenuation (Kennicutt & Evans, 2012).

Kennicutt & Evans (2012) provide a compilation of up to date relationships, across a wide range in wavelength, between SFR and both continuum and emission line luminosities.

Another common star formation indicator is the 4000 angstrom break (D_n4000), which refers to the strength of the break at 4000 Å in a galaxy's spectrum given by the ratio of the flux in the red continuum ($4000 - 4100$ Å) to the flux in the blue continuum ($3850 - 3950$ Å) (Balogh et al., 1999). Galaxies with old stellar populations and little recent star formation will show a strong D_n4000 break due to strong metal absorption in the atmospheres of old stars as well as a lack of UV emission from young, hot stars (Hamilton, 1985). Galaxies with strong recent star formation will show a correspondingly small break at 4000 Å.

Instead of determining SFRs based upon only a relatively narrow spectral region, given multiwavelength imaging, one can use spectral energy distribution (SED) fitting to synthesize the entire UV to IR spectrum. The primary assumption behind SED fitting is that the galaxy spectrum is simply the sum of the spectra of individual stars (allowing for the re-processing of stellar light by gas and dust). Therefore by inputting initial mass functions, stellar populations, stellar evolution tracks, dust distributions, etc., one can attempt to reproduce the observed SED. A successfully fit SED will contain a wealth of information such as: SFRs, star formation histories, stellar masses, stellar metallicities, and dust information (Walcher et al., 2011).

Across a wide range of environments galaxies can be divided into two main subpopulations based on their SFRs, those galaxies which are actively forming

stars and those quiescent galaxies whose star formation has ceased (Wetzel et al., 2012). One way to define the population of star-forming galaxies is to use the "star-forming main sequence" (SFMS). The SFMS is a tight correlation between SFR and stellar mass located in the upper region of SFR $- M_\star$ plane. The SFMS for low-redshift galaxies in SDSS groups is easily visible in Fig. 1.5(a) ranging between $\sim -1 < \log \mathrm{SFR} < 0$. Due to the correlation between SFR and stellar mass, it is useful to normalize SFR by galaxy stellar mass, known as the specific star formation rate (SSFR = SFR/$M_\star$). Like the distribution of galaxy color, the SSFR distribution for galaxy populations is also bimodal (see Fig. 1.5(b)). This bimodality in SSFR provides another method for distinguishing between star-forming and passive galaxies. Recent observations have shown that across many environments in the local Universe, the division between the active and quiescent populations (ie. the local minimum in the SSFR distribution) is found at SSFR $\simeq 10^{-11}\,\mathrm{yr}^{-1}$ (Wetzel et al., 2012).

Star formation activity also depends strongly on redshift. The normalization of the SFMS shifts to larger SFRs with increasing redshift (Karim et al., 2011; Whitaker et al., 2012; Lee et al., 2015; Erfanianfar et al., 2016), star-forming fractions of galaxies in groups and clusters (at a given stellar mass) increase with redshift (McGee et al., 2011; Hou et al., 2013; Nantais et al., 2013), as well the average SSFRs of galaxies increase with redshift as $(1+z)^\alpha$ where $\alpha \sim 2-4$ (Oliver et al., 2010; Whitaker et al., 2012), at least out to $z = 2$. On larger scales, the star formation rate density in the Universe has decreased to the present day from its peak at $z \simeq 2$ (e.g. Madau et al.,

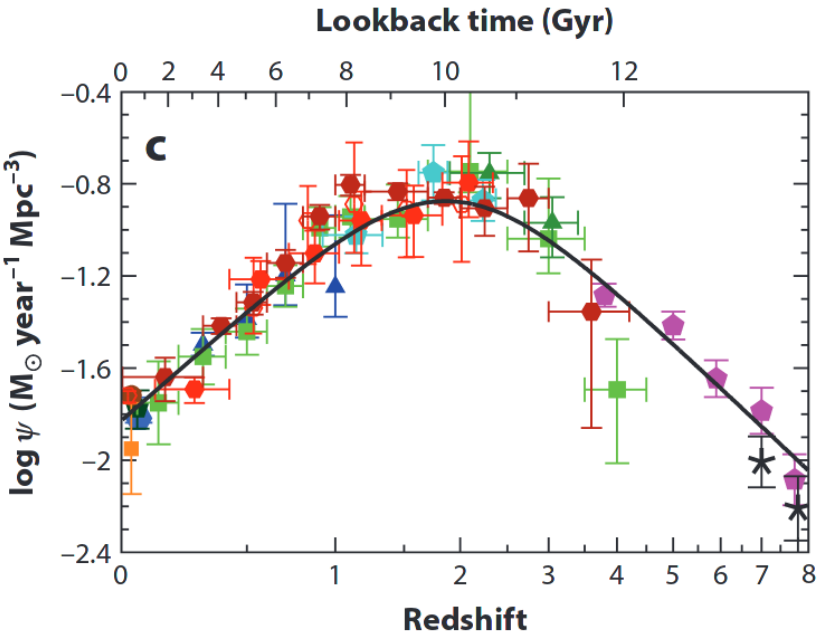

Figure 1.6: Cosmic star formation rate density as a function of redshift, using both IR and UV derived SFRs. Image credit: Madau & Dickinson (2014).

1998; Madau & Dickinson, 2014). Fig. 1.6 shows this in the form of an updated version of the famous Lilly-Madau plot taken from Madau & Dickinson (2014).

1.3 Galaxy environments

1.3.1 Galaxy groups

Galaxy groups are the most common environment in the local Universe (Geller & Huchra, 1983; Eke et al., 2005), and are also a regime in which many processes capable of driving galaxy evolution are efficient. While populations of galaxies in the isolated field and large clusters are dominated by active, late-type and passive, early-type galaxies respectively, galaxy groups are an

intermediate regime where significant numbers of different galaxy types are present (Wilman et al., 2005; McGee et al., 2011).

Figure 1.7: SDSS image of a galaxy group from the Yang et al. (2007) catalogue with: $z \simeq 0.02$, $M_H \simeq 10^{13.6}\,\mathrm{M}_\odot$, $R_{200} \simeq 0.7\,\mathrm{Mpc}$. Image credit: Sloan Digital Sky Survey.

While no strict definition exists for what constitutes a galaxy group, historically haloes referred to as groups have properties (e.g. halo mass, galaxy membership, velocity dispersion, virial radius) which lie within broadly defined (albeit, somewhat arbitrary) ranges. Generally speaking, a galaxy group is a collection of galaxies embedded within a dark matter halo which satisfy the following criteria (though the following conditions are not all independent) (Mamon, 2007; Connelly et al., 2012):

- Halo masses between $\sim 10^{12}$ and $10^{14}\,\mathrm{M}_\odot$
- Memberships of bright ($\gtrsim L_\star$) galaxies between ~ 3 and 50

- Velocity dispersions between $\sim$200 and 800 $\mathrm{km\,s^{-1}}$
- Virial radii between $\sim$0.3 and 1 Mpc

Compact groups

An interesting subclass of galaxy groups are known as compact groups. Compact groups were initially defined by Hickson (1982) by the following criteria:

- $N(\Delta m = 3) \geq 4$
- $\theta_N \geq 3\,\theta_G$
- $\mu_e \leq 26.0\,\mathrm{mag\,arcsec^{-2}}$

where $N(\Delta m = 3)$ is the number of galaxies within 3 magnitudes of the brightest galaxy in the group, μ_e is the effective surface brightness of the galaxies, θ_G is the angular diameter of the smallest circle containing the centres of all group galaxies, and θ_N is the angular diameter of the largest circle containing no galaxies brighter than the surface brightness constraint (Hickson, 1982; McConnachie et al., 2009).

Compact groups have proven to be important probes of galaxy evolution as due to the close proximity of members many galaxy interactions are favoured. When comparing the properties of galaxies in compact groups to those in loose groups (groups which do not satisfy the Hickson criteria) it has been shown that galaxies in compact groups tend to be more evolved. Namely, they have higher fractions of red, passive, early-type galaxies as well as older stellar populations and lower SSFRs (Coenda et al., 2012, 2015).

Figure 1.8: Hickson compact group 92, known as Stephan's Quintet. Image credit: NASA/Hubble Space Telescope.

Fossil groups

Due to the low velocity dispersions and relatively high galaxy densities in groups, numerical simulations suggest that most bright group members will eventually merge and form one dominant elliptical galaxy (e.g. Governato et al., 1991). While all of the bright galaxies may merge, the extended X-ray halo will persist due to the long cooling time of the IGM (beyond the high-density core) (Ponman & Bertram, 1993). Such systems with a dominant elliptical galaxy (with few, or no, bright companions) embedded within an extended X-ray halo are known as fossil groups (e.g. Fig 1.9). Fossil groups

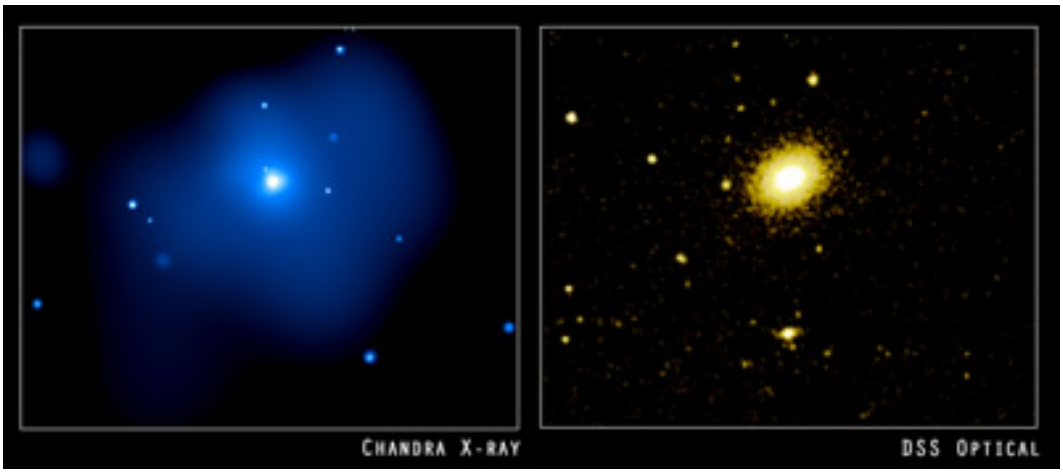

Figure 1.9: Fossil group NGC 4555. The extended X-ray halo is shown on the left and the optical image is shown on the right. Image credit: X-ray: NASA/Chandra, Optical: DSS.

are among the oldest and most evolved systems in the Universe, and tens of fossil groups have now been detected observationally (e.g. Ponman et al., 1994; Ulmer et al., 2005; Santos et al., 2007; Khosroshahi et al., 2014).

1.3.2 Galaxy clusters

Galaxy clusters are the largest bound structures in the Universe and represent important probes of both galaxy evolution and cosmology. Like galaxy groups, the precise definition of a galaxy cluster is somewhat arbitrary, however clusters can be broadly defined as bound collections of galaxies which exceed the group criteria given in Section 1.3. Galaxy populations in clusters are more evolved than field and group galaxies, and are generally dominated by red, passive, early-type galaxies (Kimm et al., 2009; Wilman & Erwin, 2012; Wetzel et al., 2012). As a result of hierarchical structure growth, clusters will be built up both through the accretion of field galaxies as well as the accre-

tion of smaller galaxy groups. Therefore, some cluster galaxies will have been quenched prior to infall in a smaller group (known as pre-processing) whereas others will have been quenched by cluster specific processes. Determining the relative balance between these two quenching pathways is important for constraining the environments in which galaxy transformations are most efficient, and is an area of active research (McGee et al., 2009; De Lucia et al., 2012; Bahé et al., 2013; Dressler et al., 2013; Hou et al., 2014; Roberts & Parker, submitted).

1.3.3 Identifying groups and clusters

The simplest method used to identify galaxy groups observationally is the so-called Friends-of-Friends (FoF) algorithm (e.g. Huchra & Geller, 1982; Press & Davis, 1982). The FoF algorithm joins galaxies into groups based upon their separations in projected distance as well as line-of-sight (LOS) velocity. In this implementation the algorithm has two free parameters known as "linking lengths". Two galaxies are linked if their seperations in projected distance as well as velocity are both smaller than the corresponding linking lengths. The process continues as more galaxies are linked together and larger and larger groups are therefore built up. The algorithm is succinctly summarized by Press & Davis (1982) in saying that pairs of galaxies are "friends", and that "any friend of a friend is a friend". While attractive in its simplicity as well as its ability to create unique groups without making any assumptions regarding group properties, there are weaknesses to generating groups via the FoF method. One example is that the algorithm does not require a well defined

group centre. To account for this, the location of the most-massive galaxy, the luminosity-weighted centre of member galaxies, or the peak of X-ray emission (given an X-ray bright group), are all used to define a group centre however there is no guarantee that these different definitions will agree. For example, George et al. (2012) find that offsets between different centre definitions are generally between $50 - 100\,\mathrm{kpc}$, with tails extending out to a few hundred kpc. Another shortcoming lies in the fact that dynamically distinct groups may be connected given a linking length that is too large, and conversely if the assumed linking length is too small then subgroups which are physically associated may not be connected by the algorithm. To attempt to account for this, linking lengths can be optimized through comparisons to mock catalogues from simulations (e.g. Nolthenius & White, 1987).

More recent work has been done in order to build off of and improve upon the simplistic FoF approach. One example is the "halo based" group finding algorithm from Yang et al. (2005, 2007) which initially seeds groups using the basic FoF algorithm with very small linking lengths, and then proceeds to further populate these seed groups based on the assumption that the phase space distribution of galaxies follows that of dark matter particles – assumed to be a spherical Navarro-Frenk-White (NFW) profile (Navarro et al., 1997).

Another modern technique of defining galaxy groups from redshift data is to use a Voronoi tessalation (Marinoni et al., 2002; Gerke et al., 2005, 2012). This technique uses a Voronoi partition to divide a survey volume into distinct subvolumes, each containing one galaxy as well as all points in the space which are closer to that galaxy than any other. These Voronoi cells provide a use-

ful measure of galaxy density, as those galaxies contained in cells with small volumes will by definition be located in dense regions. These initial Voronoi cells act as seeds for potential groups which are built up by linking closly neighbouring cells together.

At high-redshift, group finding becomes much more difficult. One main reason for this is that it is difficult to obtain enough spectra, particularly for low-mass galaxies. A method that has been used is to look for extended X-ray emission from the hot intragroup medium (IGM), though this method is biased toward finding groups with rich IGM which may not be representative of the total group population (Connelly et al., 2012). Even detecting the most X-ray bright groups at high redshift is difficult as a result of distance, and deep spectra are still required to confirm group members.

For larger clusters the cluster red sequence (CRS) method is commonly used (Gladders & Yee, 2000), which allows for cluster identification using only two filter photometry. This method relies on the fact that all galaxy clusters display a well defined red sequence in colour-magnitude space, therefore clusters can be identifed by finding galaxy overdensities on the sky which also show a tight red sequence. As well, the precise colour of the red sequence has been shown to depend on redshift, therefore providing an efficient redshift estimate for identified clusters.

A more recent method used to identify galaxy clusters is to use the electron scattering of CMB photons known as the Sunyaev-Zel'dovich (SZ) effect (Sunyaev & Zeldovich, 1970; Birkinshaw, 1999). Due to the hot, ionized ICM, CMB photons passing through large clusters will imprint a relatively strong

scattering signal on the CMB, thereby allowing the identification of galaxy clusters (Carlstrom et al., 2002; Planck Collaboration et al., 2011, 2015). The strongest asset of the SZ technique is the redshift independence of the SZ effect which makes this method particularly powerful for finding high-redshift clusters.

1.4 Star formation quenching

It has been well established that populations of galaxies are bimodal in SFR across essentially all environments (see Fig. 1.5) (e.g. Wetzel et al., 2012), with galaxies either actively forming stars as part of the blue cloud or evolving quiescently on the red sequence. An area which has received a lot of focus is determining which are the dominant mechanism(s) shutting down star formation in galaxies. In particular, it is argued that there are two main classes of SFR quenching occuring in the Universe: secular or mass-quenching, and environmental quenching. The dichotomy between these two quenching modes is outlined in detail by Peng et al. (2010), where it is concluded that low-mass ($\lesssim 10^{10.5}\,\mathrm{M}_\odot$) galaxies in the local Universe are primarily quenched by environmental mechanisms and that galaxies more massive than $\sim 10^{10.5}\,\mathrm{M}_\odot$ are quenched through internal, secular processes.

1.4.1 Environmental quenching

Significant progess has been made in identifying the processes which can affect galaxies in different environments, however there is still no consensus

regarding what the relative balance between these quenching mechanisms is. This section will outline some of the main environmental mechanisms which can impact star formation, along with a discussion of the environments in which different processes will be most efficient and how these quenching mechanisms can be constrained observationally.

Ram pressure stripping

A straight forward way to quench the star formation of a galaxy is to directly remove the cold gas reserves from the disc. A commonly invoked mechanism to achieve this is the ram pressure stripping of cold gas by the intracluster medium (ICM). Galaxies will feel a ram pressure force as they move through the ICM and if this force is enough to overcome the potential well of the gas then stripping will occur. The ram pressure felt by a galaxy scales with the density of the ICM as well as the square of the galaxy velocity relative to the ICM, $P_{RP} \propto \rho v^2$ (Gunn & Gott, 1972), and therefore should be most effective in the cores of high-mass clusters where both densities and galaxy velocities are high. One of the characteristic features of ram pressure stripping is the rapid timescales over which it is able to quench star formation. If ram pressure stripping is acting efficiently then cold gas can be removed in $\lesssim 1\,\mathrm{Gyr}$ (Abadi et al., 1999; Quilis et al., 2000; Roediger & Hensler, 2005; Steinhauser et al., 2016). Studies which require short quenching timescales to account for observational results use this fact to argue that ram pressure stripping is playing an important role (Muzzin et al., 2014; Fillingham et al., 2015; Wetzel et al., 2015). Additionally, it is possible to constrain ram pressure stripping by looking for direct evidence. For example, extended HI distributions in galaxies are

interpreted as evidence of ram pressure stripping (Kenney et al., 2004; Chung et al., 2007, 2009; Kenney et al., 2015). It is also important to note that while ram pressure stripping appears to have a measureable affect on atomic hydrogen (at least in high-mass clusters), how effectively it can remove molecular hydrogen from the disc is still a debated question (Boselli et al., 2002; Boselli & Gavazzi, 2006; Fumagalli et al., 2009; Sivanandam et al., 2014)

Starvation

As opposed to the removal of cold gas from the disc, starvation (also sometimes referred to as "strangulation") prevents the replenishment of cold gas reserves. This can occur either through the stripping of hot halo gas, or by preventing the hot halo gas from cooling and accreting onto the galactic disc. Larson et al. (1980) first proposed that preventing spiral galaxies from accreting new gas could account for the high fractions of passive S0 galaxies observed in local clusters. Compared to ram pressure stripping, quenching by starvation will occur over much longer timescales, on the order of $\sim 2 - 10\,\mathrm{Gyr}$ (Wheeler et al., 2014; Fillingham et al., 2015; Peng et al., 2015; Wetzel et al., 2015). The precise quenching time will be set by the gas consumption timescale of a given galaxy, as once a galaxy is cut-off from gas accretion it will only form stars until it has exhausted its existing cold-gas reserves. Results of previous works have shown that long quenching times are required to reproduce observational results (Balogh et al., 2000; Balogh & Morris, 2000; Wetzel et al., 2013; Wheeler et al., 2014), which tends to be interpretted as evidence for the importance of starvation as a quenching mechanism. Recently, Peng et al. (2015) have presented a novel technique for observationally constraining the

importance of starvation. Peng et al. propose that evidence for starvation can be gleaned through examining the stellar metallicities of galaxies. If a galaxy is quenched via starvation then its stellar metallicity should continue to rise as it exhausts its existing cold-gas reserves, leading to the population of passive galaxies showing, on average, higher metallicities than the population of star-forming galaxies (at a given stellar mass). Peng et al. argue that this serves as a method to distinguish between starvation and ram pressure stripping, as due to the rapid timescales over which ram pressure stripping removes cold-gas reserves, the strong metallicity difference between star-forming and passive galaxies would not be expected.

Galaxy interactions

As opposed to quenching through interactions with surrounding gas, it is possible that quenching can be driven by more direct interactions between galaxies. These interactions can be broadly divided into three main categories: major mergers, minor mergers, and impulsive interactions. Major mergers (mass ratio, $M_1/M_2 \lesssim 3-4$) have been shown to induce starburst events which can very quickly exhaust the gas reserves of a galaxy, leaving it quenched (e.g. Mihos & Hernquist, 1994b). As well, observations of closely paired galaxies show that paired galaxies of similar mass demonstrate strong enhancements in SFRs with decreasing seperation, consistent with interaction induced starbursts (Ellison et al., 2008; Davies et al., 2015). Minor mergers ($M_1/M_2 \gtrsim 3-4$) have also been shown to be capable of inducing starbursts in the primary galaxy (e.g. Mihos & Hernquist, 1994a), and seeing as minor mergers are significantly more common than major mergers (Lotz et al., 2011), this plays a potentially im-

portant role in transforming galaxies. Observations of galaxies in minor pairs have shown that star formation is enhanced in the higher mass primary, but suppressed in the secondary galaxy (Davies et al., 2015). As opposed to galaxy mergers, impulsive interactions are high-speed close encounters between galaxies, also referred to as "galaxy harassment" (Moore et al., 1996). Like galaxy mergers, harassment is capable of inducing bursty star formation as multiple high-speed encounters can funnel cold gas to the central regions of galaxies and therefore fuel intense star formation (Fujita, 1998). Tidal interactions between central galaxies and satellites can also influence gas content, either by directly stripping gas from the satellite or by transporting gas outwards allowing it to be more easily stripped by other mechanisms (Mayer et al., 2006; Chung et al., 2007).

1.4.2 Mass Quenching

While star-forming low-mass galaxies tend to be quenched via environmental mechanisms, high-mass galaxies seem to be preferentially quenched through secular processes. The most commonly invoked source of mass quenching is the feedback from Active Galactic Nuclei (AGN). Jets from and large-scale winds from AGN can not only displace cold gas from the galactic disc, but also heat surrounding gas to prevent cooling and subsequent star formation (Gabor et al., 2011). Semi-analytic models as well as hydrodynamic simulations with subgrid AGN prescriptions have shown that AGN feedback can significantly suppress star formation and therefore more closely match observations, in particular within high-mass galaxies (e.g. Somerville et al., 2008; Dubois

et al., 2013; Bongiorno et al., 2016). Though there is still no clear consensus observationally as to how strongly AGN affect star formation, with some studies finding that star-forming AGN galaxies are found preferentially below the star-forming main sequence (Gürkan et al., 2015; Mullaney et al., 2015; Ellison et al., 2016), while others find that SFRs of AGN hosts are broadly consistent, or even slightly enhanced, compared with main sequence galaxies (Santini et al., 2012; Lanzuisi et al., 2015; Stanley et al., 2015).

It has also been argued that mass quenching could be a result of the hot gas content of the dark matter haloes of large galaxies. Above a critical mass ($\sim 10^{12}\,\mathrm{M}_{\odot}$), haloes should support a hot gas component which has been heated via virial shock (Birnboim & Dekel, 2003). In a scenario similar to starvation, this hot gas corona can prevent efficient gas cooling and therefore quench the galaxy (Cattaneo et al., 2006; Gabor & Davé, 2015). A galaxy halo mass of $\sim 10^{12}\,\mathrm{M}_{\odot}$ corresponds to a stellar mass of $\sim 10^{10.5}\,\mathrm{M}_{\odot}$, which agrees well with the critical mass above which mass quenching is believed to play an important role (Peng et al., 2010). It is also worth noting that this picture may still be intimately linked to AGN, as depending on the cooling time of the hot halo gas, feedback from sources such as AGN may be required to keep the gas heated (Cattaneo et al., 2006).

1.5 Morphological evolution

Correlations between galaxy star formation and morphology have been well established observationally (e.g. Schawinski et al., 2014), where star-forming galaxies tend to show late-type morphologies and passive galaxies are pref-

erentially early-type. Therefore it is important to try to understand how the quenching mechanisms discussed in Section 1.4 affect morphology. Specifically, whether or not the same mechanisms which shut off star formation also drive morphological evolution. Taking the B/T as a proxy for the morphology of a galaxy, there are two ways in which morphologies can evolve to earlier types. Either the brightness of the disc component fades over time, or the brightness of the bulge component increases, in both cases driving the B/T to higher values.

Considering the aforementioned quenching mechanisms. Ram-pressure stripping and starvation could in principle raise the B/T through disc fading. As star formation is quenched in the disc through either process, the light profile of the galaxy would naturally evolve to being more bulge-dominated. Observationally however, previous studies have argued that disc fading alone cannot account for the morphological transformations seen in galaxies (Christlein & Zabludoff, 2004; Bundy et al., 2010). Alternatively, the B/T can be increased through the creation of a stronger bulge component. Galaxy interactions such as galaxy harrassment and minor mergers are capable of funnelling cold gas to small galactic radii, and therefore inducing central starbursts, which can increase the brightness of the central bulge. Tidal forces and impulsive heating during these interactions can also strongly influence morphology and build up a strong bulge (Moore et al., 1996; Bekki & Couch, 2011). In the most extreme case, the end product of major mergers tend to be bulge dominated galaxies with classical, de Vaucoulours profiles (e.g. Barnes, 1989).

1.6 The environmental dependence of galaxy properties

There are many ways in which one can characterize the environment of a galaxy, and previous works have shown that various galaxy properties tend to correlate with different environmental measures (Dressler, 1980; Ribeiro et al., 2010; Urquhart et al., 2010; Wilman & Erwin, 2012; Haines et al., 2015). One of the primary aims of galaxy evolution research is to obtain a self consistent picture of environmental effects, and in particular to determine which environmental correlations are strongest and which are secondary in nature. This section will lay out a number of environmental correlations which have been explored through observing the properties of galaxies across many different regimes.

1.6.1 Halo mass

Galaxy groups and clusters span a wide range of halo masses, from $\sim 10^{12}\,\mathrm{M}_{\odot}$ for low-mass groups, up to $\gtrsim 10^{15}\,\mathrm{M}_{\odot}$ for rich clusters of galaxies. The properties of galaxies in these groups and clusters depend on their host halo mass, although there is still debate as to how strong an affect that this is (De Lucia et al., 2012; Hoyle et al., 2012; Hou et al., 2013). For example, Fig. 1.10 taken from Wetzel et al. (2012), shows that galaxies in high-mass haloes tend to have large quenched fractions, in particular for low-mass galaxies, when compared to galaxies in lower mass haloes at the same stellar mass. Other studies have also found that colour and morphology correlate with halo mass

(e.g. Kimm et al., 2009; Wilman & Erwin, 2012), with galaxies in high mass haloes tending to be red and early-type.

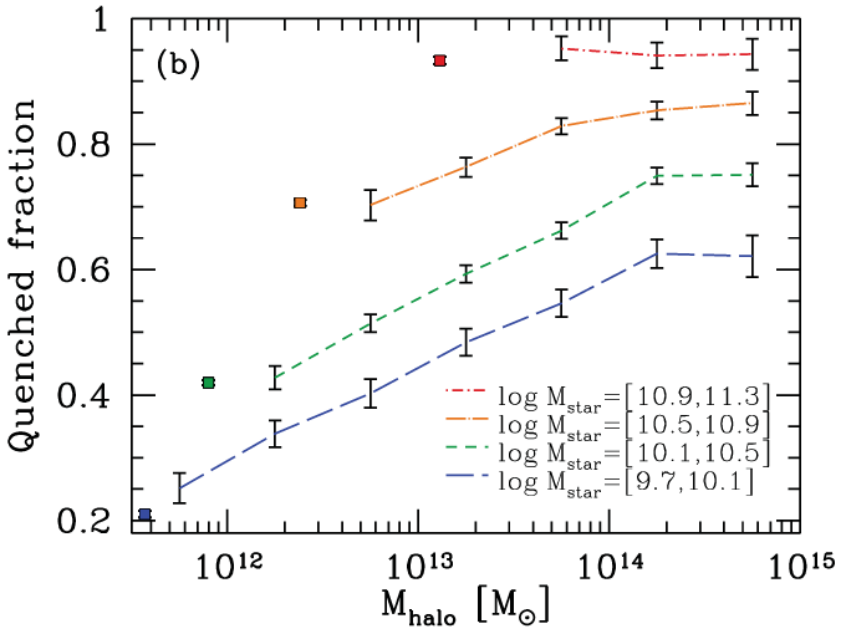

Figure 1.10: Galaxy quenched fraction (SSFR $< 10^{-11}\,\mathrm{yr}^{-1}$) versus halo mass for central galaxies (solid points) and satellite galaxies (dashed lines) in bins of stellar mass. Image credit: Wetzel et al. (2012).

1.6.2 Radial position

On top of correlating with the mass of the host halo, galaxy properties also show a strong dependence on their group-centric radius. Galaxies at small radii near the group centre have been shown to have red colours (Blanton & Berlind, 2007; Hansen et al., 2009; Li et al., 2009; Prescott et al., 2011), reduced star formation (Rasmussen et al., 2012; Wetzel et al., 2012; Haines et al., 2015), and earlier type morphologies (Whitmore et al., 1993; Goto et al., 2003; Postman et al., 2005; Fasano et al., 2015). Conversely, galaxies in the outer regions of

haloes are preferentially blue and star-forming, with late-type morphologies. Fig. 1.11 shows an example from Li et al. (2009) where a clear anti-correlation is seen between red fraction and cluster-centric radius for galaxies in clusters from the Canadian Network for Observational Cosmology (CNOC) Survey. In addition to considering the projected radial position of a galaxy, recent studies have used velocity-radius phase space to divide galaxy group and cluster populations into three main classes: those infalling onto the halo for the first time, those virialized at small radii, and those "backsplashing" beyond the virial radius after a pericentric passage (e.g. Mahajan et al., 2011). The properties of galaxies have been shown to depend on which of these subclasses they are a part of. For instance, infalling galaxies have enhanced star formation rates (Noble et al., 2016), post-starburst galaxies preferentially reside in intermediate regions of phase space (Muzzin et al., 2014), as well backsplash galaxies should have lower masses due to tidal mass loss during pericentric passage (Gill et al., 2005).

Mass segregation

Another important radial measure of galaxy properties in groups is mass segregation. A galaxy group showing strong mass segregation will have a radial gradient in galaxy mass, where the most massive galaxies are concentrated in the inner region of the halo. Mass segregation is often predicted as a result of dynamical friction (Chandrasekhar, 1943), where the drag force associated with dynamical friction will act most strongly on high-mass galaxies, thereby driving them to small radii. For the simplistic case of a mass, m, on a circular orbit in a spherical, isothermal halo, the dynamical friction timescale for the

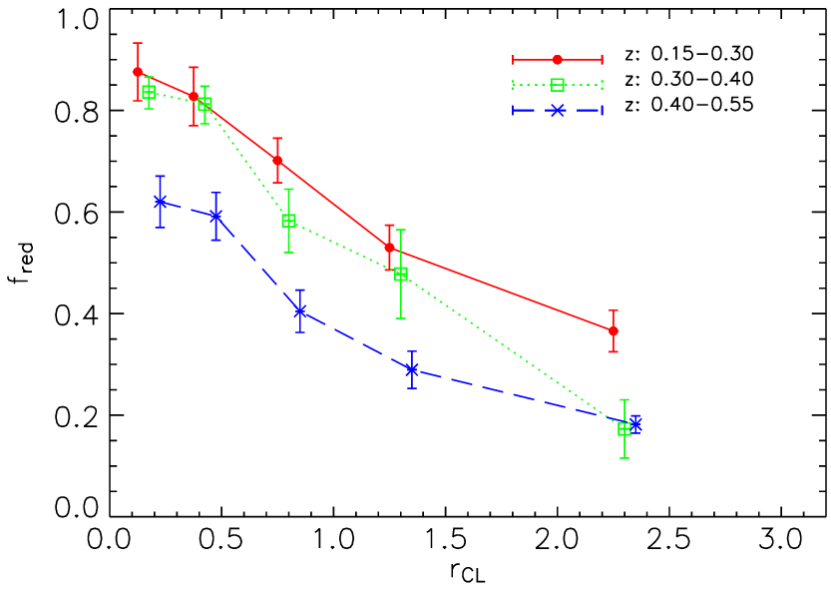

Figure 1.11: Red fraction versus cluster-centric radius for galaxies in CNOC clusters. Colours correspond to three different redshift ranges. Image credit: Li et al. (2009).

mass to migrate from $r = r_i$ to $r = 0$ is given by the following relation (Mo et al., 2010)

$$t_{df} = \frac{1.17}{\ln M_H/m} \left(\frac{r_i}{r_H}\right)^2 \left(\frac{M_H}{m}\right) \frac{r_H}{V_c}, \tag{1.2}$$

where r_H is the radius of the halo, M_H is the halo mass, and V_c is the circular velocity. Inserting characteristic values for these parameters one will find that in this simple case the dynamical friction timescale is smaller than the Hubble time only for $M_H/m \lesssim 20$.

It is important to study the distribution of galaxy mass within haloes in order to determine whether the large populations of passive, early type galaxies at low radii are due to specific mechanisms acting in dense central regions, or

a result of massive galaxies being preferentially found within the inner regions of the halo. Previous studies have attempted to elucidate the importance of mass segregation in groups and clusters, however no clear consensus exists, with some recent studies finding evidence for significant mass segregation (van den Bosch et al., 2008; Presotto et al., 2012; Balogh et al., 2014; Joshi et al., 2016) and others finding no strong evidence for a radial gradient in galaxy mass (von der Linden et al., 2010; Vulcani et al., 2013; Ziparo et al., 2013).

1.6.3 Group dynamical state

Galaxy groups can be broadly classified by their dynamical states. Galaxy populations of dynamically old, relaxed groups will show line of sight velocity distributions which are well fit by a Gaussian profile, whereas galaxy populations in dynamically young, unrelaxed groups will have velocity distributions which show stronger deviations from normality. The degree to which galaxy properties correlate with the dynamical state of their host group is still a question of active research, where no strong consensus has been reached (e.g. Biviano et al., 2002; Ribeiro et al., 2013b). Previous studies have indicated that galaxies in Gaussian (G) groups tend to be redder than galaxies in non-Gaussian (NG) groups (Ribeiro et al., 2010; Carollo et al., 2013; Ribeiro et al., 2013a). More directly investigating star-forming and morphological properties, Hou et al. (2013) find no detectable difference between the quiescent fractions of galaxies in G versus NG groups as a function of redshift. More recently, Roberts & Parker (submitted) have found that low-mass galaxies in the virialized region of NG groups have enhanced star-forming and disc fractions com-

pared to galaxies in the same region of G groups, whereas no differences are detected for infalling galaxies.

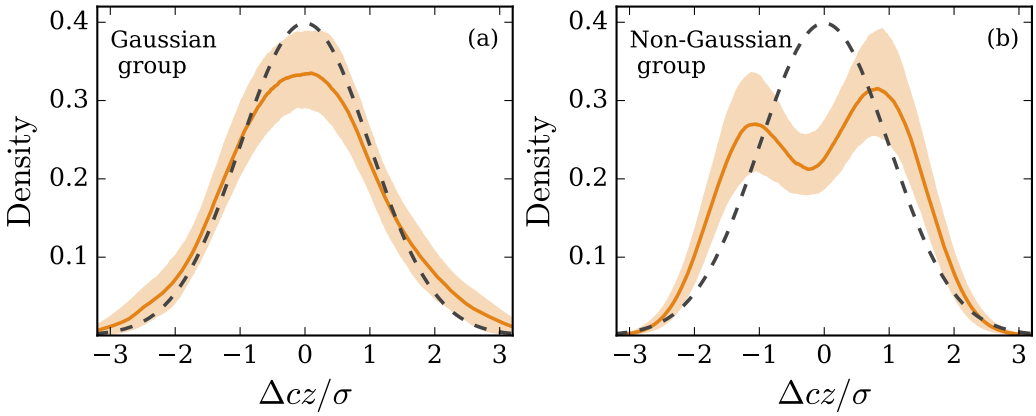

Figure 1.12: Projected velocity distributions for galaxies in a Gaussian (left) and a non-Gaussian (right) SDSS group. Solid line is the median of 1000 bootstrap resamplings and shaded regions correspond to 68 per cent confidence intervals, dashed line corresponds to the standard normal distribution.

1.6.4 X-ray luminosity

Galaxy groups and clusters can also be classified according to their X-ray luminosity, eminating from the hot IGM/ICM. Studies investigating the dependence of galaxy properties on the X-ray luminosity of their host group have been focused mostly on the higher-mass cluster regime, due to the relative ease of detecting X-ray bright clusters compared to lower-mass groups. However, even within the cluster regime, there still lacks strong consensus as to how strongly colour, star formation, and morphology correlate with X-ray luminosity. With some previous studies finding little to no correlations (Ellingson et al., 2001; Balogh et al., 2002a; Fairley et al., 2002; Wake et al., 2005; Lopes et al., 2014), and others finding evidence for redder galaxies with reduced star

formation and earlier-type morphologies in clusters with strong X-ray emission (Balogh et al., 2002b; Postman et al., 2005; Urquhart et al., 2010).

Less work has been done characterizing the properties of galaxies in lower-mass, X-ray bright groups. Connelly et al. (2012) using a sample of X-ray groups from the CNOC2 survey, study scaling relations for both X-ray and optically selected groups. More recently, Wang et al. (2014) have compiled a large sample of X-ray groups by combining ROSAT All Sky Survey X-ray images with previously identified SDSS groups (Yang et al., 2005, 2007). Wang et al. also study scaling relations between X-ray and optical properties, along with examining the red fractions of galaxies in groups with strong X-ray emission, compared to those with weak X-ray emission. Finding that galaxies in high-mass, "X-ray strong" groups have enhanced red fractions – though potential stellar mass dependences were not controlled for. Knowing that galaxy properties depend strongly on stellar and halo mass, in order to robustly characterize any correlations between X-ray luminosity and galaxy properties, potential stellar and halo mass dependences must both be properly controlled for.

1.7 Outline of this thesis

In broad terms the goal of this thesis is to further understand the influence of the group environment on various galaxy properties, across different halo mass ranges. In particular, this thesis will look to answer two main questions:

1. Do group galaxies show significant mass segregation, and how does the strength of mass segregation scale with halo mass?

2. On top of the well established dependences on stellar and halo mass, do galaxy star formation and morphology correlate with the X-ray luminosity of the host halo?

In Chapter 2, I investigate mass segregation in galaxy groups. In particular, I will use a sample of galaxies in groups from the SDSS (Yang et al., 2005, 2007) and determine the mean galaxy stellar mass as a function of group-centric radius. By dividing the group sample into bins of halo mass I explore how the strength of mass segregation (ie. the slope of the $\log M_{\star}/M_{\odot}$ vs. R/R_{200} relationship) scales with the mass of the host group. In Chapter 3, I investigate the dependence of star formation and morphology on the X-ray luminosity of their host halo. Using a large data set of galaxies in X-ray groups (Wang et al., 2014), I am able to properly control for stellar and halo mass dependences, and therefore robustly look for any residual dependence on X-ray luminosity. Lastly, in Chapter 4 I will summarize the results, discuss future work, and make concluding statements. Chapters 2 and 3 represent unchanged versions of papers that have been published (Chapter 2: Roberts et al. 2015, Chapter 3: Roberts et al. 2016) in the *Monthly Notices of the Royal Astronomical Society Letters* and *Monthly Notices of the Royal Astronomical Society* respectively, both refereed astronomical journals.

Bibliography

Abadi, M. G., Moore, B., & Bower, R. G. 1999, MNRAS, 308, 947

Bahé, Y. M., McCarthy, I. G., Balogh, M. L., & Font, A. S. 2013, MNRAS, 430, 3017

Baldry, I. K., Balogh, M. L., Bower, R. G., Glazebrook, K., Nichol, R. C., Bamford, S. P., & Budavari, T. 2006, MNRAS, 373, 469

Balogh, M., Bower, R. G., Smail, I., Ziegler, B. L., Davies, R. L., Gaztelu, A., & Fritz, A. 2002a, MNRAS, 337, 256

Balogh, M. L., Baldry, I. K., Nichol, R., Miller, C., Bower, R., & Glazebrook, K. 2004, ApJ, 615, L101

Balogh, M. L., McGee, S. L., Mok, A., Wilman, D. J., Finoguenov, A., Bower, R. G., Mulchaey, J. S., Parker, L. C., & Tanaka, M. 2014, MNRAS, 443, 2679

Balogh, M. L. & Morris, S. L. 2000, MNRAS, 318, 703

Balogh, M. L., Morris, S. L., Yee, H. K. C., Carlberg, R. G., & Ellingson, E. 1999, ApJ, 527, 54

Balogh, M. L., Navarro, J. F., & Morris, S. L. 2000, ApJ, 540, 113

Balogh, M. L., Smail, I., Bower, R. G., Ziegler, B. L., Smith, G. P., Davies, R. L., Gaztelu, A., Kneib, J.-P., & Ebeling, H. 2002b, ApJ, 566, 123

Bamford, S. P., Nichol, R. C., Baldry, I. K., Land, K., Lintott, C. J., Schawinski, K., Slosar, A., Szalay, A. S., Thomas, D., Torki, M., Andreescu, D., Edmondson, E. M., Miller, C. J., Murray, P., Raddick, M. J., & Vandenberg, J. 2009, MNRAS, 393, 1324

Barnes, J. E. 1989, Nature, 338, 123

Bekki, K. & Couch, W. J. 2011, MNRAS, 415, 1783

Birkinshaw, M. 1999, Phys. Rep., 310, 97

Birnboim, Y. & Dekel, A. 2003, MNRAS, 345, 349

Biviano, A., Katgert, P., Thomas, T., & Adami, C. 2002, A&A, 387, 8

Blanton, M. R. & Berlind, A. A. 2007, ApJ, 664, 791

Bluck, A. F. L., Mendel, J. T., Ellison, S. L., Moreno, J., Simard, L., Patton, D. R., & Starkenburg, E. 2014, MNRAS, 441, 599

Bongiorno, A., Schulze, A., Merloni, A., Zamorani, G., Ilbert, O., La Franca, F., Peng, Y., Piconcelli, E., Mainieri, V., Silverman, J. D., Brusa, M., Fiore, F., Salvato, M., & Scoville, N. 2016, A&A, 588, A78

Boselli, A. & Gavazzi, G. 2006, PASP, 118, 517

Boselli, A., Lequeux, J., & Gavazzi, G. 2002, A&A, 384, 33

Bundy, K., Scarlata, C., Carollo, C. M., Ellis, R. S., Drory, N., Hopkins, P., Salvato, M., Leauthaud, A., Koekemoer, A. M., Murray, N., Ilbert, O., Oesch, P., Ma, C.-P., Capak, P., Pozzetti, L., & Scoville, N. 2010, ApJ, 719, 1969

Butcher, H. & Oemler, Jr., A. 1978, ApJ, 219, 18

—. 1984, ApJ, 285, 426

Carlstrom, J. E., Holder, G. P., & Reese, E. D. 2002, ARA&A, 40, 643

Carollo, C. M., Cibinel, A., Lilly, S. J., Miniati, F., Norberg, P., Silverman, J. D., van Gorkom, J., Cameron, E., Finoguenov, A., Peng, Y., Pipino, A., & Rudick, C. S. 2013, ApJ, 776, 71

Cattaneo, A., Dekel, A., Devriendt, J., Guiderdoni, B., & Blaizot, J. 2006, MNRAS, 370, 1651

Chandrasekhar, S. 1943, ApJ, 97, 255

Christlein, D. & Zabludoff, A. I. 2004, ApJ, 616, 192

Chung, A., van Gorkom, J. H., Kenney, J. D. P., Crowl, H., & Vollmer, B. 2009, AJ, 138, 1741

Chung, A., van Gorkom, J. H., Kenney, J. D. P., & Vollmer, B. 2007, ApJ, 659, L115

Coenda, V., Muriel, H., & Martínez, H. J. 2012, A&A, 543, A119

—. 2015, A&A, 573, A96

Colless, M., Dalton, G., Maddox, S., Sutherland, W., Norberg, P., Cole, S., Bland-Hawthorn, J., Bridges, T., Cannon, R., Collins, C., Couch, W., Cross, N., Deeley, K., De Propris, R., Driver, S. P., Efstathiou, G., Ellis, R. S., Frenk, C. S., Glazebrook, K., Jackson, C., Lahav, O., Lewis, I., Lumsden,

S., Madgwick, D., Peacock, J. A., Peterson, B. A., Price, I., Seaborne, M., & Taylor, K. 2001, MNRAS, 328, 1039

Connelly, J. L., Wilman, D. J., Finoguenov, A., Hou, A., Mulchaey, J. S., McGee, S. L., Balogh, M. L., Parker, L. C., Saglia, R., Henderson, R. D. E., & Bower, R. G. 2012, ApJ, 756, 139

Cooper, M. C., Newman, J. A., Weiner, B. J., Yan, R., Willmer, C. N. A., Bundy, K., Coil, A. L., Conselice, C. J., Davis, M., Faber, S. M., Gerke, B. F., Guhathakurta, P., Koo, D. C., & Noeske, K. G. 2008, MNRAS, 383, 1058

Davies, L. J. M., Robotham, A. S. G., Driver, S. P., Alpaslan, M., Baldry, I. K., Bland-Hawthorn, J., Brough, S., Brown, M. J. I., Cluver, M. E., Drinkwater, M. J., Foster, C., Grootes, M. W., Konstantopoulos, I. S., Lara-López, M. A., López-Sánchez, Á. R., Loveday, J., Meyer, M. J., Moffett, A. J., Norberg, P., Owers, M. S., Popescu, C. C., De Propris, R., Sharp, R., Tuffs, R. J., Wang, L., Wilkins, S. M., Dunne, L., Bourne, N., & Smith, M. W. L. 2015, MNRAS, 452, 616

De Lucia, G., Weinmann, S., Poggianti, B. M., Aragón-Salamanca, A., & Zaritsky, D. 2012, MNRAS, 423, 1277

Dressler, A. 1980, ApJ, 236, 351

Dressler, A., Oemler, Jr., A., Couch, W. J., Smail, I., Ellis, R. S., Barger, A., Butcher, H., Poggianti, B. M., & Sharples, R. M. 1997, ApJ, 490, 577

Dressler, A., Oemler, Jr., A., Poggianti, B. M., Gladders, M. D., Abramson, L., & Vulcani, B. 2013, ApJ, 770, 62

Dubois, Y., Gavazzi, R., Peirani, S., & Silk, J. 2013, MNRAS, 433, 3297

Eke, V. R., Baugh, C. M., Cole, S., Frenk, C. S., King, H. M., & Peacock, J. A. 2005, MNRAS, 362, 1233

Ellingson, E., Lin, H., Yee, H. K. C., & Carlberg, R. G. 2001, ApJ, 547, 609

Ellison, S. L., Patton, D. R., Simard, L., & McConnachie, A. W. 2008, AJ, 135, 1877

Ellison, S. L., Teimoorinia, H., Rosario, D. J., & Mendel, J. T. 2016, MNRAS, 458, L34

Erfanianfar, G., Popesso, P., Finoguenov, A., Wilman, D., Wuyts, S., Biviano, A., Salvato, M., Mirkazemi, M., Morselli, L., Ziparo, F., Nandra, K., Lutz, D., Elbaz, D., Dickinson, M., Tanaka, M., Altieri, M. B., Aussel, H., Bauer, F., Berta, S., Bielby, R. M., Brandt, N., Cappelluti, N., Cimatti, A., Cooper, M. C., Fadda, D., Ilbert, O., Le Floch, E., Magnelli, B., Mulchaey, J. S., Nordon, R., Newman, J. A., Poglitsch, A., & Pozzi, F. 2016, MNRAS, 455, 2839

Fairley, B. W., Jones, L. R., Wake, D. A., Collins, C. A., Burke, D. J., Nichol, R. C., & Romer, A. K. 2002, MNRAS, 330, 755

Fasano, G., Poggianti, B. M., Bettoni, D., D'Onofrio, M., Dressler, A., Vulcani, B., Moretti, A., Gullieuszik, M., Fritz, J., Omizzolo, A., Cava, A., Couch, W. J., Ramella, M., & Biviano, A. 2015, MNRAS, 449, 3927

Fillingham, S. P., Cooper, M. C., Wheeler, C., Garrison-Kimmel, S., Boylan-Kolchin, M., & Bullock, J. S. 2015, MNRAS, 454, 2039

Freedman, W. L., Madore, B. F., Gibson, B. K., Ferrarese, L., Kelson, D. D., Sakai, S., Mould, J. R., Robert C. Kennicutt, J., Ford, H. C., Graham, J. A., Huchra, J. P., Hughes, S. M. G., Illingworth, G. D., Macri, L. M., & Stetson, P. B. 2001, The Astrophysical Journal, 553, 47

Fujita, Y. 1998, ApJ, 509, 587

Fumagalli, M., Krumholz, M. R., Prochaska, J. X., Gavazzi, G., & Boselli, A. 2009, ApJ, 697, 1811

Gabor, J. M. & Davé, R. 2015, MNRAS, 447, 374

Gabor, J. M., Davé, R., Oppenheimer, B. D., & Finlator, K. 2011, MNRAS, 417, 2676

Geller, M. J. & Huchra, J. P. 1983, ApJS, 52, 61

George, M. R., Leauthaud, A., Bundy, K., Finoguenov, A., Ma, C.-P., Rykoff, E. S., Tinker, J. L., Wechsler, R. H., Massey, R., & Mei, S. 2012, ApJ, 757, 2

Gerke, B. F., Newman, J. A., Davis, M., Coil, A. L., Cooper, M. C., Dutton, A. A., Faber, S. M., Guhathakurta, P., Konidaris, N., Koo, D. C., Lin, L., Noeske, K., Phillips, A. C., Rosario, D. J., Weiner, B. J., Willmer, C. N. A., & Yan, R. 2012, ApJ, 751, 50

Gerke, B. F., Newman, J. A., Davis, M., Marinoni, C., Yan, R., Coil, A. L., Conroy, C., Cooper, M. C., Faber, S. M., Finkbeiner, D. P., Guhathakurta, P., Kaiser, N., Koo, D. C., Phillips, A. C., Weiner, B. J., & Willmer, C. N. A. 2005, ApJ, 625, 6

Gill, S. P. D., Knebe, A., & Gibson, B. K. 2005, MNRAS, 356, 1327

Gladders, M. D. & Yee, H. K. C. 2000, AJ, 120, 2148

Goto, T., Yamauchi, C., Fujita, Y., Okamura, S., Sekiguchi, M., Smail, I., Bernardi, M., & Gomez, P. L. 2003, MNRAS, 346, 601

Governato, F., Bhatia, R., & Chincarini, G. 1991, ApJ, 371, L15

Grützbauch, R., Chuter, R. W., Conselice, C. J., Bauer, A. E., Bluck, A. F. L., Buitrago, F., & Mortlock, A. 2011, MNRAS, 412, 2361

Gunn, J. E. & Gott, III, J. R. 1972, ApJ, 176, 1

Gürkan, G., Hardcastle, M. J., Jarvis, M. J., Smith, D. J. B., Bourne, N., Dunne, L., Maddox, S., Ivison, R. J., & Fritz, J. 2015, MNRAS, 452, 3776

Haines, C. P., Pereira, M. J., Smith, G. P., Egami, E., Babul, A., Finoguenov, A., Ziparo, F., McGee, S. L., Rawle, T. D., Okabe, N., & Moran, S. M. 2015, ApJ, 806, 101

Hamilton, D. 1985, ApJ, 297, 371

Hansen, S. M., Sheldon, E. S., Wechsler, R. H., & Koester, B. P. 2009, ApJ, 699, 1333

Hickson, P. 1982, ApJ, 255, 382

Hinshaw, G., Spergel, D. N., Verde, L., Hill, R. S., Meyer, S. S., Barnes, C., Bennett, C. L., Halpern, M., Jarosik, N., Kogut, A., Komatsu, E., Limon, M., Page, L., Tucker, G. S., Weiland, J. L., Wollack, E., & Wright, E. L. 2003, ApJS, 148, 135

Hou, A., Parker, L. C., Balogh, M. L., McGee, S. L., Wilman, D. J., Connelly, J. L., Harris, W. E., Mok, A., Mulchaey, J. S., Bower, R. G., & Finoguenov, A. 2013, MNRAS, 435, 1715

Hou, A., Parker, L. C., & Harris, W. E. 2014, MNRAS, 442, 406

Hoyle, B., Masters, K. L., Nichol, R. C., Jimenez, R., & Bamford, S. P. 2012, MNRAS, 423, 3478

Hubble, E. 1929, PNAS, 15, 168

Hubble, E. & Humason, M. L. 1931, ApJ, 74, 43

Hubble, E. P. 1925, Popular Astronomy, 33

—. 1926, ApJ, 64

Huchra, J. P. & Geller, M. J. 1982, ApJ, 257, 423

Joshi, G. D., Parker, L. C., & Wadsley, J. 2016, MNRAS, accepted

Karim, A., Schinnerer, E., Martínez-Sansigre, A., Sargent, M. T., van der Wel, A., Rix, H.-W., Ilbert, O., Smolčić, V., Carilli, C., Pannella, M., Koekemoer, A. M., Bell, E. F., & Salvato, M. 2011, ApJ, 730, 61

Kenney, J. D. P., Abramson, A., & Bravo-Alfaro, H. 2015, AJ, 150, 59

Kenney, J. D. P., van Gorkom, J. H., & Vollmer, B. 2004, AJ, 127, 3361

Kennicutt, R. C. & Evans, N. J. 2012, ARA&A, 50, 531

Khosroshahi, H. G., Gozaliasl, G., Rasmussen, J., Molaeinezhad, A., Ponman, T., Dariush, A. A., & Sanderson, A. J. R. 2014, MNRAS, 443, 318

Kimm, T., Somerville, R. S., Yi, S. K., van den Bosch, F. C., Salim, S., Fontanot, F., Monaco, P., Mo, H., Pasquali, A., Rich, R. M., & Yang, X. 2009, MNRAS, 394, 1131

Klypin, A. A., Trujillo-Gomez, S., & Primack, J. 2011, ApJ, 740, 102

Lanzuisi, G., Ranalli, P., Georgantopoulos, I., Georgakakis, A., Delvecchio, I., Akylas, T., Berta, S., Bongiorno, A., Brusa, M., Cappelluti, N., Civano, F., Comastri, A., Gilli, R., Gruppioni, C., Hasinger, G., Iwasawa, K., Koekemoer, A., Lusso, E., Marchesi, S., Mainieri, V., Merloni, A., Mignoli, M., Piconcelli, E., Pozzi, F., Rosario, D. J., Salvato, M., Silverman, J., Trakhtenbrot, B., Vignali, C., & Zamorani, G. 2015, A&A, 573, A137

Larson, R. B., Tinsley, B. M., & Caldwell, C. N. 1980, ApJ, 237, 692

Lee, N., Sanders, D. B., Casey, C. M., Toft, S., Scoville, N. Z., Hung, C.-L., Le Floc'h, E., Ilbert, O., Zahid, H. J., Aussel, H., Capak, P., Kartaltepe, J. S., Kewley, L. J., Li, Y., Schawinski, K., Sheth, K., & Xiao, Q. 2015, ApJ, 801, 80

Li, I. H., Yee, H. K. C., & Ellingson, E. 2009, ApJ, 698, 83

Lintott, C. J., Schawinski, K., Slosar, A., Land, K., Bamford, S., Thomas, D., Raddick, M. J., Nichol, R. C., Szalay, A., Andreescu, D., Murray, P., & Vandenberg, J. 2008, MNRAS, 389, 1179

Loh, Y.-S., Ellingson, E., Yee, H. K. C., Gilbank, D. G., Gladders, M. D., & Barrientos, L. F. 2008, ApJ, 680, 214

Lopes, P. A. A., Ribeiro, A. L. B., & Rembold, S. B. 2014, MNRAS, 437, 2430

Lotz, J. M., Jonsson, P., Cox, T. J., Croton, D., Primack, J. R., Somerville, R. S., & Stewart, K. 2011, ApJ, 742, 103

Madau, P. & Dickinson, M. 2014, ARA&A, 52, 415

Madau, P., Pozzetti, L., & Dickinson, M. 1998, ApJ, 498, 106

Mahajan, S., Mamon, G. A., & Raychaudhury, S. 2011, MNRAS, 416, 2882

Mamon, G. 2007, Groups of Galaxies in the Nearby Universe: Proceedings of the ESO Workshop held at Santiago de Chile, ed. I. Saviane, V. D. Ivanov, & J. Borissova (Berlin, Heidelberg: Springer Berlin Heidelberg), 203–219

Marinoni, C., Davis, M., Newman, J. A., & Coil, A. L. 2002, ApJ, 580, 122

Mather, J. C., Cheng, E. S., Eplee, Jr., R. E., Isaacman, R. B., Meyer, S. S., Shafer, R. A., Weiss, R., Wright, E. L., Bennett, C. L., Boggess, N. W., Dwek, E., Gulkis, S., Hauser, M. G., Janssen, M., Kelsall, T., Lubin, P. M., Moseley, Jr., S. H., Murdock, T. L., Silverberg, R. F., Smoot, G. F., & Wilkinson, D. T. 1990, ApJ, 354, L37

Mayer, L., Mastropietro, C., Wadsley, J., Stadel, J., & Moore, B. 2006, MNRAS, 369, 1021

McConnachie, A. W., Patton, D. R., Ellison, S. L., & Simard, L. 2009, MNRAS, 395, 255

McGee, S. L., Balogh, M. L., Bower, R. G., Font, A. S., & McCarthy, I. G. 2009, MNRAS, 400, 937

McGee, S. L., Balogh, M. L., Wilman, D. J., Bower, R. G., Mulchaey, J. S., Parker, L. C., & Oemler, A. 2011, MNRAS, 413, 996

Mihos, J. C. & Hernquist, L. 1994a, ApJ, 425, L13

—. 1994b, ApJ, 431, L9

Mo, H., van den Bosch, F., & White, S. 2010, Galaxy Formation and Evolution, Galaxy Formation and Evolution (Cambridge University Press)

Moore, B., Katz, N., Lake, G., Dressler, A., & Oemler, A. 1996, Nature, 379, 613

Mullaney, J. R., Alexander, D. M., Aird, J., Bernhard, E., Daddi, E., Del Moro, A., Dickinson, M., Elbaz, D., Harrison, C. M., Juneau, S., Liu, D., Pannella, M., Rosario, D., Santini, P., Sargent, M., Schreiber, C., Simpson, J., & Stanley, F. 2015, MNRAS, 453, L83

Muzzin, A., van der Burg, R. F. J., McGee, S. L., Balogh, M., Franx, M., Hoekstra, H., Hudson, M. J., Noble, A., Taranu, D. S., Webb, T., Wilson, G., & Yee, H. K. C. 2014, ApJ, 796, 65

Nair, P. B. & Abraham, R. G. 2010, ApJS, 186, 427

Nantais, J. B., Rettura, A., Lidman, C., Demarco, R., Gobat, R., Rosati, P., & Jee, M. J. 2013, A&A, 556, A112

Navarro, J. F., Frenk, C. S., & White, S. D. M. 1997, ApJ, 490, 493

Newman, J. A., Cooper, M. C., Davis, M., Faber, S. M., Coil, A. L., Guhathakurta, P., Koo, D. C., Phillips, A. C., Conroy, C., Dutton, A. A., Finkbeiner, D. P., Gerke, B. F., Rosario, D. J., Weiner, B. J., Willmer, C. N. A., Yan, R., Harker, J. J., Kassin, S. A., Konidaris, N. P., Lai, K., Madgwick, D. S., Noeske, K. G., Wirth, G. D., Connolly, A. J., Kaiser, N., Kirby, E. N., Lemaux, B. C., Lin, L., Lotz, J. M., Luppino, G. A., Marinoni, C., Matthews, D. J., Metevier, A., & Schiavon, R. P. 2013, ApJS, 208, 5

Noble, A. G., Webb, T. M. A., Yee, H. K. C., Muzzin, A., Wilson, G., van der Burg, R. F. J., Balogh, M. L., & Shupe, D. L. 2016, ApJ, 816, 48

Nolthenius, R. & White, S. D. M. 1987, MNRAS, 225, 505

Oliver, S., Frost, M., Farrah, D., Gonzalez-Solares, E., Shupe, D. L., Henriques, B., Roseboom, I., Alfonso-Luis, A., Babbedge, T. S. R., Frayer, D., Lencz, C., Lonsdale, C. J., Masci, F., Padgett, D., Polletta, M., Rowan-Robinson, M., Siana, B., Smith, H. E., Surace, J. A., & Vaccari, M. 2010, MNRAS, 405, 2279

Opik, E. 1922, ApJ, 55

Peng, Y., Maiolino, R., & Cochrane, R. 2015, Nature, 521, 192

Peng, Y.-j., Lilly, S. J., Kovač, K., Bolzonella, M., Pozzetti, L., Renzini, A., Zamorani, G., Ilbert, O., Knobel, C., Iovino, A., Maier, C., Cucciati, O., Tasca, L., Carollo, C. M., Silverman, J., Kampczyk, P., de Ravel, L., Sanders, D., Scoville, N., Contini, T., Mainieri, V., Scodeggio, M., Kneib, J.-P., Le Fèvre, O., Bardelli, S., Bongiorno, A., Caputi, K., Coppa, G., de la Torre, S., Franzetti, P., Garilli, B., Lamareille, F., Le Borgne, J.-F., Le Brun, V., Mignoli, M., Perez Montero, E., Pello, R., Ricciardelli, E., Tanaka, M., Tresse, L., Vergani, D., Welikala, N., Zucca, E., Oesch, P., Abbas, U., Barnes, L., Bordoloi, R., Bottini, D., Cappi, A., Cassata, P., Cimatti, A., Fumana, M., Hasinger, G., Koekemoer, A., Leauthaud, A., Maccagni, D., Marinoni, C., McCracken, H., Memeo, P., Meneux, B., Nair, P., Porciani, C., Presotto, V., & Scaramella, R. 2010, ApJ, 721, 193

Penzias, A. A. & Wilson, R. W. 1965, ApJ, 142, 419

Planck Collaboration, Ade, P. A. R., Aghanim, N., Armitage-Caplan, C., Arnaud, M., Ashdown, M., Atrio-Barandela, F., Aumont, J., Baccigalupi, C., Banday, A. J., & et al. 2014, A&A, 571, A16

Planck Collaboration, Ade, P. A. R., Aghanim, N., Arnaud, M., Ashdown, M., Aumont, J., Baccigalupi, C., Balbi, A., Banday, A. J., Barreiro, R. B., & et al. 2011, A&A, 536, A8

Planck Collaboration, Ade, P. A. R., Aghanim, N., Arnaud, M., Ashdown, M., Aumont, J., Baccigalupi, C., Banday, A. J., Barreiro, R. B., Barrena, R., & et al. 2015, ArXiv e-prints

Ponman, T. J., Allan, D. J., Jones, L. R., Merrifield, M., McHardy, I. M., Lehto, H. J., & Luppino, G. A. 1994, Nature, 369, 462

Ponman, T. J. & Bertram, D. 1993, Nature, 363, 51

Postman, M., Franx, M., Cross, N. J. G., Holden, B., Ford, H. C., Illingworth, G. D., Goto, T., Demarco, R., Rosati, P., Blakeslee, J. P., Tran, K.-V., Benítez, N., Clampin, M., Hartig, G. F., Homeier, N., Ardila, D. R., Bartko, F., Bouwens, R. J., Bradley, L. D., Broadhurst, T. J., Brown, R. A., Burrows, C. J., Cheng, E. S., Feldman, P. D., Golimowski, D. A., Gronwall, C., Infante, L., Kimble, R. A., Krist, J. E., Lesser, M. P., Martel, A. R., Mei, S., Menanteau, F., Meurer, G. R., Miley, G. K., Motta, V., Sirianni, M., Sparks, W. B., Tran, H. D., Tsvetanov, Z. I., White, R. L., & Zheng, W. 2005, ApJ, 623, 721

Prescott, M., Baldry, I. K., James, P. A., Bamford, S. P., Bland-Hawthorn, J., Brough, S., Brown, M. J. I., Cameron, E., Conselice, C. J., Croom, S. M., Driver, S. P., Frenk, C. S., Gunawardhana, M., Hill, D. T., Hopkins, A. M., Jones, D. H., Kelvin, L. S., Kuijken, K., Liske, J., Loveday, J., Nichol, R. C., Norberg, P., Parkinson, H. R., Peacock, J. A., Phillipps, S., Pimbblet, K. A., Popescu, C. C., Robotham, A. S. G., Sharp, R. G., Sutherland, W. J., Taylor, E. N., Tuffs, R. J., van Kampen, E., & Wijesinghe, D. 2011, MNRAS, 417, 1374

Presotto, V., Iovino, A., Scodeggio, M., Cucciati, O., Knobel, C., Bolzonella, M., Oesch, P., Finoguenov, A., Tanaka, M., Kovač, K., Peng, Y., Zamorani, G., Bardelli, S., Pozzetti, L., Kampczyk, P., López-Sanjuan, C., Vergani,

D., Zucca, E., Tasca, L. A. M., Carollo, C. M., Contini, T., Kneib, J.-P., Le Fèvre, O., Lilly, S., Mainieri, V., Renzini, A., Bongiorno, A., Caputi, K., de la Torre, S., de Ravel, L., Franzetti, P., Garilli, B., Lamareille, F., Le Borgne, J.-F., Le Brun, V., Maier, C., Mignoli, M., Pellò, R., Perez-Montero, E., Ricciardelli, E., Silverman, J. D., Tresse, L., Barnes, L., Bordoloi, R., Cappi, A., Cimatti, A., Coppa, G., Koekemoer, A. M., McCracken, H. J., Moresco, M., Nair, P., & Welikala, N. 2012, A&A, 539, A55

Press, W. H. & Davis, M. 1982, ApJ, 259, 449

Press, W. H. & Schechter, P. 1974, ApJ, 187, 425

Quilis, V., Moore, B., & Bower, R. 2000, Science, 288, 1617

Rasmussen, J., Mulchaey, J. S., Bai, L., Ponman, T. J., Raychaudhury, S., & Dariush, A. 2012, ApJ, 757, 122

Ribeiro, A. L. B., de Carvalho, R. R., Trevisan, M., Capelato, H. V., La Barbera, F., Lopes, P. A. A., & Schilling, A. C. 2013a, MNRAS, 434, 784

Ribeiro, A. L. B., Lopes, P. A. A., & Rembold, S. B. 2013b, A&A, 556, A74

Ribeiro, A. L. B., Lopes, P. A. A., & Trevisan, M. 2010, MNRAS, 409, L124

Roberts, I. D. & Parker, L. C. submitted, MNRAS

Roberts, I. D., Parker, L. C., Joshi, G. D., & Evans, F. A. 2015, MNRAS, 448, L1

Roberts, I. D., Parker, L. C., & Karunakaran, A. 2016, MNRAS, 455, 3628

Roediger, E. & Hensler, G. 2005, A&A, 433, 875

Santini, P., Rosario, D. J., Shao, L., Lutz, D., Maiolino, R., Alexander, D. M., Altieri, B., Andreani, P., Aussel, H., Bauer, F. E., Berta, S., Bongiovanni, A., Brandt, W. N., Brusa, M., Cepa, J., Cimatti, A., Daddi, E., Elbaz, D., Fontana, A., Förster Schreiber, N. M., Genzel, R., Grazian, A., Le Floc'h, E., Magnelli, B., Mainieri, V., Nordon, R., Pérez Garcia, A. M., Poglitsch, A., Popesso, P., Pozzi, F., Riguccini, L., Rodighiero, G., Salvato, M., Sanchez-Portal, M., Sturm, E., Tacconi, L. J., Valtchanov, I., & Wuyts, S. 2012, A&A, 540, A109

Santos, W. A., Mendes de Oliveira, C., & Sodré, Jr., L. 2007, AJ, 134, 1551

Schawinski, K., Urry, C. M., Simmons, B. D., Fortson, L., Kaviraj, S., Keel, W. C., Lintott, C. J., Masters, K. L., Nichol, R. C., Sarzi, M., Skibba, R., Treister, E., Willett, K. W., Wong, O. I., & Yi, S. K. 2014, MNRAS, 440, 889

Scoville, N., Aussel, H., Brusa, M., Capak, P., Carollo, C. M., Elvis, M., Giavalisco, M., Guzzo, L., Hasinger, G., Impey, C., Kneib, J.-P., LeFevre, O., Lilly, S. J., Mobasher, B., Renzini, A., Rich, R. M., Sanders, D. B., Schinnerer, E., Schminovich, D., Shopbell, P., Taniguchi, Y., & Tyson, N. D. 2007, ApJS, 172, 1

Sersic, J. L. 1968, Atlas de galaxias australes (Observatorio Astronomico, Universidad Nacional de Cordoba)

Simard, L., Willmer, C. N. A., Vogt, N. P., Sarajedini, V. L., Phillips, A. C., Weiner, B. J., Koo, D. C., Im, M., Illingworth, G. D., & Faber, S. M. 2002, ApJS, 142, 1

Sivanandam, S., Rieke, M. J., & Rieke, G. H. 2014, ApJ, 796, 89

Slipher, V. M. 1917, The Observatory, 40, 304

Somerville, R. S., Hopkins, P. F., Cox, T. J., Robertson, B. E., & Hernquist, L. 2008, MNRAS, 391, 481

Springel, V., White, S. D. M., Jenkins, A., Frenk, C. S., Yoshida, N., Gao, L., Navarro, J., Thacker, R., Croton, D., Helly, J., Peacock, J. A., Cole, S., Thomas, P., Couchman, H., Evrard, A., Colberg, J., & Pearce, F. 2005, Nature, 435, 629

Stanley, F., Harrison, C. M., Alexander, D. M., Swinbank, A. M., Aird, J. A., Del Moro, A., Hickox, R. C., & Mullaney, J. R. 2015, MNRAS, 453, 591

Steinhauser, D., Schindler, S., & Springel, V. 2016, ArXiv e-prints

Sunyaev, R. A. & Zeldovich, Y. B. 1970, Ap&SS, 7, 3

Trayford, J. W., Theuns, T., Bower, R. G., Crain, R. A., Lagos, C. d. P., Schaller, M., & Schaye, J. 2016, ArXiv e-prints

Ulmer, M. P., Adami, C., Covone, G., Durret, F., Lima Neto, G. B., Sabirli, K., Holden, B., Kron, R. G., & Romer, A. K. 2005, ApJ, 624, 124

Urquhart, S. A., Willis, J. P., Hoekstra, H., & Pierre, M. 2010, MNRAS, 406, 368

van den Bosch, F. C., Pasquali, A., Yang, X., Mo, H. J., Weinmann, S., McIntosh, D. H., & Aquino, D. 2008, ArXiv e-prints

van der Wel, A. 2008, ApJ, 675, L13

von der Linden, A., Wild, V., Kauffmann, G., White, S. D. M., & Weinmann, S. 2010, MNRAS, 404, 1231

Vulcani, B., Poggianti, B. M., Oemler, A., Dressler, A., Aragón-Salamanca, A., De Lucia, G., Moretti, A., Gladders, M., Abramson, L., & Halliday, C. 2013, A&A, 550, A58

Wake, D. A., Collins, C. A., Nichol, R. C., Jones, L. R., & Burke, D. J. 2005, ApJ, 627, 186

Walcher, J., Groves, B., Budavári, T., & Dale, D. 2011, Ap&SS, 331, 1

Wang, L., Yang, X., Shen, S., Mo, H. J., van den Bosch, F. C., Luo, W., Wang, Y., Lau, E. T., Wang, Q. D., Kang, X., & Li, R. 2014, MNRAS, 439, 611

Wetzel, A. R., Tinker, J. L., & Conroy, C. 2012, MNRAS, 424, 232

Wetzel, A. R., Tinker, J. L., Conroy, C., & van den Bosch, F. C. 2013, MNRAS, 432, 336

Wetzel, A. R., Tollerud, E. J., & Weisz, D. R. 2015, ApJ, 808, L27

Wheeler, C., Phillips, J. I., Cooper, M. C., Boylan-Kolchin, M., & Bullock, J. S. 2014, MNRAS, 442, 1396

Whitaker, K. E., van Dokkum, P. G., Brammer, G., & Franx, M. 2012, ApJ, 754, L29

Whitmore, B. C., Gilmore, D. M., & Jones, C. 1993, ApJ, 407, 489

Wilman, D. J., Balogh, M. L., Bower, R. G., Mulchaey, J. S., Oemler, A., Carlberg, R. G., Eke, V. R., Lewis, I., Morris, S. L., & Whitaker, R. J. 2005, MNRAS, 358, 88

Wilman, D. J. & Erwin, P. 2012, ApJ, 746, 160

Yang, X., Mo, H. J., van den Bosch, F. C., & Jing, Y. P. 2005, MNRAS, 356, 1293

Yang, X., Mo, H. J., van den Bosch, F. C., Pasquali, A., Li, C., & Barden, M. 2007, ApJ, 671, 153

York, D. G., Adelman, J., Anderson, Jr., J. E., Anderson, S. F., Annis, J., Bahcall, N. A., Bakken, J. A., Barkhouser, R., Bastian, S., Berman, E., Boroski, W. N., Bracker, S., Briegel, C., Briggs, J. W., Brinkmann, J., Brunner, R., Burles, S., Carey, L., Carr, M. A., Castander, F. J., Chen, B., Colestock, P. L., Connolly, A. J., Crocker, J. H., Csabai, I., Czarapata, P. C., Davis, J. E., Doi, M., Dombeck, T., Eisenstein, D., Ellman, N., Elms, B. R., Evans, M. L., Fan, X., Federwitz, G. R., Fiscelli, L., Friedman, S., Frieman, J. A., Fukugita, M., Gillespie, B., Gunn, J. E., Gurbani, V. K., de Haas, E., Haldeman, M., Harris, F. H., Hayes, J., Heckman, T. M., Hennessy, G. S., Hindsley, R. B., Holm, S., Holmgren, D. J., Huang, C.-h., Hull, C., Husby, D., Ichikawa, S.-I., Ichikawa, T., Ivezić, Ž., Kent, S., Kim, R. S. J., Kinney, E., Klaene, M., Kleinman, A. N., Kleinman, S., Knapp, G. R., Korienek, J., Kron, R. G., Kunszt, P. Z., Lamb, D. Q., Lee, B., Leger, R. F., Limmongkol, S., Lindenmeyer, C., Long, D. C., Loomis, C., Loveday, J., Lucinio, R., Lupton, R. H., MacKinnon, B., Mannery, E. J., Mantsch, P. M., Margon, B.,

McGehee, P., McKay, T. A., Meiksin, A., Merelli, A., Monet, D. G., Munn, J. A., Narayanan, V. K., Nash, T., Neilsen, E., Neswold, R., Newberg, H. J., Nichol, R. C., Nicinski, T., Nonino, M., Okada, N., Okamura, S., Ostriker, J. P., Owen, R., Pauls, A. G., Peoples, J., Peterson, R. L., Petravick, D., Pier, J. R., Pope, A., Pordes, R., Prosapio, A., Rechenmacher, R., Quinn, T. R., Richards, G. T., Richmond, M. W., Rivetta, C. H., Rockosi, C. M., Ruthmansdorfer, K., Sandford, D., Schlegel, D. J., Schneider, D. P., Sekiguchi, M., Sergey, G., Shimasaku, K., Siegmund, W. A., Smee, S., Smith, J. A., Snedden, S., Stone, R., Stoughton, C., Strauss, M. A., Stubbs, C., SubbaRao, M., Szalay, A. S., Szapudi, I., Szokoly, G. P., Thakar, A. R., Tremonti, C., Tucker, D. L., Uomoto, A., Vanden Berk, D., Vogeley, M. S., Waddell, P., Wang, S.-i., Watanabe, M., Weinberg, D. H., Yanny, B., Yasuda, N., & SDSS Collaboration. 2000, AJ, 120, 1579

Ziparo, F., Popesso, P., Biviano, A., Finoguenov, A., Wuyts, S., Wilman, D., Salvato, M., Tanaka, M., Ilbert, O., Nandra, K., Lutz, D., Elbaz, D., Dickinson, M., Altieri, B., Aussel, H., Berta, S., Cimatti, A., Fadda, D., Genzel, R., Le Flo'ch, E., Magnelli, B., Nordon, R., Poglitsch, A., Pozzi, F., Portal, M. S., Tacconi, L., Bauer, F. E., Brandt, W. N., Cappelluti, N., Cooper, M. C., & Mulchaey, J. S. 2013, MNRAS, 434, 3089

Chapter 2

Mass segregation trends in SDSS galaxy groups

This chapter represents an unchanged version of the paper, "*Mass-segregation trends in SDSS galaxy groups*", published in the refereed journal, *Monthly Notices of the Royal Astronomical Society Letters*. The full reference is given below:

Roberts I.D., Parker L.C., Joshi G.D., Evans F.A., 2015,

MNRAS, Volume 448, Issue 1, pp. L1-L5

Department of Physics & Astronomy, McMaster University, Hamilton ON L8S 4M1, Canada

Abstract

It has been shown that galaxy properties depend strongly on their host environment. In order to understand the relevant physical processes driving galaxy evolution it is important to study the observed properties of galaxies in different environments. Mass segregation in bound galaxy structures is an important indicator of evolutionary history and dynamical friction time-scales. Using group catalogues derived from the Sloan Digital Sky Survey Data Release 7 (SDSS DR7), we investigate mass-segregation trends in galaxy groups at low redshift. We investigate average galaxy stellar mass as a function of group-centric radius and find evidence for weak mass segregation in SDSS groups. The magnitude of the mass segregation depends on both galaxy stellar mass limits and group halo mass. We show that the inclusion of low-mass galaxies tends to strengthen mass-segregation trends, and that the strength of mass segregation tends to decrease with increasing group halo mass. We find the same trends if we use the fraction of massive galaxies as a function of group-centric radius as an alternative probe of mass segregation. The magnitude of mass segregation that we measure, particularly in high-mass haloes, indicates that dynamical friction is not acting efficiently.

2.1 Introduction

It has been well established that galaxy properties depend strongly on local environment (e.g. Oemler, 1974; Hogg et al., 2004; Blanton et al., 2005a; Tal et al., 2014). Galaxies in dense environments such as clusters tend to have lower star formation rates (SFRs), while isolated field galaxies are generally actively forming stars (e.g. Balogh et al., 2000; Ball et al., 2008; Wetzel et al., 2012). It is also well known that galaxy properties, such as SFR, depend strongly on galaxy mass (e.g. Poggianti et al., 2008). It is critical to study the distribution of galaxy masses within haloes of different masses in order to ascertain whether the variations in galaxy properties with environment are due to physical mechanisms acting in dense environments, or simply due to the fact that high-density environments contain more high-mass galaxies. Intermediate-density environments, galaxy groups, represent not only the most common environment in the local Universe (Geller & Huchra, 1983; Eke et al., 2005), but also represent the environment where many physical processes are efficient. Galaxy interactions such as mergers and harassment are favoured in this environment because of the low relative velocities between galaxies (Zabludoff & Mulchaey, 1998; Brough et al., 2006).

The study of mass segregation in groups can be used to elucidate information on physical processes such as dynamical friction, galaxy mergers, and tidal stripping. Mass segregation in bound structures has generally been predicted as a result of dynamical friction (Chandrasekhar, 1943). Dynamical friction acts as a drag force on orbiting bodies and massive galaxies within groups and clusters are expected to migrate to smaller radii as time progresses. If

dynamical friction is a dominant factor, then clear mass segregation should be observed in evolved groups and clusters.

Galaxy groups are not static systems, but are constantly being replenished by infalling galaxies from the field. Infalling galaxies are preferentially found at large radii (Wetzel et al., 2013) and the difference in stellar mass distributions between evolved group members and infalling galaxies could affect the strength of mass segregation.

If significant mass segregation is not found, then this implies that either: the time-scale associated with dynamical friction is greater than the age of the group/cluster, or that there are other physical processes, such as merging, tidal stripping, or pre-processing, which are playing a more important role than dynamical friction.

Recent work has shown conflicting results with regards to the presence of mass segregation in groups and clusters. Ziparo et al. (2013) find no evidence for strong mass segregation in X-ray selected groups out to $z = 1.6$, for a sample of galaxies with $M_{\rm star} > 10^{10.3}\,{\rm M}_{\odot}$. von der Linden et al. (2010) examine Sloan Digital Sky Survey (SDSS) galaxy clusters and find no evidence for mass segregation in four different redshift bins at $z < 0.1$. von der Linden et al. make redshift-dependent stellar mass cuts ranging from $10^{9.6}$ to $10^{10.5}\,{\rm M}_{\odot}$. Vulcani et al. (2013) use mass-limited samples at $0.3 \leq z \leq 0.8$ from the IMACS Cluster Building Survey and the ESO Distant Cluster Survey, with stellar mass cuts at $M_{\rm star} > 10^{10.5}\,{\rm M}_{\odot}$ and $M_{\rm star} > 10^{10.2}\,{\rm M}_{\odot}$, respectively, to study galaxy stellar mass functions in different environments. Vulcani et al. find no

statistical differences between mass functions of galaxies located at different cluster-centric distances.

Conversely, Balogh et al. (2014) find evidence for mass segregation in Group Environment Evolution Collaboration 2 (GEEC2) groups at $0.8 < z < 1$, using a stellar-mass-limited sample with $M_{\rm star} > 10^{10.3}\,{\rm M}_{\odot}$. Using a volume limited sample of zCOSMOS groups, Presotto et al. (2012) find evidence for mass segregation in their whole sample at both $0.2 \leq z \leq 0.45$ and $0.45 \leq z \leq 0.8$. Presotto et al. also break their sample into rich and poor groups at $0.2 \leq z \leq 0.45$, and find evidence for mass segregation within rich groups but find no evidence for mass segregation within poor groups. Using a $V_{\rm max}$-weighted sample with a stellar mass cut at $10^{9.0}\,{\rm M}_{\odot}$, van den Bosch et al. (2008) find evidence for mass segregation in SDSS groups.

It is clear that there is no consensus regarding the strength of mass segregation in groups and clusters or its halo mass dependence.

In this Letter, we present evidence of the presence of a small, but significant, amount of mass segregation in SDSS galaxy groups. We show that the detection of mass segregation is dependent on stellar mass completeness, with completeness cuts at relatively high stellar masses potentially masking underlying mass segregation trends. We also show that the strength of mass segregation scales inversely with halo mass, with cluster-sized haloes showing little to no observable mass segregation. In Section 2.2, we briefly describe our data set, in Section 2.3 we present our results from this work, in Section 2.4 we provide a discussion of our results, and in Section 2.5 we give a summary of the results and make concluding statements.

In this Letter, we assume a flat Λ cold dark matter cosmology with $\Omega_M = 0.3$, $\Omega_\Lambda = 0.7$, and $H_0 = 70\,\mathrm{km\,s^{-1}\,Mpc^{-1}}$.

2.2 Data

The results presented in this Letter utilize the group catalogue of Yang et al. (2007). This catalogue is contructed by applying the halo-based group finder of Yang et al. (2005, 2007) to the New York University Value-Added Galaxy Catalogue (NYU-VAGC; Blanton et al. 2005b), which is based on the SDSS Data Release 7 (DR7; Abazajian et al. 2009). Stellar masses are obtained from the NYU-VAGC and are computed using the methodology of Blanton & Roweis (2007), assuming a Chabrier (2003) initial mass function. Halo masses are determined using the ranking of the characteristic stellar mass, $M_{\star,\mathrm{grp}}$, and assuming a relationship between M_{halo} and $M_{\star,\mathrm{grp}}$ (Yang et al., 2007). $M_{\star,\mathrm{grp}}$ is defined by Yang et al. as

$$M_{\star,\mathrm{grp}} = \frac{1}{g(L_{19.5},\, L_{\mathrm{lim}})} \sum_i \frac{M_{\mathrm{star},i}}{C_i}, \tag{2.1}$$

where $M_{\mathrm{star},i}$ is the stellar mass of the ith member galaxy, C_i is the completeness of the survey at the position of that galaxy, and $g(L_{19.5},\, L_{\mathrm{lim}})$ is a correction factor which accounts for galaxies missed due to the magnitude limit of the survey.

Halo-centric distance for each galaxy is not given explicitly in the Yang catalogue; however, we calculate it using the redshift of the group and the angular separation of the galaxy and halo centre on the sky. We measure

group-centric radius from the luminosity-weighted centre of each group, and normalize our group-centric radii by R_{200}. We use the definition for R_{200} as given in Carlberg et al. (1997)

$$R_{200} = \frac{\sqrt{3}\sigma}{10H(z)}, \tag{2.2}$$

where the Hubble parameter, $H(z)$, is defined as

$$H(z) = H_0\sqrt{\Omega_M(1+z)^3 + \Omega_\Lambda}, \tag{2.3}$$

and we calculate the velocity dispersion, σ, as

$$\sigma = 397.9\,\mathrm{km\,s^{-1}}\left(\frac{M_{\mathrm{halo}}}{10^{14}\,h^{-1}\,\mathrm{M_\odot}}\right)^{0.3214}, \tag{2.4}$$

where the above is a fitting function given in Yang et al. (2007).

For our analysis we select group galaxies with redshift, $z < 0.1$, that are within two virial radii of the group centre, and groups with a minimum of three galaxy members – although our results are not sensitive to these specific cuts. For our sample over 95 per cent of group galaxies reside within two virial radii of the group centre. We also subtract the most massive galaxy (MMG) from each group, to ensure that any underlying radial mass trend is not contaminated by the MMG.

This sample is not volume limited, therefore, the sample will suffer from the Malmquist bias. This leads to a bias towards objects of higher luminosity and stellar mass, with increasing redshift. To account for this bias we weight

our sample by $1/V_{\rm max}$, where $V_{\rm max}$ is the comoving volume of the Universe out to a comoving radius at which the galaxy would have met the selection criteria for the sample. For our $V_{\rm max}$ weights we apply the values presented in the catalogue of Simard et al. (2011) to our sample.

In order to investigate the effect of stellar mass limits on the detection of mass segregation, we use samples corresponding to various stellar mass cuts. We perform our analysis on an unweighted sample with two mass cuts corresponding to $M_{\rm star} > 10^{10.5}\,{\rm M}_{\odot}$ (4152 galaxies in 1970 groups) and $M_{\rm star} > 10^{10.0}\,{\rm M}_{\odot}$ (26 774 galaxies in 4534 groups); and a $V_{\rm max}$-weighted sample with mass cuts at $M_{\rm star} > 10^{9.0}\,{\rm M}_{\odot}$ (56 957 galaxies in 7217 groups) and $M_{\rm star} > 10^{8.5}\,{\rm M}_{\odot}$ (59 791 galaxies in 7289 groups). The unweighted sample is stellar mass complete down to $M_{\rm star} > 10^{10.0}\,{\rm M}_{\odot}$. Therefore, for both the weighted and unweighted sample, we have two different stellar mass cuts, giving us four separate samples in total.

2.3 Results

2.3.1 Mass segregation in SDSS groups

In Fig. 2.1 we plot mean stellar mass as a function of radial distance from the group centre for various halo mass bins. Fig 2.1(a) corresponds to our high-mass cut, unweighted sample; Fig 2.1(b) corresponds to our low-mass cut, unweighted sample; Fig 2.1(c) corresponds to our high-mass cut, weighted sample; and Fig 2.1(d) corresponds to our low-mass cut, weighted sample.

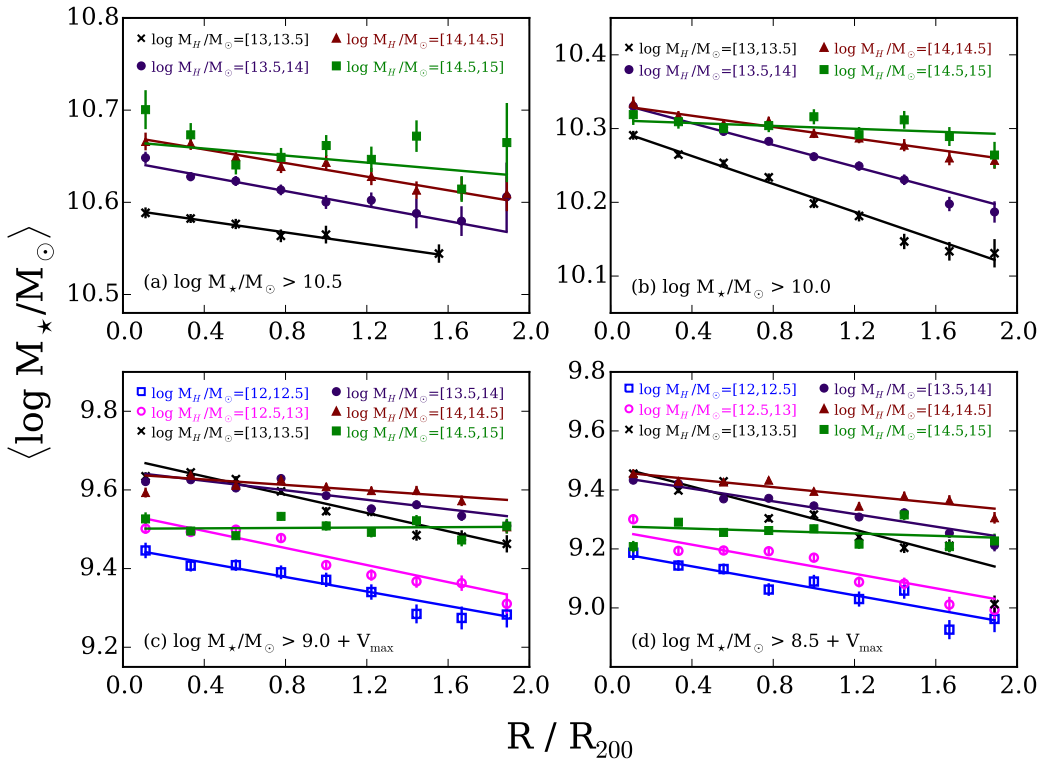

Figure 2.1: All panels show mean mass as a function of normalized distance for various halo mass bins, with error bars corresponding to 1σ statistical errors. The solid lines correspond to weighted least-squares fits for each halo mass bin. Top left: unweighted sample, for galaxies with $\log(M_{\rm star}/\,{\rm M}_\odot) > 10.5$. Top right: unweighted sample, for galaxies with $\log(M_{\rm star}/\,{\rm M}_\odot) > 10.0$. Bottom left: $V_{\rm max}$-weighted sample, for galaxies with $\log(M_{\rm star}/\,{\rm M}_\odot) > 9.0$. Bottom right: $V_{\rm max}$-weighted sample, for galaxies with $\log(M_{\rm star}/\,{\rm M}_\odot) > 8.5$. Note that different mass scales are used in each panel. There are more halo mass bins in the bottom row due to the increased number of low-mass galaxies as a result of $V_{\rm max}$ weighting.

For all halo mass bins, and regardless of the mass cut, the unweighted sample shows statistically significant mass segregation with a weighted linear least-squares fit. The $V_{\rm max}$-weighted sample shows statistically significant mass segregation for the five lower halo mass bins, whereas the highest halo mass bin has a best-fitting slope consistent with zero – this trend hold for both mass cuts. For both the weighted and unweighted samples there is a clear trend of the slope with halo mass – more massive haloes show weaker mass segregation. This result will be discussed in Section 2.4.

We find that our highest halo mass sample ($M_{\rm halo} > 10^{14.5}\,{\rm M}_{\odot}$) has a large number of low-mass galaxies when compared to the high-halo-mass samples, which leads to a smaller mean stellar mass in the $V_{\rm max}$-weighted results shown in Figs 2.1(c) and (d). While this introduces a shift in normalization, it does not affect the mass segregation trend and therefore does not change the key result that mass segregation depends on halo mass.

2.3.2 Massive galaxy fraction

An alternative way to investigate galaxy populations within the group sample is to study the fraction of 'massive' galaxies at various group-centric radii. In Fig. 2.2, we plot the fraction of massive galaxies as a function of radial distance for two different definitions of what constitutes a massive galaxy. We calculate the massive fraction for each radial bin as

$$f_m(M_{\rm cut}) = \frac{\#\text{ galaxies with } M_{\rm star} > M_{\rm cut}}{\#\text{ galaxies with } M_{\rm star} > 10^{10}\,{\rm M}_{\odot}}, \tag{2.5}$$

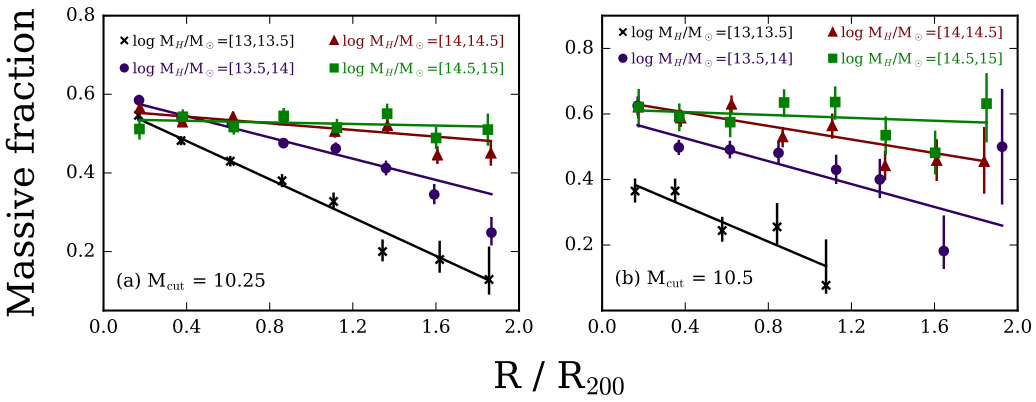

Figure 2.2: Fraction of massive galaxies with respect to normalized radial distance. Error bars are given by a 1σ binomial confidence interval, calculated using the beta distribution as outlined in Cameron (2011). The solid lines correspond to weighted least-squares fits for each halo mass bin. Left-hand panel: the fraction of galaxies with $\log(M_{\rm star}/\,{\rm M}_\odot) > 10.25$ as a function of radial distance, for the unweighted sample with $M_{\rm star} > 10^{10}\,{\rm M}_\odot$. Right-hand panel: the fraction of galaxies with $\log(M_{\rm star}/\,{\rm M}_\odot) > 10.5$ as a function of radial distance, for the unweighted sample with $M_{\rm star} > 10^{10}\,{\rm M}_\odot$.

where $M_{\rm cut}$ is a stellar mass cut-off above which we define a massive galaxy. We initially apply a high-mass galaxy cut, $M_{\rm cut}$, at $10^{10.25}\,{\rm M}_\odot$, corresponding to the median stellar mass of the unweighted sample (with the low-mass cut at $10^{10}\,{\rm M}_\odot$). Comparing Figs 2.1(b) and 2.2(a) we see essentially identical trends. We observe the same trends of mass segregation whether we look at the average galaxy mass at a given radius, or consider the fraction of massive galaxies.

To confirm that this trend is robust regardless of the mass cut-off used to define a massive galaxy, we make the same plot but now use $M_{\rm cut} = 10^{10.5}\,{\rm M}_\odot$. Comparing Figs 2.2(a) and (b) we see that while the overall fractions of massive galaxies decrease with increasing the stellar mass cut, the trend essentially stays the same. There is clear evidence for mass segregation and the strength of mass segregation depends on halo mass.

2.4 Discussion

2.4.1 Effect of including low-mass galaxies

The results in Fig. 2.1 show that mass segregation generally increases when lower mass galaxies are included. To quantify this effect we can compare the best-fitting slopes corresponding to the high-mass and the low-mass cut samples.

For a given halo mass, the low-mass cut sample displays larger slopes than the high-mass cut sample for two of the halo mass bins. The slopes corresponding to the other two halo mass bins are consistent with being equal. For the weighted samples we find similar results with the low-mass cut sample showing larger slopes for three of the halo mass bins, and the other three halo mass bins showing slopes consistent with being equal.

This suggests that the inclusion of low-mass galaxies has a measurable effect on the observation of mass-segregation. Studies which make mass cuts at moderate to high-stellar mass, are potentially missing a mass segregation contribution from low-mass galaxies. The observation of mild mass segregation is consistent with the low redshift sample of Ziparo et al. (2013); however, they see similar mass-radius relations regardless of the stellar mass cut applied.

2.4.2 Halo mass dependence

Figs 2.1 and 2.2 clearly indicate that the highest halo mass bins show the least mass segregation. This trend is consistent in all cases, regardless of

stellar mass cut or whether the sample had $V_{\rm max}$ weights applied. Our observed dependence on halo mass is consistent with results finding no measurable mass segregation in galaxy clusters (Pracy et al., 2005; von der Linden et al., 2010; Vulcani et al., 2013)

It has been shown through N-body simulations that the dynamical friction time-scale scales with M_h/M_s (e.g. Taffoni et al., 2003; Conroy et al., 2007; Boylan-Kolchin et al., 2008), where M_s is the initial satellite mass and M_h is the mass of the host halo. For a given satellite mass, this implies a longer dynamical friction time-scale for larger haloes, which is consistent with our result. This can be interpreted as an increase in tidal stripping efficiency as M_h/M_s increases (Taffoni et al., 2003). Gan et al. (2010) have shown that for an infalling satellite the dynamical friction time-scale increases with a stronger tidal field. This is due to tidal stripping retarding the decay of satellite angular momentum, which increases the dynamical friction time-scale.

It should be noted that the merger time-scale scales with M_s/M_h (Jiang et al., 2008), which implies a higher merger efficiency in low-mass haloes, for a given satellite mass. The build-up of massive objects through galaxy mergers could enhance mass segregation in low-mass haloes, in accordance with our results.

There has been evidence of cluster galaxies having their star formation quenched in lower mass groups ($\sim 10^{13}\,{\rm M}_\odot$) prior to accretion into the cluster environment (e.g. Zabludoff & Mulchaey, 1998; McGee et al., 2009; De Lucia et al., 2012; Hou et al., 2014). This pre-processing could potentially provide an explanation of our observed mass segregation trends with halo mass. If mass

segregation is present in the group environment as a result of pre-processing, the recent accretion of multiple pre-processed groups to form a galaxy cluster could result in little to no observed mass segregation in the cluster as a whole. In other words, if the cluster environment consists of multiple subhaloes at various cluster-centric radii, while individual subhaloes may show mass segregation, the total effect of these subhaloes together may leave the cluster with a relatively uniform radial mass distribution.

Vulcani et al. (2014) apply semi-analytic models to the Millenium Simulation (Springel et al., 2005) to study galaxy mass functions in different environments. Vulcani et al. simulate galaxy mass functions for three halo masses, $\log(M_{\rm halo}/M_{\odot}) = \{13.4, 14.1, 15.1\}$, as a function of cluster-centric radius. In the lowest mass halo they find the mass function depends slightly on cluster-centric radius, with the innermost regions showing flatter mass functions at low and intermediate masses. This trend persists, but is not as strong at intermediate halo mass. The highest halo mass bin shows virtually identical mass function shapes for all cluster-centric radii. This result is indicative of measurable mass segregation for the low- and intermediate-mass haloes, with the strength of mass segregation decreasing with increasing halo mass. These simulation trends show excellent agreement with our observed dependence of mass segregation on halo mass.

2.4.3 Reconciling previous results

In Section 2.1, we mention previous literature results which present evidence both for and against the presence of mass segregation in groups and

clusters. We argue that the majority of these results can be reconciled with our two main findings.

(i) Mass segregation is enhanced with the inclusion of low-mass galaxies in a sample.

(ii) Mass segregation decreases with increasing halo mass, with high-mass haloes showing little to no mass segregation.

Of the studies mentioned in Section 2.1, those which observe no evidence for mass segregation either: make a mass completeness cut at intermediate to high stellar mass, or observe this lack of mass segregation only in high-mass haloes. Therefore, the lack of observed mass segregation can potentially be explained through the lack of low-mass galaxies in the study survey, or the study being limited to high-halo-mass environments.

2.5 Conclusion

In this Letter, we examine mass segregation trends in the Yang et al. (2007) SDSS DR7 groups for various stellar and halo mass cuts. We show that a small, but significant, amount of mass segregation is present in these groups. This mass segregation shows consistent trends, with lower stellar mass samples showing stronger mass segregation, and galaxies in large haloes showing little to no mass segregation.

The magnitude of mass segregation we measure, especially in high-mass haloes, is potentially indicative of dynamical friction not acting efficiently. We

discuss previous literature to provide possible explanations for the observed trends, showing that our observed trends with halo mass agree with prior results. Further work with hydrodynamic simulations would be helpful to further constrain the important mechanisms responsible for our observed mass trends and the lack of mass segregation in high-mass haloes.

2.6 Acknowledgements

We thank the anonymous referee for their various helpful comments and suggestions. IDR and LCP thank the National Science and Engineering Research Council of Canada for funding. We thank X. Yang et al. for making their SDSS DR7 group catalogue public, L. Simard et al. for the publication of their SDSS DR7 morphology catalogue, and the NYU-VAGC team for the publication of their SDSS DR7 catalogue. This research would not have been possible without these public catalogues.

Funding for the SDSS has been provided by the Alfred P. Sloan Foundation, the Participating Institutions, the National Science Foundation, the US Department of Energy, the National Aeronautics and Space Administration, the Japanese Monbukagakusho, the Max Planck Society, and the Higher Education Funding Council for England. The SDSS website is http://www.sdss.org/.

Bibliography

Abazajian, K. N., Adelman-McCarthy, J. K., Agüeros, M. A., Allam, S. S., Allende Prieto, C., An, D., Anderson, K. S. J., Anderson, S. F., Annis, J., Bahcall, N. A., & et al. 2009, ApJS, 182, 543

Ball, N. M., Loveday, J., & Brunner, R. J. 2008, MNRAS, 383, 907

Balogh, M. L., McGee, S. L., Mok, A., Wilman, D. J., Finoguenov, A., Bower, R. G., Mulchaey, J. S., Parker, L. C., & Tanaka, M. 2014, MNRAS, 443, 2679

Balogh, M. L., Navarro, J. F., & Morris, S. L. 2000, ApJ, 540, 113

Blanton, M. R., Eisenstein, D., Hogg, D. W., Schlegel, D. J., & Brinkmann, J. 2005a, ApJ, 629, 143

Blanton, M. R. & Roweis, S. 2007, AJ, 133, 734

Blanton, M. R., Schlegel, D. J., Strauss, M. A., Brinkmann, J., Finkbeiner, D., Fukugita, M., Gunn, J. E., Hogg, D. W., Ivezić, Ž., Knapp, G. R., Lupton, R. H., Munn, J. A., Schneider, D. P., Tegmark, M., & Zehavi, I. 2005b, AJ, 129, 2562

Boylan-Kolchin, M., Ma, C.-P., & Quataert, E. 2008, MNRAS, 383, 93

Brough, S., Forbes, D. A., Kilborn, V. A., & Couch, W. 2006, MNRAS, 370, 1223

Cameron, E. 2011, PASA, 28, 128

Carlberg, R. G., Yee, H. K. C., Ellingson, E., Morris, S. L., Abraham, R., Gravel, P., Pritchet, C. J., Smecker-Hane, T., Hartwick, F. D. A., Hesser, J. E., Hutchings, J. B., & Oke, J. B. 1997, ApJ, 485, L13

Chabrier, G. 2003, PASP, 115, 763

Chandrasekhar, S. 1943, ApJ, 97, 255

Conroy, C., Ho, S., & White, M. 2007, MNRAS, 379, 1491

De Lucia, G., Weinmann, S., Poggianti, B. M., Aragón-Salamanca, A., & Zaritsky, D. 2012, MNRAS, 423, 1277

Eke, V. R., Baugh, C. M., Cole, S., Frenk, C. S., King, H. M., & Peacock, J. A. 2005, MNRAS, 362, 1233

Gan, J.-L., Kang, X., Hou, J.-L., & Chang, R.-X. 2010, Research in Astronomy and Astrophysics, 10, 1242

Geller, M. J. & Huchra, J. P. 1983, ApJS, 52, 61

Hogg, D. W., Blanton, M. R., Brinchmann, J., Eisenstein, D. J., Schlegel, D. J., Gunn, J. E., McKay, T. A., Rix, H.-W., Bahcall, N. A., Brinkmann, J., & Meiksin, A. 2004, ApJ, 601, L29

Hou, A., Parker, L. C., & Harris, W. E. 2014, MNRAS, 442, 406

Jiang, C. Y., Jing, Y. P., Faltenbacher, A., Lin, W. P., & Li, C. 2008, ApJ, 675, 1095

McGee, S. L., Balogh, M. L., Bower, R. G., Font, A. S., & McCarthy, I. G. 2009, MNRAS, 400, 937

Oemler, Jr., A. 1974, ApJ, 194, 1

Poggianti, B. M., Desai, V., Finn, R., Bamford, S., De Lucia, G., Varela, J., Aragón-Salamanca, A., Halliday, C., Noll, S., Saglia, R., Zaritsky, D., Best, P., Clowe, D., Milvang-Jensen, B., Jablonka, P., Pelló, R., Rudnick, G., Simard, L., von der Linden, A., & White, S. 2008, ApJ, 684, 888

Pracy, M. B., Driver, S. P., De Propris, R., Couch, W. J., & Nulsen, P. E. J. 2005, MNRAS, 364, 1147

Presotto, V., Iovino, A., Scodeggio, M., Cucciati, O., Knobel, C., Bolzonella, M., Oesch, P., Finoguenov, A., Tanaka, M., Kovač, K., Peng, Y., Zamorani, G., Bardelli, S., Pozzetti, L., Kampczyk, P., López-Sanjuan, C., Vergani, D., Zucca, E., Tasca, L. A. M., Carollo, C. M., Contini, T., Kneib, J.-P., Le Fèvre, O., Lilly, S., Mainieri, V., Renzini, A., Bongiorno, A., Caputi, K., de la Torre, S., de Ravel, L., Franzetti, P., Garilli, B., Lamareille, F., Le Borgne, J.-F., Le Brun, V., Maier, C., Mignoli, M., Pellò, R., Perez-Montero, E., Ricciardelli, E., Silverman, J. D., Tresse, L., Barnes, L., Bordoloi, R., Cappi, A., Cimatti, A., Coppa, G., Koekemoer, A. M., McCracken, H. J., Moresco, M., Nair, P., & Welikala, N. 2012, A&A, 539, A55

Simard, L., Mendel, J. T., Patton, D. R., Ellison, S. L., & McConnachie, A. W. 2011, ApJS, 196, 11

Springel, V., White, S. D. M., Jenkins, A., Frenk, C. S., Yoshida, N., Gao, L., Navarro, J., Thacker, R., Croton, D., Helly, J., Peacock, J. A., Cole,

S., Thomas, P., Couchman, H., Evrard, A., Colberg, J., & Pearce, F. 2005, Nature, 435, 629

Taffoni, G., Mayer, L., Colpi, M., & Governato, F. 2003, MNRAS, 341, 434

Tal, T., Dekel, A., Oesch, P., Muzzin, A., Brammer, G. B., van Dokkum, P. G., Franx, M., Illingworth, G. D., Leja, J., Magee, D., Marchesini, D., Momcheva, I., Nelson, E. J., Patel, S. G., Quadri, R. F., Rix, H.-W., Skelton, R. E., Wake, D. A., & Whitaker, K. E. 2014, ApJ, 789, 164

van den Bosch, F. C., Pasquali, A., Yang, X., Mo, H. J., Weinmann, S., McIntosh, D. H., & Aquino, D. 2008, ArXiv e-prints

von der Linden, A., Wild, V., Kauffmann, G., White, S. D. M., & Weinmann, S. 2010, MNRAS, 404, 1231

Vulcani, B., De Lucia, G., Poggianti, B. M., Bundy, K., More, S., & Calvi, R. 2014, ApJ, 788, 57

Vulcani, B., Poggianti, B. M., Oemler, A., Dressler, A., Aragón-Salamanca, A., De Lucia, G., Moretti, A., Gladders, M., Abramson, L., & Halliday, C. 2013, A&A, 550, A58

Wetzel, A. R., Tinker, J. L., & Conroy, C. 2012, MNRAS, 424, 232

Wetzel, A. R., Tinker, J. L., Conroy, C., & van den Bosch, F. C. 2013, MNRAS, 432, 336

Yang, X., Mo, H. J., van den Bosch, F. C., & Jing, Y. P. 2005, MNRAS, 356, 1293

Yang, X., Mo, H. J., van den Bosch, F. C., Pasquali, A., Li, C., & Barden, M. 2007, ApJ, 671, 153

Zabludoff, A. I. & Mulchaey, J. S. 1998, ApJ, 496, 39

Ziparo, F., Popesso, P., Biviano, A., Finoguenov, A., Wuyts, S., Wilman, D., Salvato, M., Tanaka, M., Ilbert, O., Nandra, K., Lutz, D., Elbaz, D., Dickinson, M., Altieri, B., Aussel, H., Berta, S., Cimatti, A., Fadda, D., Genzel, R., Le Flo'ch, E., Magnelli, B., Nordon, R., Poglitsch, A., Pozzi, F., Portal, M. S., Tacconi, L., Bauer, F. E., Brandt, W. N., Cappelluti, N., Cooper, M. C., & Mulchaey, J. S. 2013, MNRAS, 434, 3089

Chapter 3

Comparing galaxy morphology and star formation properties in X-ray bright and faint groups and clusters

This chapter represents an unchanged version of the paper, "*Comparing galaxy morphology and star formation properties in X-ray bright and faint groups and clusters*", published in the refereed journal, *Monthly Notices of the Royal Astronomical Society*. The full reference is given below:

Roberts I.D., Parker L.C., Karunakaran A., 2016, MNRAS,

Volume 455, Issue 4, pp. 3628-3639

Department of Physics & Astronomy, McMaster University, Hamilton ON L8S 4M1, Canada

Abstract

Galaxy morphologies and star formation rates depend on environment. Galaxies in underdense regions are generally star-forming and discy whereas galaxies in overdense regions tend to be early-type and not actively forming stars. The mechanism(s) responsible for star formation quenching and morphological transformation remain unclear, although many processes have been proposed. We study the dependence of star formation and morphology on X-ray luminosity for galaxies in Sloan Digital Sky Survey Data Release 7 (SDSS-DR7) groups and clusters. While controlling for stellar and halo mass dependences, we find that galaxies in X-ray strong groups and clusters have preferentially low star-forming and disc fractions - with the differences being strongest at low stellar masses. The trends that we observe do not change when considering only galaxies found within or outside of the X-ray radius of the host group. When considering central and satellite galaxies separately we find that this dependence on X-ray luminosity is only present for satellites, and we show that our results are consistent with 'galaxy strangulation' as a mechanism for quenching these satellites. We investigate the dynamics of the groups and clusters in the sample, and find that the velocity distributions of galaxies beyond the virial radius in low X-ray luminosity haloes tend to be less Gaussian in nature than the rest of the data set. This may be indicative of low X-ray luminosity groups and clusters having enhanced populations of star-forming and disc galaxies as a result of recent accretion.

3.1 Introduction

Numerous studies have shown a strong environmental dependence on the star-forming and morphological properties of galaxies (e.g. Butcher & Oemler, 1978; Dressler, 1980; Postman & Geller, 1984; Dressler et al., 1999; Blanton et al., 2005a; Wetzel et al., 2012). Low-density regimes tend to be dominated by star-forming, late-type galaxies whereas high-density areas, such as galaxy clusters, tend to be primarily populated by quiescent, early-type galaxies. Within individual clusters, galaxy morphologies tend to distribute as a function of local density (or equivalently cluster-centric radius), with high fractions of late-type galaxies being found at large radii and the regions near the cluster core being dominated by early-types (e.g. Dressler, 1980; Postman & Geller, 1984; Postman et al., 2005). This effect has become known as the morphology-density relation. While galaxies distribute based on their star-forming and morphological properties, the mechanism(s) responsible for the quenching of star formation and morphological transformations in galaxies are not well constrained – although many have been proposed. Both mergers and impulsive galaxy-galaxy interactions ('harassment') (e.g. Moore et al., 1996) can induce starburst events in galaxies leading to rapid consumption of gas reserves and star formation quenching. Within the virial radius of a group or cluster the stripping of gas from galaxies becomes efficient. Both the stripping of hot halo gas ('strangulation') (e.g. Kawata & Mulchaey, 2008) and cold gas stripping due to a dense intracluster medium ('ram-pressure') (e.g. Gunn & Gott, 1972) can quench star formation. As well, tidal interactions can affect gas reservoirs by transporting gas from the galactic halo outwards which sub-

sequently allows it to more easily be stripped from the galaxy (Chung et al., 2007).

On top of these environmental quenching mechanisms, previous authors have found that secular processes, which depend on galaxy mass, appear to play a significant role in star formation quenching (Balogh et al., 2004; Muzzin et al., 2012). The emergent picture for star formation quenching appears to be some combination of environmental quenching mechanisms and internal, secular processes. In particular, Peng et al. (2010) suggest that in the low-redshift Universe, environmental quenching is dominant for galaxies with $M_\star \lesssim 10^{10.5}\,\mathrm{M}_\odot$, whereas for galaxies with $M_\star \gtrsim 10^{10.5}\,\mathrm{M}_\odot$ mass quenching plays the more important role.

While environmental and mass quenching within individual haloes are seemingly strong effects, it is important to realize that groups and clusters are not isolated structures. In particular, galaxies can be pre-quenched in group haloes prior to infall into a larger cluster. This 'pre-processing' suggests that many galaxies may already be quenched upon cluster infall. Simulations have shown that between $\sim$ 25 and 45 per cent of infalling cluster galaxies may have been pre-processed (McGee et al., 2009; De Lucia et al., 2012). Observationally, Hou et al. (2014) find that $\sim$ 25 per cent of the infall population reside in subhaloes for massive clusters ($M_H \gtrsim 10^{14.5}\,\mathrm{M}_\odot$). This pre-quenching of galaxies in groups could potentially be driven by galaxy interactions and mergers which are favoured in the group regime as a result of lower relative velocities between member galaxies (Barnes, 1985; Brough et al., 2006).

An important method for studying the quenching mechanisms in groups and clusters is to study the dependence of the star formation and morphological properties of galaxies on the conditions of their host halo (e.g. halo mass, X-ray luminosity, etc.). In particular, if quenching mechanisms depend on the density of the intra-group/cluster medium (IGM/ICM) – for example, ram-pressure stripping of cold gas – then one would expect to see galaxy populations which are preferentially passive in haloes with high X-ray luminosities. Such correlations have been looked for in previous studies, primarily within cluster environments.

In particular, Ellingson et al. (2001) find no positive correlation between the fraction of old galaxies and X-ray gas density. Balogh et al. (2002a) conclude that the level of star formation found in their 'low-L_X' sample is consistent with the levels seen in their CNOC1 sample consisting of higher mass clusters. Fairley et al. (2002) and Wake et al. (2005) both study the fractions of blue galaxies at intermediate redshifts and find no discernible trend between blue fraction and X-ray luminosity. Using multivariate regression Popesso et al. (2007b) find that cluster star formation depends on cluster richness but find no additional dependence on X-ray luminosity. In addition, they find no significant correlation between star-forming fraction and any global cluster property (M_{200}, σ_v, $N_{\rm gal}$, and L_X). Lopes et al. (2014) find no dependence of blue fraction on X-ray luminosity and the only slight dependence they find between disc fraction and X-ray luminosity is within the central and most dense regions.

Conversely, Balogh et al. (2002b) find that galaxies in their 'low-L_X' sample have preferentially high disc fractions compared to galaxies in their 'high-

L_X' sample. Postman et al. (2005) find that the bulge-dominated fraction for galaxies in high X-ray luminosity clusters is higher than for those in low X-ray luminosity clusters. In contrast with their star formation results, Popesso et al. (2007b) do find a significant anticorrelation between blue fraction and X-ray luminosity. Finally, Urquhart et al. (2010) find an anticorrelation between blue fraction and X-ray temperature for galaxies in intermediate redshift clusters.

In this paper we revisit the dependence of galaxy star formation and morphological properties on the X-ray luminosity of the host halo. Specifically, as a result of the large SDSS X-ray sample presented in Wang et al. (2014), we are able to control for stellar mass, halo mass, and radial dependences through fine-binning of the data set. This allows us to more directly investigate the effect of X-ray luminosity on galaxies in different environments.

The results of this study are presented as follows. In Section 3.2 we briefly describe the SDSS group catalogues utilized in this work, as well as the star formation and morphology catalogues which we match to the group data set. In Section 3.3 we present the primary results of this paper, specifically, the differences between star-forming and morphological trends in environments with different X-ray luminosities. In Section 3.4 we provide a discussion of the results presented in this paper. Finally, in Section 3.5 we provide a summary of the key results and make concluding statements.

In this paper we assume a Λ cold dark matter cosmology with $\Omega_M = 0.3$, $\Omega_\Lambda = 0.7$, and $H_0 = 70\,\mathrm{km\,s^{-1}\,Mpc^{-1}}$.

3.2 Data

3.2.1 Yang group catalogue

This work relies heavily on the group catalogue of Yang et al. (2007). The Yang group catalogue is constructed by applying the iterative halo-based group finder of Yang et al. (2005, 2007) to the New York University Value-Added Galaxy Catalogue (NYU-VAGC; Blanton et al. 2005b), which is based on the Sloan Digital Sky Survey Data Release 7 (SDSS-DR7; Abazajian et al. 2009). The Yang group catalogue has a wide range of halo masses, spanning from $\sim 10^{12}\,\mathrm{M}_\odot$ to $\sim 10^{15}\,\mathrm{M}_\odot$. The catalogue contains both objects which would be classified as groups ($10^{12} \lesssim M_H \lesssim 10^{14}$) and as clusters ($M_H \gtrsim 10^{14}\,\mathrm{M}_\odot$), however for brevity we will refer to all systems as groups regardless of mass.

Groups are initially populated using the traditional friends-of-friends (FOF) algorithm (e.g. Huchra & Geller, 1982), as well as assigning galaxies not yet linked to FOF groups as the centres of potential groups. Next, the characteristic luminosity, $L_{19.5}$, defined as the combined luminosity of all group members with ${}^{0.1}M_r - 5\log h \leq -19.5$, is calculated for each group. Using the value of $L_{19.5}$ along with an assumption for the group mass-to-light ratio, $M_H/L_{19.5}$, a tentative halo mass is assigned on a group-by-group basis. The tentative halo mass is used to calculate a virial radius and velocity dispersion for each group, which are then used to add or remove galaxies from the system. Galaxies are assigned to groups under the assumption that the distribution of galaxies in phase space follows that of dark matter particles – the distribution of which is

assumed to follow a spherical NFW profile (Navarro et al., 1997). This process is iterated until the group memberships no longer change.

Final halo masses given in the Yang group catalogue are determined using the ranking of the characteristic stellar mass, $M_{\star,\mathrm{grp}}$, and assuming a relationship between M_H and $M_{\star,\mathrm{grp}}$ (Yang et al., 2007). $M_{\star,\mathrm{grp}}$ is defined by Yang et al. as

$$M_{\star,\mathrm{grp}} = \frac{1}{g(L_{19.5},\, L_{\mathrm{lim}})} \sum_i \frac{M_{\star,i}}{C_i}, \tag{3.1}$$

where $M_{\star,i}$ is the stellar mass of the ith member galaxy, C_i is the completeness of the survey at the position of that galaxy, and $g(L_{19.5},\, L_{\mathrm{lim}})$ is a correction factor which accounts for galaxies missed due to the magnitude limit of the survey. The statistical error in M_H is on the order of 0.3 dex and mostly independent of halo mass (Yang et al., 2007).

3.2.2 SDSS X-ray catalogue

To study the X-ray properties of the group sample, we utilize the SDSS X-ray catalogue of Wang et al. (2014), which combines ROSAT All Sky Survey (RASS) X-ray images in conjunction with optical groups identified from SDSS-DR7 (Yang et al., 2007) to estimate X-ray luminosities around $\sim 65\,000$ spectroscopic groups.

To identify X-ray luminosities for individual groups, the algorithm of Shen et al. (2008) is employed. Beginning from an optical group, the most massive galaxies (MMGs) of that group are identifed – up to four MMGs are kept.

The RASS field in which the MMGs reside are then identified, and an X-ray source catalogue is generated in the $0.5-2.0\,\mathrm{keV}$ band (Wang et al., 2014). The maximum X-ray emission density point is used to identify the X-ray centre of the group, and any X-ray sources not associated with the group (e.g. point source quasars or stellar object cross-matched from RASS and SDSS-DR7), within one virial radius, are masked out. Values for the X-ray background, centred on the X-ray centre, are determined and subtracted off and the X-ray luminosity, L_X, is calculated by integrating the source count profile within the X-ray radius.

Determining X-ray luminosities in this manner is susceptible to 'source confusion'. Due to projection it is possible for more than one group to contribute to the X-ray emission within the X-ray radius, leading to an overestimation of the X-ray luminosity for a given group. To account for this effect Wang et al. (2014) calculate the 'expected' average X-ray flux, $F_{X,i}$, for each group using the average $L_X - M_H$ relation taken from Mantz et al. (2010). They then calculate the sum of the expected fluxes from each group for multigroup systems and determine the contribution fraction, $f_{\mathrm{mult},i}$, for each group defined as

$$f_{\mathrm{mult},i} = F_{X,i}/\Sigma_i F_{X,i}. \tag{3.2}$$

The contribution factor will approximate the fraction of the observed X-ray luminosity intrinsic to the individual group in question, therefore applying this fraction to each group will act to debias the measured X-ray luminosity from source confusion contamination.

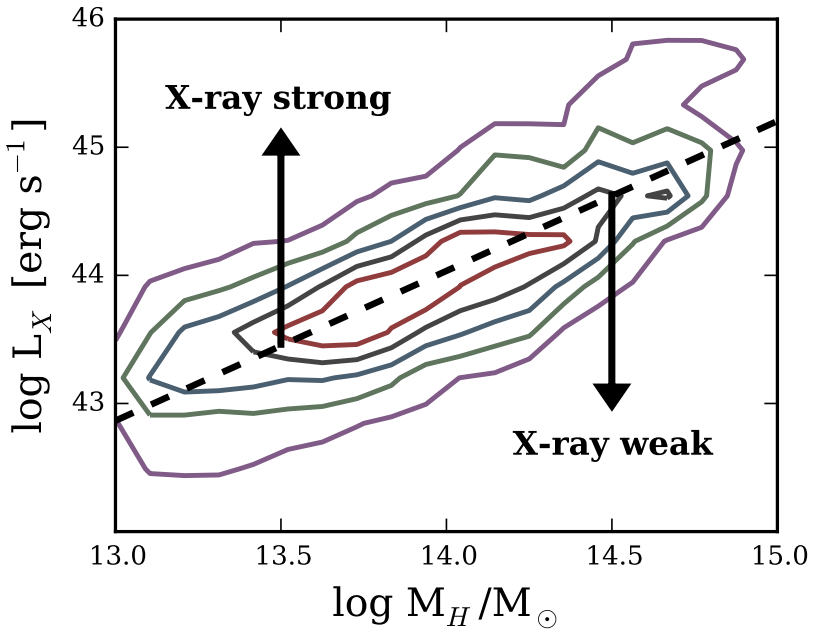

Figure 3.1: Density contours for log X-ray luminosity versus log halo mass. Dashed line corresponds to the linear least-squares best-fitting relationship.

Within the Wang catalogue 817 groups have S/N $>$ 3, compared to the total of 34 522 groups with positive detections (positive count rates after background subtraction) and S/N $>$ 0. We run our analysis for groups with S/N $>$ 3 as well as groups with S/N $>$ 0 and find that our choice of signal-to-noise cut does not change the trends that we observe, therefore we focus on the total sample (S/N $>$ 0) to ensure a sample size which is large enough to finely bin the data in various properties simultaneously.

3.2.3 Final data set

To obtain the final data set, we match the Wang SDSS X-ray catalogue to the Yang SDSS group catalogue, giving us both optical and X-ray group

properties for the sample. To obtain individual galaxy properties we further match the data set to various public SDSS catalogues as follows.

We utilize stellar masses given in the NYU-VAGC, which are computed following the methodology of Blanton & Roweis (2007).

To obtain star formation rates (SFRs) and specific star formation rates (SSFR = SFR/$M_\star$) we match the catalogue of Brinchmann et al. (2004) to the sample. SFRs given by Brinchmann et al. are determined using emission line fluxes whenever possible; however, in the case of no clear emission lines or contamination from active galactic nuclei (AGNs), SFRs are determined using the strength of the 4000 Å break (D_n4000) (Brinchmann et al., 2004).

We obtain galaxy morphologies from the catalogue of Simard et al. (2011). Simard et al. perform two-dimensional bulge + disc decompositions for over one million galaxies from the Legacy area of the SDSS-DR7, using three different fitting models: a pure Sérsic model, a bulge + disc model with a de Vaucouleurs ($n_b = 4$) bulge, and a bulge + disc model with a free n_b. To distinguish between discy and elliptical galaxies we utilize the galaxy Sérsic index, n_g, from the pure Sérsic decomposition. We also use the $V_{\rm max}$ weights given by Simard et al. to correct for the incompleteness of our sample.

We calculate group-centric distances for each galaxy using the redshift of the group and the angular separation between the galaxy and the luminosity-weighted centre of its host group. We normalize all of the galaxy radii by the virial radius of the host group, R_{180}, which we calculate as in Yang et al. (2007)

$$R_{180} = 1.26\,h^{-1}\,\mathrm{Mpc}\left(\frac{M_H}{10^{14}\,h^{-1}\ \mathrm{M}_\odot}\right)^{1/3}(1+z_g)^{-1}, \tag{3.3}$$

where z_g is the redshift of the group centre.

The final data set includes groups with halo masses ranging between $10^{13} - 10^{15}$ $\mathrm{M}_\odot$, and galaxies with stellar masses ranging from $10^9 - 10^{11.3}$ $\mathrm{M}_\odot$. Group X-ray luminosities in the data set are between $10^{39.6} - 10^{46.4}\,\mathrm{erg\,s^{-1}}$, with a median value of $10^{43.9}\,\mathrm{erg\,s^{-1}}$, and are strongly correlated with halo mass (see Fig. 3.1). We do not make an explicit radial cut, however over 99 per cent of member galaxies fall within 1.5 virial radii. Our final sample contains 3 902 low-redshift ($z < 0.1$) groups hosting 41 173 galaxies. The catalogue of Wang et al. (2014) contains $\sim 35\,000$ groups. The fact that the final sample in this work is significantly smaller than the original catalogue is twofold. First, we restrict our sample to redshifts smaller than 0.1 which reduces the number of groups from $\sim 35\,000$ at $z < 0.2$ to $\sim 18\,000$ at $z < 0.1$. The second important cut is that we require $10^{13} < M_H < 10^{15}\,\mathrm{M}_\odot$ and a number of groups in the Wang catalogue have halo masses, $M_H < 10^{13}\,\mathrm{M}_\odot$ (where halo masses have been obtained from the catalogue of Yang et al. 2007). This cut reduces the remaining number of groups from $\sim$ 18 000 to $\sim$ 3 900. It should be noted that the majority of the $M_H < 10^{13}\,\mathrm{M}_\odot$ groups removed from the data set are groups with very low membership.

To determine the effect of X-ray luminosity on star formation and morphology we consider two X-ray luminosity samples for the majority of our analysis, which we refer to as the X-ray weak (XRW) and X-ray strong (XRS) samples. Similar to Wang et al. (2014), we define the XRS sample to con-

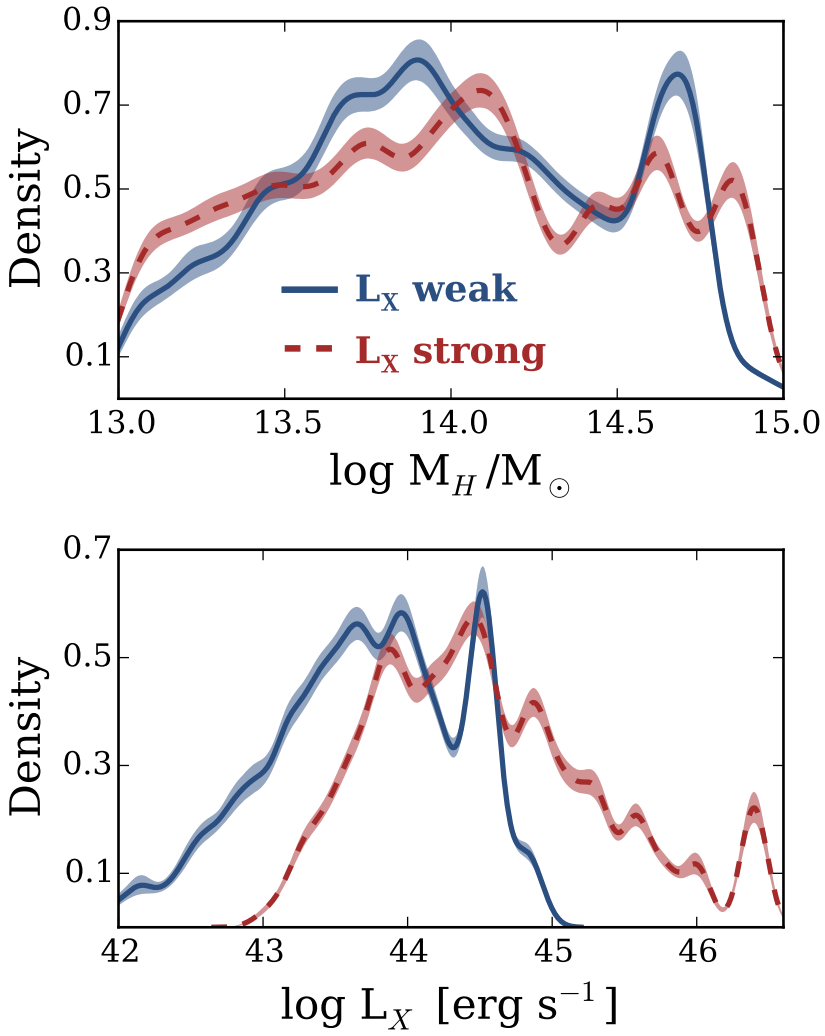

Figure 3.2: Smoothed distributions for halo mass and X-ray luminosity within the sample. Distributions are shown for both the X-ray strong (red, dashed) and the X-ray weak (blue, solid) samples. Shaded regions correspond to 2σ confidence intervals obtained from random bootstrap resampling.

sist of all galaxies found above the $\log M_H - \log L_X$ trend line (see Fig. 3.1), and correspondingly the XRW sample consists of all galaxies found below the $\log M_H - \log L_X$ trend line. This leads to an approximately equal number of galaxies within the XRW and XRS samples. We also performed our analysis with a cut between the two X-ray samples at the median X-ray luminosity of the data set, as well as defining the two samples using the first and the fourth quartiles, however these alternative definitions of the two X-ray samples do not change the trends that we observe.

Smoothed distributions for halo mass and X-ray luminosity are shown in Fig. 3.2 for both X-ray luminosity samples. Density distributions are calculated using the `density` {`stats`} function in the statistical computing language R (R Core Team, 2013)[†] using a Gaussian kernel.

We study the dependence of star formation rates and morphology on stellar mass by binning the data by stellar mass and calculating the disc and star-forming fractions for each bin. Binning by stellar mass is important to account for the systematic dependence of star formation and morphology on stellar mass (e.g. Brinchmann et al., 2004; Whitaker et al., 2012). Additionally, as the relative balance between environmental and mass quenching is not well understood, it is important to investigate the effects of environment at a given stellar mass.

We define the star-forming fraction, f_{SF}, as the fraction of galaxies in each bin with $\log \mathrm{SSFR} > -11$. Wetzel et al. (2012) show that at low redshift the division between the red sequence and the blue cloud is found at $\log \mathrm{SSFR} \simeq$

[†]http://www.R-project.org/

-11 across a wide range of halo masses. For each stellar mass bin the star-forming fraction is given by

$$f_{SF} = \frac{V_{\max} \text{ weighted no. of galaxies with } \log \mathrm{SSFR} > -11}{V_{\max} \text{ weighted total no. of galaxies}}. \tag{3.4}$$

Similarly we define the disc fraction, f_D, as the fraction of galaxies in each bin with Sérsic index, $n < 1.5$. For each stellar mass bin this is given by

$$f_D = \frac{V_{\max} \text{ weighted no. of galaxies with } n < 1.5}{V_{\max} \text{ weighted total no. of galaxies}}. \tag{3.5}$$

We also ran our analysis using a dividing cut at Sérsic indices of $n = 1.0$ and $n = 2.0$ to define a disc galaxy, however using these alternative definitions for a disc galaxy does not alter the trends that we observe.

3.3 Results

3.3.1 Star-forming and morphology trends in strong and weak L_X samples

To investigate the effect of X-ray luminosity on galaxy properties, in Fig. 3.3 we show star-forming and disc fractions, as a function of stellar mass, for sub-samples corresponding to the four X-ray luminosity quartiles of the data set. Examination of Figs 3.3(a) and (b) show that star-forming and disc fractions follow a consistent marching order with respect to X-ray luminosity. The disc and star-forming fractions decrease as X-ray luminosity increases.

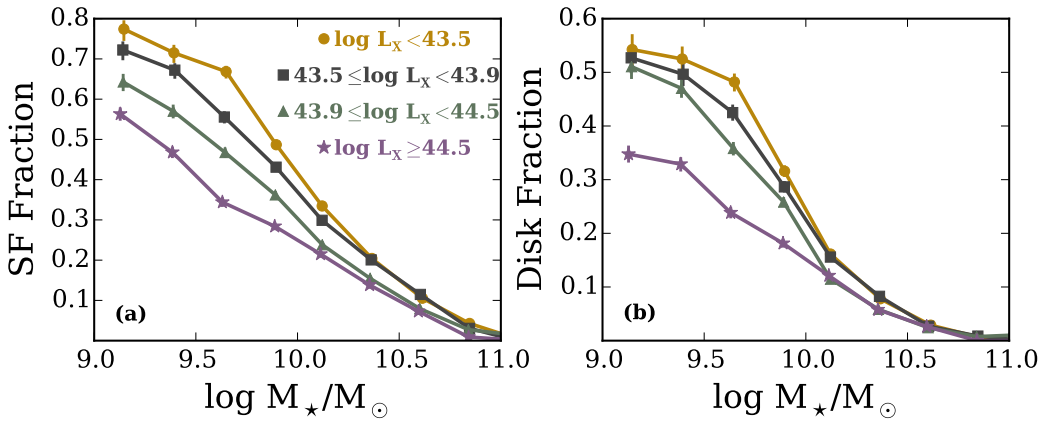

Figure 3.3: Left: star-forming fraction versus stellar mass for the four X-ray luminosity quartiles of the data sample. Right: disc fraction versus stellar mass for the four X-ray luminosity quartiles of the sample. Error bars correspond to 1σ Bayesian binomial confidence intervals given in Cameron (2011).

We note that the results in Fig. 3.3 consider all halo masses in the sample, however it has been found that galaxy morphology and star formation depend on local density and halo mass (Dressler, 1980; Balogh et al., 2004; Wetzel et al., 2012; Lackner & Gunn, 2013) (however also see: De Lucia et al. 2012; Hoyle et al. 2012; Hou et al. 2013). As shown in Fig. 3.1 the data show a strong correlation between X-ray luminosity and halo mass, therefore we must determine if differences shown in Fig. 3.3 are simply a result of galaxies in higher L_X environments being housed in preferentially high-mass haloes.

To control for any potential halo mass effect, we further bin the data into narrow halo mass bins and re-examine the dependence of galaxy properties on X-ray luminosity, considering now the XRW and XRS samples from Fig. 3.1. Fig. 3.4 shows star-forming (solid) and disc (dashed) fractions as a function of stellar mass for four different halo mass bins – ranging from 10^{13} to $10^{15}\,\mathrm{M}_\odot$ with bin widths of 0.5 dex. Data are binned according to stellar mass and

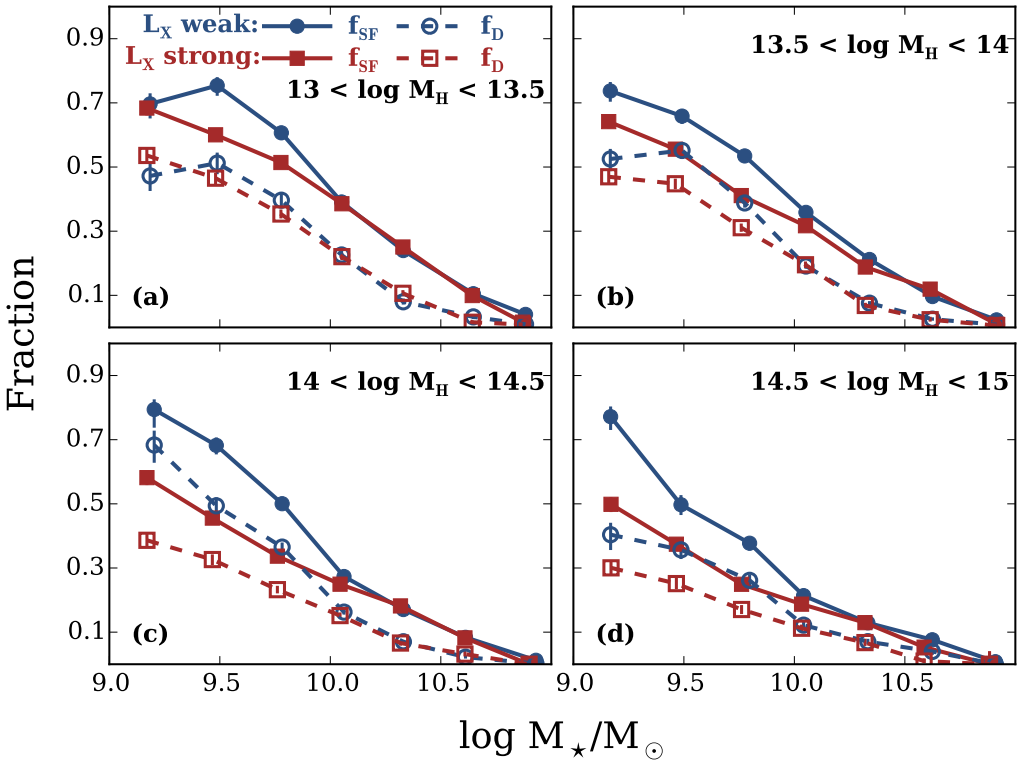

Figure 3.4: Star-forming (solid lines) and disc (dashed lines) fractions versus stellar mass, for different halo mass bins and the XRW (blue) and XRS (red) samples. Error bars correspond to 1σ Bayesian binomial confidence intervals given in Cameron (2011).

markers are plotted at the median bin values. For each halo mass bin we show star-forming and disc fractions from the X-ray strong and X-ray weak samples.

For both star-forming and disc fractions we continue to see a residual trend with X-ray luminosity, even after controlling for any halo mass dependence: star-forming and disc fractions are systematically higher in the XRW sample. We see the strongest trends in the intermediate and high-mass haloes. The difference between the strong (red) and weak (blue) X-ray luminosity samples is clearest at low stellar mass, and in all haloes the two samples converge at moderate to high stellar mass.

3.3.2 Radial dependence of star-forming and morphology trends

Within host groups X-ray emission is concentrated at relatively small group-centric radii, with X-ray emission generally extending out to half a virial radius (Wang et al., 2014). If the trends we are observing are a result of increased gas density, we would expect to see enhanced trends (i.e. a larger difference between the XRS and XRW samples) at small group-centric radii and suppressed trends at large radii. To test this we further divide the data into subsets corresponding to those galaxies that lie within the X-ray emission radius (using the X-ray radius, $R_{\rm Xray}$, given in Wang et al. 2014) and those galaxies that lie outside of the X-ray radius. We again plot star-forming/disc fraction versus stellar mass, in narrow halo mass bins, for the large and small radius subsamples. The results of this analysis are shown in Figs 3.5 and 3.6, where the two figures correspond to disc fraction and star-forming fraction trends for the large and small radius subsamples, respectively.

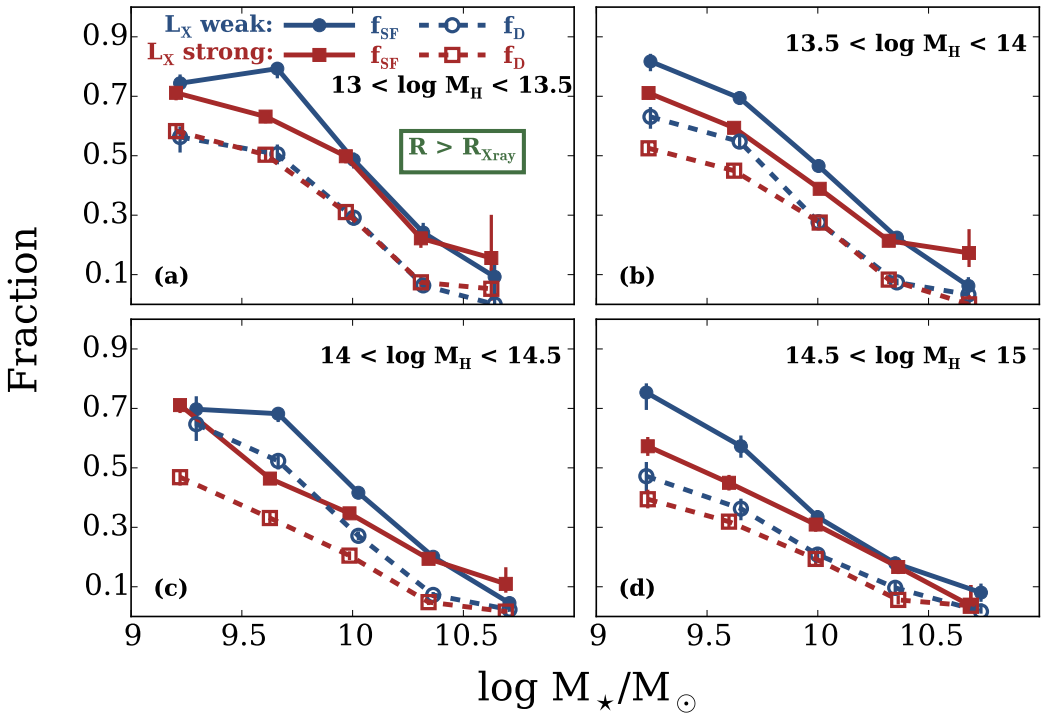

Figure 3.5: Star-forming (solid lines) and disc (dashed lines) fractions versus stellar mass, for galaxies outside of their host X-ray radius and for different halo mass bins and the two L_X samples. Error bars correspond to 1σ Bayesian binomial confidence intervals given in Cameron (2011).

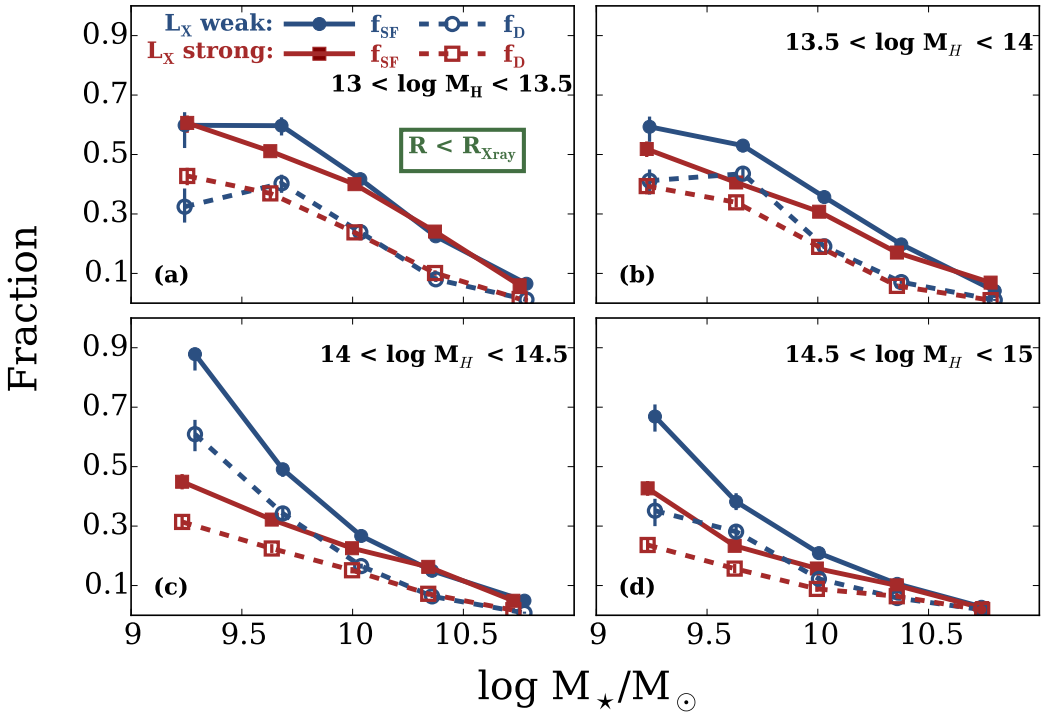

Figure 3.6: Same as Fig. 3.5 for galaxies inside of their host X-ray radius.

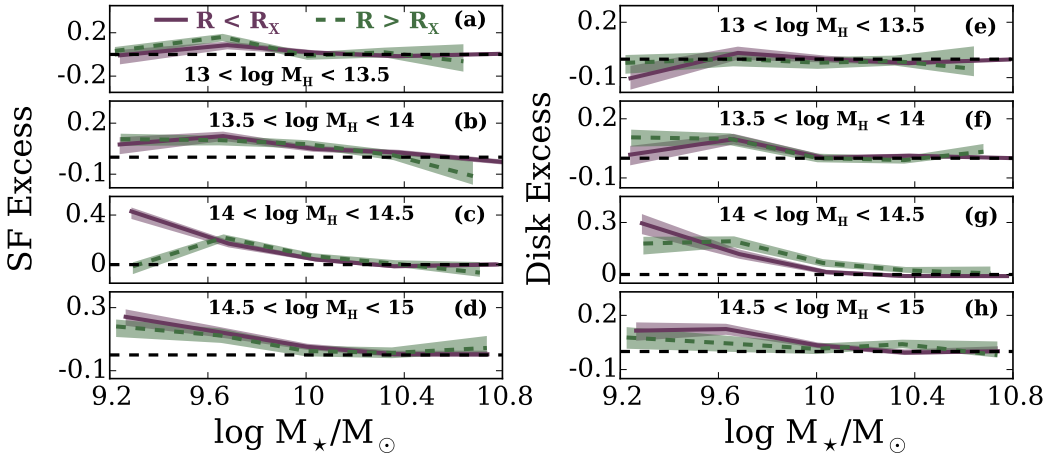

Figure 3.7: SF and disc excess versus stellar mass for both galaxies within (purple, solid) and outside (green, dashed) of the X-ray radius. Panels a-d show SF excess for four halo mass bins and panels e-h show disc excess for four halo mass bins. Shaded regions represent 1σ confidence intervals.

Examination of Figs 3.5 and 3.6 shows that for both galaxies found within their host halo's X-ray radius and those found outside, we still see an increase in star-forming and disc fractions in the XRW sample – as before this effect is strongest in the intermediate-to high-mass haloes and at low stellar mass. Also the disc and star-forming fractions tend to be higher at large radii, which is consistent with the morphology-density relation.

To further investigate if the increase in star-forming and disc fractions in the XRW sample compared to the XRS sample – which we will refer to as the 'SF excess' and the 'disc excess' – depends on whether you consider galaxies within or outside of the X-ray radius, we show SF and disc excess versus stellar mass in Fig. 3.7. We quantitatively define SF and disc excess as

$$\text{SF excess} = f_{SF}(\text{XRW}) - f_{SF}(\text{XRS}) \tag{3.6}$$

$$\text{Disc excess} = f_{D}(\text{XRW}) - f_{D}(\text{XRS}) \tag{3.7}$$

where f_{SF}(XRW) and f_{SF}(XRS) are the star-forming fractions in the XRW and XRS samples respectively, and analogously for f_D(XRW) and f_D(XRS).

We find no radial dependence for SF and disc excess as the two radial subsamples in Fig. 3.7 show overlap for all halo and stellar masses. With the exception in Fig. 3.7(c) where the SF excess, for low-mass galaxies, is stronger for galaxies within the X-ray radius.

3.4 Discussion

We find that star-forming and disc fractions are systematically lower in the XRS sample than galaxies in XRW environments. This trend persists even upon controlling for any halo mass dependence, however the observed difference between the XRS and the XRW sample is not enhanced when considering only those galaxies within the X-ray radius of the host halo.

There are two major observed effects which have been found to impact the distributions of early-type and late-type galaxies within cluster environments. The so called 'Butcher-Oemler' (BO) effect is the observational trend that the blue fraction of cluster galaxies are positively correlated with redshift (e.g. Butcher & Oemler, 1984; Ellingson et al., 2001; Loh et al., 2008; Urquhart et al., 2010). However, it should be noted that there is still debate when it comes to the physical nature of the BO effect (for example, see: Andreon &

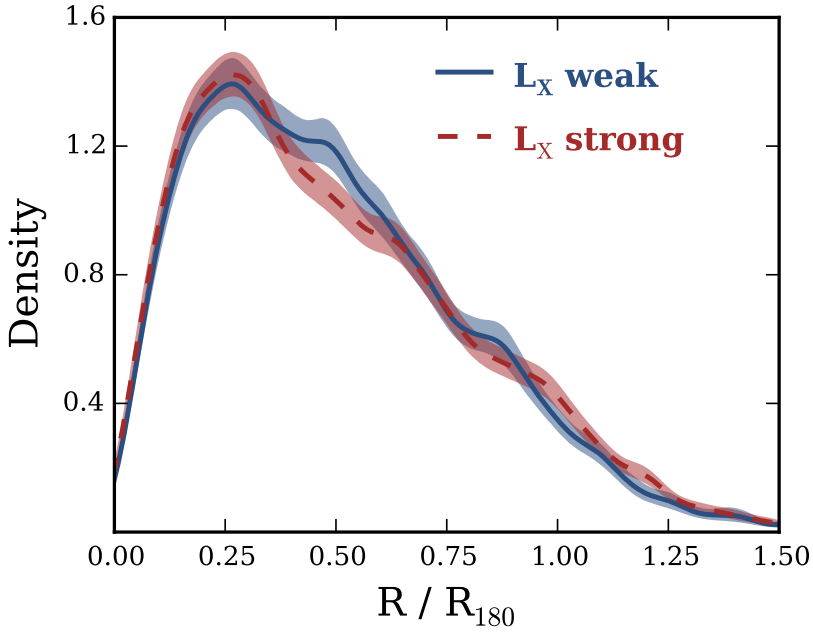

Figure 3.8: Smoothed radial distributions of galaxies in the XRW (blue, solid) and XRS (red, dashed) samples. Shaded regions correspond to 2σ confidence intervals obtained from random bootstrap resampling.

Ettori 1999; Andreon et al. 2004, 2006). Since we are only considering low-redshift ($z < 0.1$) galaxies the BO effect should be negligible.

The second major effect is the previously mentioned morphology-density relationship. In order to determine if the morphology-density relation is affecting the trends we observe, we must check if there are significant differences in the radial distributions of the XRS and the XRW samples. For instance, if the XRW sample is found at systematically high group-centric radii compared to the XRS sample, then the morphology-density relation could explain why we find systematically larger star-forming and disc fractions in the XRW sample. In Fig. 3.8 we plot the smoothed radial distributions for both the XRS and the XRW samples. We see no systematic difference between the two distributions, in fact they are nearly indistinguishable from one another, and therefore any observed differences between the XRS and XRW samples are not being driven by difffering radial distributions.

3.4.1 AGN contamination

When considering X-ray properties of galaxy groups it is important to ensure that the observed X-ray emission is due to the hot IGM and not due to contamination from AGN or other X-ray sources. In Wang et al. (2014) bright point sources, such as stars and quasars, are masked out, however it is still important to ensure that our results are not being contaminated by galaxies housing non-point source AGN.

In Fig. 3.9 we plot AGN fraction versus stellar mass for the XRW and XRS samples. We use AGN classified by Kauffmann et al. (2003), which are

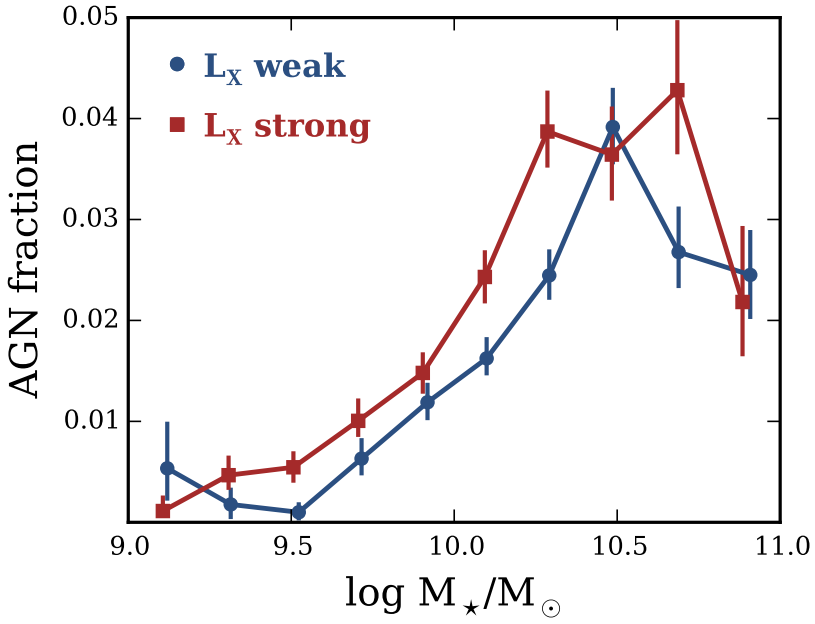

Figure 3.9: BPT identified AGN fraction versus stellar mass for the XRW and XRS samples. Error bars correspond to 1σ Bayesian binomial confidence intervals given in Cameron (2011).

identified using the location of galaxies on the BPT diagram (Baldwin et al., 1981). It should be noted that Trouille & Barger (2010) show that between 20 and 50 per cent (depending on the dividing line between AGN and star-forming galaxies used) of X-ray identified AGN fail to be classified as AGN on the BPT diagram.

We see that the AGN fraction tends to be larger within the XRS sample, however at all stellar masses the number of AGN galaxies is a modest fraction (less than 5 per cent) of the total sample, for both XRS and XRW galaxies. Most relevant is the fact that at low stellar mass the AGN fraction is consistently below one per cent, for both the XRW and XRS samples, whereas the trends we observe with X-ray luminosity are exclusively seen at low stellar mass (e.g. Fig. 3.4). We examined disc and star-forming fractions for a subsample of the data with galaxies identified as AGN removed and found that removing AGN galaxies from the sample does not change the observed trends. Furthermore, we examined trends after removing all groups that house galaxies identified as AGN and again found no change in the observed trends. Therefore we conclude that AGN are not a significant contributor to the observed trends in star-forming and disc fractions.

3.4.2 Implications for star formation quenching

The relative importance of various galaxy quenching mechanisms is an important, open question. Galaxy populations in groups can be classified as either 'central' (located at the centre of the group dark matter halo) or 'satellite' galaxies. These two populations are expected to evolve differently (e.g. van den

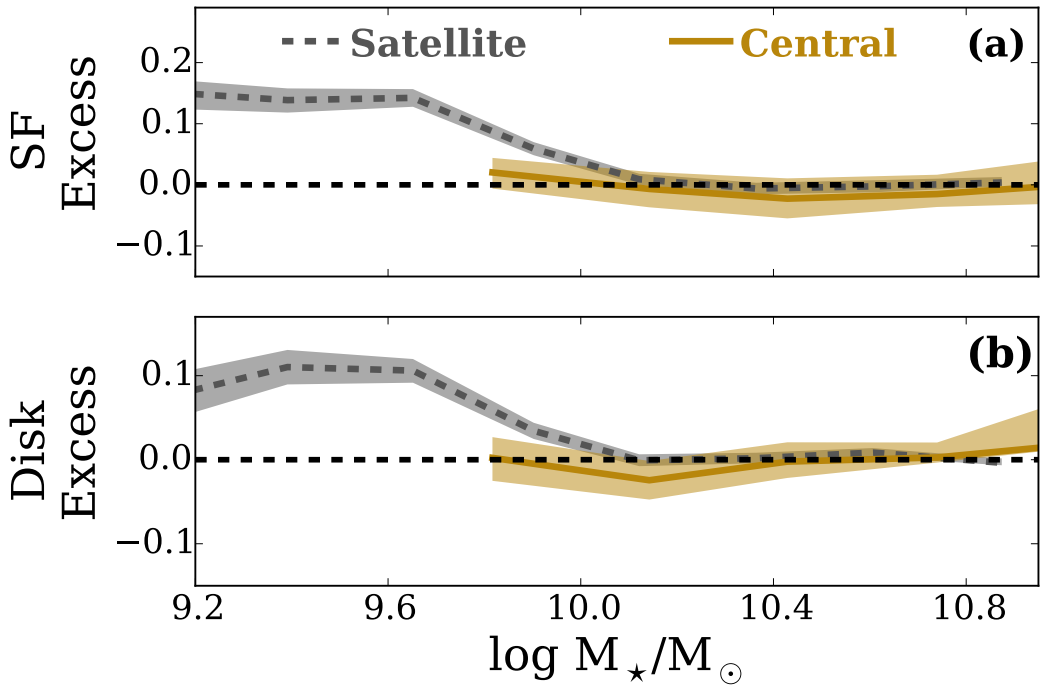

Figure 3.10: SF and disc excess versus stellar mass for both centrals (gold, solid) and satellites (grey, dashed). Shaded regions correspond to 1σ confidence intervals.

Bosch et al., 2008), and therefore when attempting to elucidate information on the quenching of galaxies it is important to consider centrals and satellites as distinct populations. In Fig. 3.10 we plot SF and disc excess (equations 3.6 and 3.7) versus stellar mass, considering separately central and satellite galaxies. Central galaxies are defined as the most massive group galaxies and satellite galaxies are defined as all galaxies which have not been classified as centrals.

When considering satellite galaxies in Fig. 3.10(a) we find that galaxies within the XRW sample have consistently larger star-forming fractions at low stellar mass (SF excess > 0), while at large stellar mass the XRW and XRS samples are indistinguishable. When considering only central galaxies we find that there is no difference between the XRW and XRS samples (SF excess ≈ 0) when considering star-forming fraction. We observe qualitatively similar trends for disc excess in Fig. 3.10(b). This implies that whatever effect X-ray luminosity has on star-forming and morphological properties it only affects satellite galaxies, central galaxies are insensitive to the group X-ray properties. This is not surprising given that central galaxies are massive, and we see no difference between the XRS and XRW at large stellar mass.

One interpretation of the differences we observe between the XRW and XRS samples would be to invoke the ram-pressure stripping of satellite galaxies. The rate at which galaxies will lose gas through ram-pressure stripping will increase in proportion to L_X (Fairley et al., 2002). Therefore if ram-pressure is an important mechanism when it comes to the quenching of galaxies, a decrease in star-forming fraction should be observed with increasing X-ray luminosity. It should be noted that although we observe very similar trends for

star-forming and disc fractions, it is not clear whether ram-pressure stripping can efficiently drive galaxy morphology transformations from late to early type (Christlein & Zabludoff, 2004). Prior studies (e.g. Gavazzi et al., 2003; Kenney et al., 2004; Muzzin et al., 2014) have found evidence of ram-pressure stripping. We note as well that other studies (e.g. Balogh et al., 2002a; Fairley et al., 2002; Wake et al., 2005; Lopes et al., 2014) have found no clear trend between star-forming or blue fractions and X-ray luminosity. At first glance the results shown in Fig. 3.4 are consistent with ram-pressure stripping; at low stellar masses there are lower star-forming fractions in the XRS sample. One difference between the results we observe and previous studies is that we narrowly bin our data in stellar mass. Since star-forming and morphological properties depend strongly on stellar mass, any residual dependence on X-ray luminosity may be lost without controlling for stellar mass. In addition our sample size is significantly larger than most previous studies, so it may be that trends with X-ray luminosity are subtle enough to be missed without large statistics.

If the trends we detect are driven by ram-pressure we would expect a radial dependence of our trends with X-ray luminosity. The efficiency of ram-pressure stripping is proportional to ρv^2 (Wake et al., 2005; Popesso et al., 2007b), where ρ is the IGM density and v is the speed of the member galaxies. Since the IGM density is highest at small group-centric radii, the efficiency of ram-pressure stripping should increase towards small radii. In Fig. 3.7 we showed that the observed SF excess does not strongly depend on radius. We conclude that this lack of radial dependence is inconsistent with the ram-pressure stripping scenario.

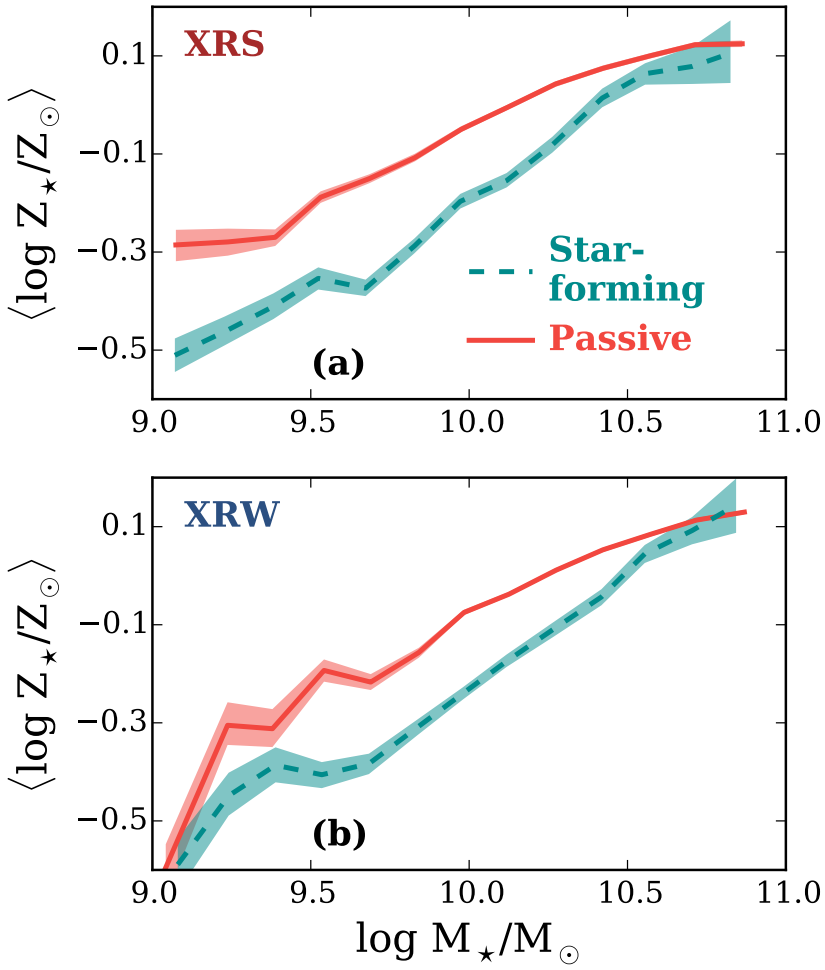

Figure 3.11: Mean stellar metallicity versus stellar mass for star-forming (blue, dashed) and passive (red, solid) galaxies, divided by galaxies in the XRS (top) and XRW (bottom) samples. Shaded regions correspond to 1σ confidence intervals obtained from random bootstrap resampling.

Another often-envoked mechanism for regulating star formation is 'galaxy strangulation' (Larson et al., 1980; Balogh et al., 2000; Kawata & Mulchaey, 2008; Peng et al., 2015). Strangulation is a mechanism in which the replenishment of cold gas onto galaxies is halted, which in turn leads to galaxy quenching once the galaxy has exhausted its existing cold gas reservoirs. The time-scales over which a galaxy will be quenched by strangulation are longer than the times associated with the direct stripping of cold gas reserves (ram-pressure). Recently, Peng et al. (2015) have argued that it is possible to differentiate between strangulation and direct stripping using metallicity differences between star-forming and quiescent galaxy populations. We direct the reader to Peng et al. (2015) for a more complete discussion, however the main idea is that quenching by strangulation will result in higher metallicities for passive galaxies compared to star-forming galaxies. This is a result of star formation continuing even after the gas supply has been halted which will increase stellar metallicity until the cold gas reserves have been exhausted and the galaxy has therefore been quenched. This trend in metallicity is not expected from direct stripping, where star formation shuts off quickly after the removal of cold gas.

To investigate the effect of strangulation on the galaxy sample in this study we follow Peng et al. (2015) and calculate mean stellar metallicity versus stellar mass considering star-forming and passive galaxies separately, for galaxies within our XRW sample as well as our XRS sample. Metallicities are matched to our sample from the catalogue of Gallazzi et al. (2005), and mean metallicities are calculated in stellar mass bins with widths of 0.15 dex. Not all of the galaxies within this sample have measured metallicities, and our XRW and

XRS samples are reduced to 10 939 (52 per cent of total sample) and 8 851 (44 per cent of total sample) member galaxies respectively.

In Fig. 3.11 we see higher stellar metallicities for passive galaxies compared to star-formers, which we interpret as evidence for strangulation playing a significant role in star formation quenching. Of particular interest for this work is the behaviour at low stellar mass which is where the dependence of star formation and morphology on X-ray luminosity is observed (see Fig. 3.4). We see a somewhat stronger strangulation signal (ie. difference between passive and star-former metallicity) for galaxies in the XRS sample compared to the XRW sample, at low stellar mass.

In light of this observed difference, it is important to note that compiling this subsample of galaxies with measured metallicities does not affect all stellar masses equally. Specifically, low-mass galaxies are preferentially removed from the sample when matching to the metallicity catalogue. In particular, 69 per cent of low-mass ($M_\star < 10^{9.5}\,\mathrm{M}_\odot$) galaxies in the XRS sample do not have measured metallicities, whereas in the XRW sample 75 per cent of low-mass galaxies do not have measured metallicities. Not only are low-mass galaxies being preferentially lost, but the fraction of low-mass galaxies being lost is slightly different between the two X-ray samples. Therefore, although the results in Fig. 3.11 are consistent with strangulation – and more specifically, somewhat stronger strangulation at the low-mass end of the XRS sample – we suggest that this trend be interpreted with caution as completeness differences could be playing some role.

3.4.3 Group evolutionary/dynamical state

The dynamical state of galaxy groups is an important evolutionary indicator and can potentially influence galaxy properties. Trends with X-ray luminosity may reflect that the XRW and XRS samples have different dynamical properties as it is expected that more evolved groups with relaxed dynamics would be more X-ray luminous (Popesso et al., 2007a).

Theoretically the velocity distribution of galaxies within a group in dynamical equilibrium should have a characteristic Gaussian shape. Groups lacking this Gaussian distribution can therefore be considered as being unevolved, dynamically young systems. To investigate the dependence on the dynamical state of the groups in our data set we follow the procedure of Hou et al. (2009) and apply the Anderson-Darling normality (ADN) test to the velocity distributions of the galaxies in the group sample. The ADN test is a non-parametric test which compares the cumulative distribution function (CDF) of the data to the CDF of a normal distribution to determine the probability (p-value) that the difference between the distribution of the data and that of a Gaussian is as large as observed (or larger), under the assumption that the data is in fact normally distributed. For our dynamical analysis we use a subset of the data consisting of only those groups with eight or more members (31 820 galaxies in 1 456 groups), in order to ensure reasonable statistics when applying the ADN test. To obtain values for the ADN statistic for each of our groups we employ the `ad.test {nortest}` function in the statistical computing language R (R Core Team, 2013) – large values of the ADN statistic are indicative of less Gaussian distributions.

Initially, we examine the dynamical states of galaxies within the XRW and XRS samples globally (ie. no radial cuts) and we find no systematic differences between the dynamical states of XRW and XRS galaxies. Popesso et al. (2007a) study the difference between X-ray underluminous Abell (AXU) clusters and normal Abell clusters. They find that while both AXU and normal Abell clusters show Gaussian velocity distributions within the virialized region ($R < 1.5\,\mathrm{R}_{200}$), within the exterior regions ($1.5 \leq R \leq 3.5\,\mathrm{r}_{200}$) the AXU cluster show sharply peaked, non-Gaussian velocity distributions. The authors interpret these leptokurtic velocity distributions in the outer cluster regions as evidence that AXU clusters have experienced recent accretion/merging. If the XRW groups have experienced more recent accretion of galaxies from the field and smaller groups than the XRS groups, then this could contribute to the dependence we observe between star-forming and disc fractions on X-ray luminosity. Galaxies in underdense regions (the field, low-mass groups) have been found to be preferentially star- forming with late-type morphologies. Accordingly, groups experiencing recent accretion may contain more star-forming, late-type, galaxies when compared to groups which are dynamically older.

To investigate this possibility we study the dynamical states of groups in both the XRW and XRS samples, and divide member galaxies into two radial subsamples: those found in the inner regions ($R < R_{180}$) of their host group, and those found in the outer regions ($R \geq R_{180}$) of their host group. This is similar to the analysis performed by Popesso et al. (2007a). Instead of making an arbitrary, discrete cut to define Gaussian and non-Gaussian groups we treat the AD statistic values as continuous and compare the distributions of ADN statistics from the four subsamples (XRW inner, XRW outer, XRS

inner, XRS outer) to determine whether there are any significant differences in dynamical state. To quantitatively compare the distributions we utilize the two-sample Anderson-Darling (AD2) test. The AD2 test is similar to the ADN test, however instead of comparing observed data to the normal distribution, it compares the CDFs of two data samples to determine whether they are drawn from the same underlying distribution. We apply the AD2 test to the distributions of ADN statistic values for the XRW and XRS samples to determine if the dynamical states vary between the inner and the outer regions. To perform the AD2 test between the subsamples we use the `ad.test {kSamples}` function in the statistical computing language R (R Core Team, 2013).

We find no evidence ($\mathrm{p-value} = 0.38$) for different dynamical states in the inner and outer regions of the XRS sample, however for the XRW sample we find strong evidence ($\mathrm{p-value} = 3 \times 10^{-7}$) that the dynamical state of galaxies in the outer region is different from those in the inner region. When we examine the distributions of ADN statistics for the four subsamples we find that the ADN statistic values for the XRW outer subsample are systematically higher than for the other three subsamples. This suggests that the velocity distributions for galaxies outside of the virial radius in the XRW sample are less Gaussian than the rest of the data set.

This result is consistent with Popesso et al. (2007a), who find non-Gaussian velocity distributions for galaxies in the outer regions of X-ray underluminous Abell clusters. This result supports the notion that the increased number of star-forming and late-type galaxies we observe in the XRW sample can potentially be explained by underluminous X-ray groups experiencing recent accre-

tion of field galaxies and small galaxy groups, as this recent accretion can give rise to less Gaussian velocity distributions in the exteriors of these groups.

We do note that it remains difficult to simultaneously explain the dynamical results together with the fact that we observe no dependence of SF and disc excess on radius (Fig. 3.7).

3.5 Summary & Conclusions

We have used a sample of galaxies taken from X-ray emitting groups and clusters in the SDSS to study the effect of X-ray luminosity on galaxy star formation and morphological properties. Using a data set spanning a large range in stellar mass ($10^{9} - 10^{11.3}\,\mathrm{M}_{\odot}$), halo mass ($10^{13} - 10^{15}\,\mathrm{M}_{\odot}$), and X-ray luminosity ($10^{39.6} - 10^{46.4}\mathrm{erg\,s^{-1}}$) we have investigated the differences between disc and star-forming fractions within different X-ray environments. The main results of this paper are as follows.

(i) Star-forming and disc fractions are preferentially lower within the X-ray strong sample when compared to galaxies within the X-ray weak sample – this trend remains after controlling for any halo mass dependence.

(ii) This difference between the X-ray strong and X-ray weak samples is most apparent at intermediate to high halo mass and at low stellar mass.

(iii) The differences we observe between the X-ray weak and X-ray strong samples do not depend on whether we consider galaxies inside of, or outside their host halo's X-ray radius.

(iv) The enhancement of star-forming and disc fractions we observe in the X-ray weak sample is present for satellites but not central galaxies, which is not surprising given that the difference between X-ray samples is only seen at low stellar mass.

(v) Our results are consistent with quenching by strangulation, in particular we see a somewhat stronger strangulation signal at low stellar mass within the XRS sample.

Bibliography

Abazajian, K. N., Adelman-McCarthy, J. K., Agüeros, M. A., Allam, S. S., Allende Prieto, C., An, D., Anderson, K. S. J., Anderson, S. F., Annis, J., Bahcall, N. A., & et al. 2009, ApJS, 182, 543

Andreon, S. & Ettori, S. 1999, ApJ, 516, 647

Andreon, S., Lobo, C., & Iovino, A. 2004, MNRAS, 349, 889

Andreon, S., Quintana, H., Tajer, M., Galaz, G., & Surdej, J. 2006, MNRAS, 365, 915

Baldwin, J. A., Phillips, M. M., & Terlevich, R. 1981, PASP, 93, 5

Balogh, M., Bower, R. G., Smail, I., Ziegler, B. L., Davies, R. L., Gaztelu, A., & Fritz, A. 2002a, MNRAS, 337, 256

Balogh, M. L., Baldry, I. K., Nichol, R., Miller, C., Bower, R., & Glazebrook, K. 2004, ApJ, 615, L101

Balogh, M. L., Navarro, J. F., & Morris, S. L. 2000, ApJ, 540, 113

Balogh, M. L., Smail, I., Bower, R. G., Ziegler, B. L., Smith, G. P., Davies, R. L., Gaztelu, A., Kneib, J.-P., & Ebeling, H. 2002b, ApJ, 566, 123

Barnes, J. 1985, MNRAS, 215, 517

Blanton, M. R., Eisenstein, D., Hogg, D. W., Schlegel, D. J., & Brinkmann, J. 2005a, ApJ, 629, 143

Blanton, M. R. & Roweis, S. 2007, AJ, 133, 734

Blanton, M. R., Schlegel, D. J., Strauss, M. A., Brinkmann, J., Finkbeiner, D., Fukugita, M., Gunn, J. E., Hogg, D. W., Ivezić, Ž., Knapp, G. R., Lupton, R. H., Munn, J. A., Schneider, D. P., Tegmark, M., & Zehavi, I. 2005b, AJ, 129, 2562

Brinchmann, J., Charlot, S., White, S. D. M., Tremonti, C., Kauffmann, G., Heckman, T., & Brinkmann, J. 2004, MNRAS, 351, 1151

Brough, S., Forbes, D. A., Kilborn, V. A., & Couch, W. 2006, MNRAS, 370, 1223

Butcher, H. & Oemler, Jr., A. 1978, ApJ, 219, 18

—. 1984, ApJ, 285, 426

Cameron, E. 2011, PASA, 28, 128

Christlein, D. & Zabludoff, A. I. 2004, ApJ, 616, 192

Chung, A., van Gorkom, J. H., Kenney, J. D. P., & Vollmer, B. 2007, ApJ, 659, L115

De Lucia, G., Weinmann, S., Poggianti, B. M., Aragón-Salamanca, A., & Zaritsky, D. 2012, MNRAS, 423, 1277

Dressler, A. 1980, ApJ, 236, 351

Dressler, A., Smail, I., Poggianti, B. M., Butcher, H., Couch, W. J., Ellis, R. S., & Oemler, Jr., A. 1999, ApJS, 122, 51

Ellingson, E., Lin, H., Yee, H. K. C., & Carlberg, R. G. 2001, ApJ, 547, 609

Fairley, B. W., Jones, L. R., Wake, D. A., Collins, C. A., Burke, D. J., Nichol, R. C., & Romer, A. K. 2002, MNRAS, 330, 755

Gallazzi, A., Charlot, S., Brinchmann, J., White, S. D. M., & Tremonti, C. A. 2005, MNRAS, 362, 41

Gavazzi, G., Cortese, L., Boselli, A., Iglesias-Paramo, J., Vílchez, J. M., & Carrasco, L. 2003, ApJ, 597, 210

Gunn, J. E. & Gott, III, J. R. 1972, ApJ, 176, 1

Hou, A., Parker, L. C., Balogh, M. L., McGee, S. L., Wilman, D. J., Connelly, J. L., Harris, W. E., Mok, A., Mulchaey, J. S., Bower, R. G., & Finoguenov, A. 2013, MNRAS, 435, 1715

Hou, A., Parker, L. C., & Harris, W. E. 2014, MNRAS, 442, 406

Hou, A., Parker, L. C., Harris, W. E., & Wilman, D. J. 2009, ApJ, 702, 1199

Hoyle, B., Masters, K. L., Nichol, R. C., Jimenez, R., & Bamford, S. P. 2012, MNRAS, 423, 3478

Huchra, J. P. & Geller, M. J. 1982, ApJ, 257, 423

Kauffmann, G., Heckman, T. M., Tremonti, C., Brinchmann, J., Charlot, S., White, S. D. M., Ridgway, S. E., Brinkmann, J., Fukugita, M., Hall, P. B., Ivezić, Ž., Richards, G. T., & Schneider, D. P. 2003, MNRAS, 346, 1055

Kawata, D. & Mulchaey, J. S. 2008, ApJ, 672, L103

Kenney, J. D. P., van Gorkom, J. H., & Vollmer, B. 2004, AJ, 127, 3361

Lackner, C. N. & Gunn, J. E. 2013, MNRAS, 428, 2141

Larson, R. B., Tinsley, B. M., & Caldwell, C. N. 1980, ApJ, 237, 692

Loh, Y.-S., Ellingson, E., Yee, H. K. C., Gilbank, D. G., Gladders, M. D., & Barrientos, L. F. 2008, ApJ, 680, 214

Lopes, P. A. A., Ribeiro, A. L. B., & Rembold, S. B. 2014, MNRAS, 437, 2430

Mantz, A., Allen, S. W., Ebeling, H., Rapetti, D., & Drlica-Wagner, A. 2010, MNRAS, 406, 1773

McGee, S. L., Balogh, M. L., Bower, R. G., Font, A. S., & McCarthy, I. G. 2009, MNRAS, 400, 937

Moore, B., Katz, N., Lake, G., Dressler, A., & Oemler, A. 1996, Nature, 379, 613

Muzzin, A., van der Burg, R. F. J., McGee, S. L., Balogh, M., Franx, M., Hoekstra, H., Hudson, M. J., Noble, A., Taranu, D. S., Webb, T., Wilson, G., & Yee, H. K. C. 2014, ApJ, 796, 65

Muzzin, A., Wilson, G., Yee, H. K. C., Gilbank, D., Hoekstra, H., Demarco, R., Balogh, M., van Dokkum, P., Franx, M., Ellingson, E., Hicks, A., Nantais, J., Noble, A., Lacy, M., Lidman, C., Rettura, A., Surace, J., & Webb, T. 2012, ApJ, 746, 188

Navarro, J. F., Frenk, C. S., & White, S. D. M. 1997, ApJ, 490, 493

Peng, Y., Maiolino, R., & Cochrane, R. 2015, Nature, 521, 192

Peng, Y.-j., Lilly, S. J., Kovač, K., Bolzonella, M., Pozzetti, L., Renzini, A., Zamorani, G., Ilbert, O., Knobel, C., Iovino, A., Maier, C., Cucciati, O., Tasca, L., Carollo, C. M., Silverman, J., Kampczyk, P., de Ravel, L., Sanders, D., Scoville, N., Contini, T., Mainieri, V., Scodeggio, M., Kneib, J.-P., Le Fèvre, O., Bardelli, S., Bongiorno, A., Caputi, K., Coppa, G., de la Torre, S., Franzetti, P., Garilli, B., Lamareille, F., Le Borgne, J.-F., Le Brun, V., Mignoli, M., Perez Montero, E., Pello, R., Ricciardelli, E., Tanaka, M., Tresse, L., Vergani, D., Welikala, N., Zucca, E., Oesch, P., Abbas, U., Barnes, L., Bordoloi, R., Bottini, D., Cappi, A., Cassata, P., Cimatti, A., Fumana, M., Hasinger, G., Koekemoer, A., Leauthaud, A., Maccagni, D., Marinoni, C., McCracken, H., Memeo, P., Meneux, B., Nair, P., Porciani, C., Presotto, V., & Scaramella, R. 2010, ApJ, 721, 193

Popesso, P., Biviano, A., Böhringer, H., & Romaniello, M. 2007a, A&A, 461, 397

Popesso, P., Biviano, A., Romaniello, M., & Böhringer, H. 2007b, A&A, 461, 411

Postman, M., Franx, M., Cross, N. J. G., Holden, B., Ford, H. C., Illingworth, G. D., Goto, T., Demarco, R., Rosati, P., Blakeslee, J. P., Tran, K.-V., Benítez, N., Clampin, M., Hartig, G. F., Homeier, N., Ardila, D. R., Bartko, F., Bouwens, R. J., Bradley, L. D., Broadhurst, T. J., Brown, R. A., Burrows, C. J., Cheng, E. S., Feldman, P. D., Golimowski, D. A., Gronwall, C., Infante, L., Kimble, R. A., Krist, J. E., Lesser, M. P., Martel, A. R., Mei, S., Menanteau, F., Meurer, G. R., Miley, G. K., Motta, V., Sirianni,

M., Sparks, W. B., Tran, H. D., Tsvetanov, Z. I., White, R. L., & Zheng, W. 2005, ApJ, 623, 721

Postman, M. & Geller, M. J. 1984, ApJ, 281, 95

R Core Team. 2013, R: A Language and Environment for Statistical Computing, R Foundation for Statistical Computing, Vienna, Austria

Shen, S., Kauffmann, G., von der Linden, A., White, S. D. M., & Best, P. N. 2008, MNRAS, 389, 1074

Simard, L., Mendel, J. T., Patton, D. R., Ellison, S. L., & McConnachie, A. W. 2011, ApJS, 196, 11

Trouille, L. & Barger, A. J. 2010, ApJ, 722, 212

Urquhart, S. A., Willis, J. P., Hoekstra, H., & Pierre, M. 2010, MNRAS, 406, 368

van den Bosch, F. C., Aquino, D., Yang, X., Mo, H. J., Pasquali, A., McIntosh, D. H., Weinmann, S. M., & Kang, X. 2008, MNRAS, 387, 79

Wake, D. A., Collins, C. A., Nichol, R. C., Jones, L. R., & Burke, D. J. 2005, ApJ, 627, 186

Wang, L., Yang, X., Shen, S., Mo, H. J., van den Bosch, F. C., Luo, W., Wang, Y., Lau, E. T., Wang, Q. D., Kang, X., & Li, R. 2014, MNRAS, 439, 611

Wetzel, A. R., Tinker, J. L., & Conroy, C. 2012, MNRAS, 424, 232

Whitaker, K. E., van Dokkum, P. G., Brammer, G., & Franx, M. 2012, ApJ, 754, L29

Yang, X., Mo, H. J., van den Bosch, F. C., & Jing, Y. P. 2005, MNRAS, 356, 1293

Yang, X., Mo, H. J., van den Bosch, F. C., Pasquali, A., Li, C., & Barden, M. 2007, ApJ, 671, 153

Chapter 4

Summary & Conclusions

The field of galaxy evolution is a broad one with many areas of research focus, however one of the most fundamental questions involves determining which mechanisms are driving the tranformations of blue, active, late-type galaxies to red, passive, early-type galaxies, and additionally what the relative balance is between different mechanisms across varying environments. Dense environments such as galaxy groups or clusters seem to efficiently drive these galaxy transformations, for low-mass galaxies especially, whereas high-mass galaxies appear to evolve more agnostically with respect to their environment (Peng et al., 2010).

In this thesis we have probed the dependence of galaxy properties on their environment to further elucidate the regimes in which galaxy evolution occurs. By taking advantage of a large sample of SDSS galaxies in groups (Yang et al., 2005, 2007) we have investigated trends in galaxy mass as well as star-forming and disc fractions across a wide range of halo environments, considering not only haloes of different masses, but also those which show relatively strong and weak X-ray emission (Wang et al., 2014).

In Chapter 2 we investigate the presence of mass segregation, or lackthereof, in galaxy groups and clusters. It is important to understand the role of mass segregation in dense environments in order to correctly interpret star formation and morphology trends with radius in groups and clusters. Specifically, radial trends in star formation and morphology (Goto et al., 2003; Postman et al., 2005; Rasmussen et al., 2012; Wetzel et al., 2012; Fasano et al., 2015; Haines et al., 2015) could be driven, at least in part, by mass segregation effects. For example, high-mass galaxies are preferentially passive and early-type and therefore mass segregation would drive an excess of passive early-type galaxies at small radii irrespective of environmental effects.

We explore the mean galaxy mass as a function of radius for galaxies in groups and clusters across a wide range in halo mass, reaching two main conclusions regarding the nature of the mass segregation of galaxies. First, we find that the strength of mass segregation depends on host halo mass. Significant mass segregation is measured for lower mass groups but not for large clusters, the strength of mass segregation decreases toward higher halo masses in a clear marching order. Second, we find that the strength of mass segregation generally increases with the inclusion of lower mass galaxies, therefore surveys which are only complete to relatively high stellar masses may miss intrinsic mass segregation trends. These two conclusions can be used to explain why recent observations (van den Bosch et al., 2008; von der Linden et al., 2010; Presotto et al., 2012; Vulcani et al., 2013; Ziparo et al., 2013; Balogh et al., 2014) have come to seemingly contradictory conclusions regarding the presence of mass segregation in dense structures.

In addition to previous studies, more recent studies published after Roberts et al. (2015) have investigated mass segregation in groups and clusters using simulations. Contini & Kang (2015) use semi-analytic models to explore mass segregation of galaxies in groups and clusters, finding that within the virial radius the strength of mass segregation decreases with increasing halo mass, consistent with the results of this thesis. However, Contini & Kang also see an upturn (i.e. a positive correlation) in the stellar mass - radius relationship beyond the virial radius which is not seen observationally in this work. van den Bosch et al. (2016) use N-body simulations from the Bolshoi and Chinchilla simulations to study the segregation of many different subhalo properties. Relevant to this work, they study the segregation of both subhalo mass at accretion as well as present day subhalo mass, finding that subhalo mass at accretion shows an anti-correlation with radius whereas radial trends in present day mass are more complex. Present day stellar mass has been shown to trace mass at accretion (e.g. Conroy et al., 2006) therefore trends with mass at accretion should correspond more closely to observations. van den Bosch et al. find that trends with present day mass are very sensitive to selection effects and can show a positive or a negative correlation with radius depending on which subhalos are included. In this work we also find that selection effects can influence observed mass segregation, with stronger mass segregation generally being observed when lower mass galaxies are included. Most recently, Joshi et al. (2016) have performed N-body simulations using the ChaNGa code to study the mass segregation of galaxy analogues across different host halo and galaxy analogue masses. Joshi et al. detect mass segregation of galaxy analogues, at least within $0.5\,\mathrm{R_{vir}}$, and find stronger mass segregation trends

when including lower mass analogues and for galaxy analogues in lower mass haloes, in agreement with the two main conclusions of this work. We note that Joshi et al. do see a mild positive correlation between average mass and radius beyond R_{vir} which is not observed in this work.

Interpreting mass segregation trends requires understanding the complicated balance between accretion history, dynamical friction, and tidal mass loss in group haloes. While observationally it is difficult to disentangle these various effects, simulations provide an important tool to break these potential degeneracies. As well, the fact that we do not see strong segregation when considering massive galaxies suggests that dynamical friction may not be the dominant effect.

In Chapter 3 we explore beyond the well established dependences of observed galaxy properties on stellar and halo mass to determine if star-forming and disc fractions of group galaxies display any residual trends with the X-ray luminosity of their host halo. Since the X-ray luminosity of a halo is driven by the hot IGM/ICM, this provides a method to probe connections between galaxy transformations and the halo content.

To accomplish this we split the group sample into groups which, for a given halo mass, show enhanced or suppressed X-ray emission – referred to as X-ray strong (XRS) and X-ray weak (XRW). We show that for a given stellar and halo mass, low-mass galaxies in XRW groups show enhanced star-forming and disc fractions. By applying the Anderson-Darling (AD) test to the LOS velocity profiles of member galaxies, we then explore the dynamical states of the inner and outer regions of X-ray strong and X-ray weak groups. Fig. 4.1

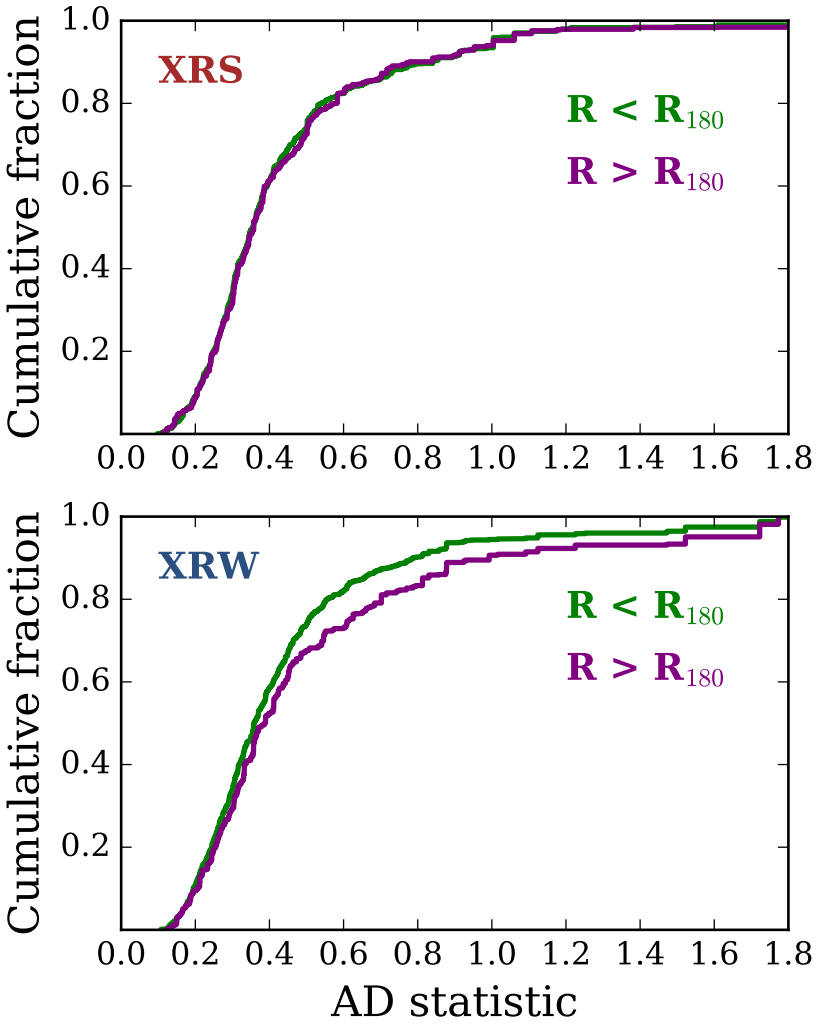

Figure 4.1: Cumulative distribution functions of Anderson-Darling statistics for velocity profiles of XRS and XRW galaxies, both in the inner and outer regions of the halo.

shows the distribution of AD statistics for both the XRS and XRW samples, separately for galaxies in the inner and outer regions of the halo. We see that velocity profiles of galaxies in the outer regions of XRW groups show stronger deviations from normality (high AD statistics), perhaps signifying recently formed, dynamically young systems which could drive the observed excess of star-forming, late-type galaxies. Using the novel technique presented by Peng et al. (2015), we also find evidence for starvation as a quenching mechanism for both XRW and XRS groups. When comparing the strength of the starvation signal between XRW and XRS groups we find that starvation is potentially more efficient in XRS groups, however this result is marginal and requires further work to determine its robustness. Other methods which could constrain the timescales/efficiency of starvation could involve determining estimates for quenching times either using observations at different redshifts, or through fitting observational trends with simple quenching models.

Comparing to previous results, the dependence on X-ray luminosity we observe for low-mass galaxies is consistent with the established notion that low-mass galaxies are quenched primarily environmentally whereas high-mass galaxies are quenched more through secular processes (Peng et al., 2010). In particular, the mass at which we no longer see a dependence on X-ray luminosity is $\gtrsim 10^{10}\,\mathrm{M}_{\odot}$ which is in broad agreement with the expected transition mass between environmental and mass quenching. The quenching mechanism favoured in this work is quenching by starvation. Starvation is a mechanism which has also been invoked by many previous studies in order to account for observational trends (Balogh et al., 2000; Balogh & Morris, 2000; Wetzel et al., 2013; Wheeler et al., 2014; Peng et al., 2015). In this work we see

a marginally stronger starvation signal for low-mass galaxies in XRS groups compared to XRW groups. Should this prove robust, it indicates a connection between the efficiency of starvation and the X-ray luminosity of a host halo. This may be expected, given that a dense/hot IGM/ICM (i.e. a high X-ray luminosity) should be able to more efficiently strip hot halo gas and prevent cold gas accretion, thereby quenching via starvation. It is also possible that our results are being driven by the fact that our XRW groups could represent younger, more unevolved systems. If this is the case then the enhanced star-forming and disc fractions in XRW groups could be simply a result of galaxies in these systems being exposed to dense environments for less time. This is consistent with the fact that we find the velocity profiles of galaxies in XRW groups to show stronger deviations from normality than XRS systems. Future work examining the X-ray morphologies of these groups could help further constrain the connection between X-ray luminosity and dynamical state, as unrelaxed groups should show X-ray profiles which are more irregular in nature. Detailed studies of the X-ray morphologies of the groups in this work are somewhat limited by the low resolution of ROSAT maps, however more detailed follow-ups with the higher resolution Chandra X-ray Observatory could make a significant addition.

Our results find similar trends when considering either star-forming or disc fraction, begging the question whether or not the same mechanism drives both changes in star formation and morphology. Recent work has tended to favour starvation and/or ram pressure stripping as the dominant environmental mechanisms for quenching star formation (Muzzin et al., 2014; Peng et al., 2015; Fillingham et al., 2015; Weisz et al., 2015; Wetzel et al., 2015). These mecha-

nisms could potentially drive morphological transformations through disc fading, however this is at odds with results suggesting that an enhancement to the bulge luminosity is required to reproduce observed morphological trends (Christlein & Zabludoff, 2004; Bundy et al., 2010). If morphological transformations are therefore driven by building up a strong bulge then galaxy interactions such as harassment or mergers are more likely candidates. If star formation quenching and morphological transformations are being driven by different mechanisms, then it is important to understand the balance which gives rise to the tight correlations between star formation and morphology which are seen observationally (e.g. Schawinski et al., 2014). Simulations have shown that gas-poor discs can be more easily disrupted by galaxy interactions (Hopkins et al., 2009), therefore it is possible that star formation is initially quenched by exhausting the gas in the disc and subsequently a strong bulge is built up through minor mergers and harassment (Bundy et al., 2010). The above scenario implies a distinct order in which star formation is quenched first followed by a morphological transformation, or put another way, the characteristic time over which a galaxy is star-forming is shorter than the timescale which a galaxy is late-type. This is consistent with previous studies which have found that the timescales for morphological transformation are somewhat longer than quenching timescales (Sánchez-Blázquez et al., 2009; Skibba et al., 2009; Kovač et al., 2010).

One example of potential future work using this sample of X-ray groups would be to closely study AGN influence on the IGM. For example, by identifying AGN signatures in galaxies it would be then possible to investigate AGN influence on diffuse gas across a wide range in halo mass. Are groups

simply scaled down clusters in this respect, or is diffuse gas in groups more strongly affected by AGN from member galaxies? It would also be possible to study AGN influence by searching for groups from this sample with evidence for X-ray cavities to further study both how common X-ray cavities are in group-mass haloes, as well as determine if galaxy properties correlate with the presence of X-ray cavities.

In addition to X-ray luminosity, another of these secondary environmental effects which has been studied somewhat in previous literature is the dependence of galaxy properties on group dynamical state. In Chapter 3 we do see dynamical differences between the XRS and XRW samples which further motivates understanding how dynamical differences can influence galaxy properties. In ongoing work we are interested in determining at which point during a galaxy's infall history (if at all) dependences on host dynamical state set in place. This again will require controlling carefully for stronger effects (e.g. stellar mass, halo mass, redshift) in order to make a fair comparison between galaxies in groups with dynamical differences.

While the two scientific sections of this thesis are relatively distinct studies, they both contribute to furthering the understanding of how galaxies evolve and determining in which environments this evolution is strongest. That being said, there is still much about galaxy evolution which is not understood and future observational surveys providing better statistics, probing lower galaxy masses, and probing higher redshifts will continue to push the field forward. Surveys such as GOGREEN will vastly increase the number of spectroscopic members of groups and clusters at $1 \leq z \leq 1.5$, thereby allowing the environ-

mental quenching of satellites as well as the influence of group/cluster dynamical state to be probed at high-redshift. As well, wide field imaging surveys ($\sim$ thousands of square degrees) such as the Dark Energy Survey (Flaugher, 2005), Pan-STARRS (Kaiser et al., 2002), and the Large Synoptic Survey Telescope (Ivezic et al., 2008) will provide enormous data sets with photometric redshifts from which interesting subsets can be chosen for detailed spectroscopic follow up.

Bibliography

Balogh, M. L., McGee, S. L., Mok, A., Wilman, D. J., Finoguenov, A., Bower, R. G., Mulchaey, J. S., Parker, L. C., & Tanaka, M. 2014, MNRAS, 443, 2679

Balogh, M. L. & Morris, S. L. 2000, MNRAS, 318, 703

Balogh, M. L., Navarro, J. F., & Morris, S. L. 2000, ApJ, 540, 113

Bundy, K., Scarlata, C., Carollo, C. M., Ellis, R. S., Drory, N., Hopkins, P., Salvato, M., Leauthaud, A., Koekemoer, A. M., Murray, N., Ilbert, O., Oesch, P., Ma, C.-P., Capak, P., Pozzetti, L., & Scoville, N. 2010, ApJ, 719, 1969

Christlein, D. & Zabludoff, A. I. 2004, ApJ, 616, 192

Conroy, C., Wechsler, R. H., & Kravtsov, A. V. 2006, ApJ, 647, 201

Contini, E. & Kang, X. 2015, MNRAS, 453, L53

Fasano, G., Poggianti, B. M., Bettoni, D., D'Onofrio, M., Dressler, A., Vulcani, B., Moretti, A., Gullieuszik, M., Fritz, J., Omizzolo, A., Cava, A., Couch, W. J., Ramella, M., & Biviano, A. 2015, MNRAS, 449, 3927

Fillingham, S. P., Cooper, M. C., Wheeler, C., Garrison-Kimmel, S., Boylan-Kolchin, M., & Bullock, J. S. 2015, MNRAS, 454, 2039

Flaugher, B. 2005, International Journal of Modern Physics A, 20, 3121

Goto, T., Yamauchi, C., Fujita, Y., Okamura, S., Sekiguchi, M., Smail, I., Bernardi, M., & Gomez, P. L. 2003, MNRAS, 346, 601

Haines, C. P., Pereira, M. J., Smith, G. P., Egami, E., Babul, A., Finoguenov, A., Ziparo, F., McGee, S. L., Rawle, T. D., Okabe, N., & Moran, S. M. 2015, ApJ, 806, 101

Hopkins, P. F., Cox, T. J., Younger, J. D., & Hernquist, L. 2009, ApJ, 691, 1168

Ivezic, Z., Tyson, J. A., Abel, B., Acosta, E., Allsman, R., AlSayyad, Y., Anderson, S. F., Andrew, J., Angel, R., Angeli, G., Ansari, R., Antilogus, P., Arndt, K. T., Astier, P., Aubourg, E., Axelrod, T., Bard, D. J., Barr, J. D., Barrau, A., Bartlett, J. G., Bauman, B. J., Beaumont, S., Becker, A. C., Becla, J., Beldica, C., Bellavia, S., Blanc, G., Blandford, R. D., Bloom, J. S., Bogart, J., Borne, K., Bosch, J. F., Boutigny, D., Brandt, W. N., Brown, M. E., Bullock, J. S., Burchat, P., Burke, D. L., Cagnoli, G., Calabrese, D., Chandrasekharan, S., Chesley, S., Cheu, E. C., Chiang, J., Claver, C. F., Connolly, A. J., Cook, K. H., Cooray, A., Covey, K. R., Cribbs, C., Cui, W., Cutri, R., Daubard, G., Daues, G., Delgado, F., Digel, S., Doherty, P., Dubois, R., Dubois-Felsmann, G. P., Durech, J., Eracleous, M., Ferguson, H., Frank, J., Freemon, M., Gangler, E., Gawiser, E., Geary, J. C., Gee, P., Geha, M., Gibson, R. R., Gilmore, D. K., Glanzman, T., Goodenow, I., Gressler, W. J., Gris, P., Guyonnet, A., Hascall, P. A., Haupt, J., Hernandez, F., Hogan, C., Huang, D., Huffer, M. E., Innes, W. R., Jacoby, S. H., Jain, B., Jee, J., Jernigan, J. G., Jevremovic, D., Johns, K., Jones, R. L., Juramy-Gilles, C., Juric, M., Kahn, S. M., Kalirai, J. S., Kallivayalil, N., Kalmbach,

B., Kantor, J. P., Kasliwal, M. M., Kessler, R., Kirkby, D., Knox, L., Kotov, I., Krabbendam, V. L., Krughoff, S., Kubanek, P., Kuczewski, J., Kulkarni, S., Lambert, R., Le Guillou, L., Levine, D., Liang, M., Lim, K., Lintott, C., Lupton, R. H., Mahabal, A., Marshall, P., Marshall, S., May, M., McKercher, R., Migliore, M., Miller, M., Mills, D. J., Monet, D. G., Moniez, M., Neill, D. R., Nief, J., Nomerotski, A., Nordby, M., O'Connor, P., Oliver, J., Olivier, S. S., Olsen, K., Ortiz, S., Owen, R. E., Pain, R., Peterson, J. R., Petry, C. E., Pierfederici, F., Pietrowicz, S., Pike, R., Pinto, P. A., Plante, R., Plate, S., Price, P. A., Prouza, M., Radeka, V., Rajagopal, J., Rasmussen, A., Regnault, N., Ridgway, S. T., Ritz, S., Rosing, W., Roucelle, C., Rumore, M. R., Russo, S., Saha, A., Sassolas, B., Schalk, T. L., Schindler, R. H., Schneider, D. P., Schumacher, G., Sebag, J., Sembroski, G. H., Seppala, L. G., Shipsey, I., Silvestri, N., Smith, J. A., Smith, R. C., Strauss, M. A., Stubbs, C. W., Sweeney, D., Szalay, A., Takacs, P., Thaler, J. J., Van Berg, R., Vanden Berk, D., Vetter, K., Virieux, F., Xin, B., Walkowicz, L., Walter, C. W., Wang, D. L., Warner, M., Willman, B., Wittman, D., Wolff, S. C., Wood-Vasey, W. M., Yoachim, P., Zhan, H., & for the LSST Collaboration. 2008, ArXiv e-prints

Joshi, G. D., Parker, L. C., & Wadsley, J. 2016, MNRAS, accepted

Kaiser, N., Aussel, H., Burke, B. E., Boesgaard, H., Chambers, K., Chun, M. R., Heasley, J. N., Hodapp, K.-W., Hunt, B., Jedicke, R., Jewitt, D., Kudritzki, R., Luppino, G. A., Maberry, M., Magnier, E., Monet, D. G., Onaka, P. M., Pickles, A. J., Rhoads, P. H. H., Simon, T., Szalay, A., Szapudi, I., Tholen, D. J., Tonry, J. L., Waterson, M., & Wick, J. 2002, in

Proc. SPIE, Vol. 4836, Survey and Other Telescope Technologies and Discoveries, ed. J. A. Tyson & S. Wolff, 154–164

Kovač, K., Lilly, S. J., Knobel, C., Bolzonella, M., Iovino, A., Carollo, C. M., Scarlata, C., Sargent, M., Cucciati, O., Zamorani, G., Pozzetti, L., Tasca, L. A. M., Scodeggio, M., Kampczyk, P., Peng, Y., Oesch, P., Zucca, E., Finoguenov, A., Contini, T., Kneib, J.-P., Le Fèvre, O., Mainieri, V., Renzini, A., Bardelli, S., Bongiorno, A., Caputi, K., Coppa, G., de la Torre, S., de Ravel, L., Franzetti, P., Garilli, B., Lamareille, F., Le Borgne, J.-F., Le Brun, V., Maier, C., Mignoli, M., Pello, R., Perez Montero, E., Ricciardelli, E., Silverman, J. D., Tanaka, M., Tresse, L., Vergani, D., Abbas, U., Bottini, D., Cappi, A., Cassata, P., Cimatti, A., Fumana, M., Guzzo, L., Koekemoer, A. M., Leauthaud, A., Maccagni, D., Marinoni, C., McCracken, H. J., Memeo, P., Meneux, B., Porciani, C., Scaramella, R., & Scoville, N. Z. 2010, ApJ, 718, 86

Muzzin, A., van der Burg, R. F. J., McGee, S. L., Balogh, M., Franx, M., Hoekstra, H., Hudson, M. J., Noble, A., Taranu, D. S., Webb, T., Wilson, G., & Yee, H. K. C. 2014, ApJ, 796, 65

Peng, Y., Maiolino, R., & Cochrane, R. 2015, Nature, 521, 192

Peng, Y.-j., Lilly, S. J., Kovač, K., Bolzonella, M., Pozzetti, L., Renzini, A., Zamorani, G., Ilbert, O., Knobel, C., Iovino, A., Maier, C., Cucciati, O., Tasca, L., Carollo, C. M., Silverman, J., Kampczyk, P., de Ravel, L., Sanders, D., Scoville, N., Contini, T., Mainieri, V., Scodeggio, M., Kneib, J.-P., Le Fèvre, O., Bardelli, S., Bongiorno, A., Caputi, K., Coppa, G., de

la Torre, S., Franzetti, P., Garilli, B., Lamareille, F., Le Borgne, J.-F., Le Brun, V., Mignoli, M., Perez Montero, E., Pello, R., Ricciardelli, E., Tanaka, M., Tresse, L., Vergani, D., Welikala, N., Zucca, E., Oesch, P., Abbas, U., Barnes, L., Bordoloi, R., Bottini, D., Cappi, A., Cassata, P., Cimatti, A., Fumana, M., Hasinger, G., Koekemoer, A., Leauthaud, A., Maccagni, D., Marinoni, C., McCracken, H., Memeo, P., Meneux, B., Nair, P., Porciani, C., Presotto, V., & Scaramella, R. 2010, ApJ, 721, 193

Postman, M., Franx, M., Cross, N. J. G., Holden, B., Ford, H. C., Illingworth, G. D., Goto, T., Demarco, R., Rosati, P., Blakeslee, J. P., Tran, K.-V., Benítez, N., Clampin, M., Hartig, G. F., Homeier, N., Ardila, D. R., Bartko, F., Bouwens, R. J., Bradley, L. D., Broadhurst, T. J., Brown, R. A., Burrows, C. J., Cheng, E. S., Feldman, P. D., Golimowski, D. A., Gronwall, C., Infante, L., Kimble, R. A., Krist, J. E., Lesser, M. P., Martel, A. R., Mei, S., Menanteau, F., Meurer, G. R., Miley, G. K., Motta, V., Sirianni, M., Sparks, W. B., Tran, H. D., Tsvetanov, Z. I., White, R. L., & Zheng, W. 2005, ApJ, 623, 721

Presotto, V., Iovino, A., Scodeggio, M., Cucciati, O., Knobel, C., Bolzonella, M., Oesch, P., Finoguenov, A., Tanaka, M., Kovač, K., Peng, Y., Zamorani, G., Bardelli, S., Pozzetti, L., Kampczyk, P., López-Sanjuan, C., Vergani, D., Zucca, E., Tasca, L. A. M., Carollo, C. M., Contini, T., Kneib, J.-P., Le Fèvre, O., Lilly, S., Mainieri, V., Renzini, A., Bongiorno, A., Caputi, K., de la Torre, S., de Ravel, L., Franzetti, P., Garilli, B., Lamareille, F., Le Borgne, J.-F., Le Brun, V., Maier, C., Mignoli, M., Pellò, R., Perez-Montero, E., Ricciardelli, E., Silverman, J. D., Tresse, L., Barnes, L., Bordoloi, R.,

Cappi, A., Cimatti, A., Coppa, G., Koekemoer, A. M., McCracken, H. J., Moresco, M., Nair, P., & Welikala, N. 2012, A&A, 539, A55

Rasmussen, J., Mulchaey, J. S., Bai, L., Ponman, T. J., Raychaudhury, S., & Dariush, A. 2012, ApJ, 757, 122

Roberts, I. D., Parker, L. C., Joshi, G. D., & Evans, F. A. 2015, MNRAS, 448, L1

Sánchez-Blázquez, P., Jablonka, P., Noll, S., Poggianti, B. M., Moustakas, J., Milvang-Jensen, B., Halliday, C., Aragón-Salamanca, A., Saglia, R. P., Desai, V., De Lucia, G., Clowe, D. I., Pelló, R., Rudnick, G., Simard, L., White, S. D. M., & Zaritsky, D. 2009, A&A, 499, 47

Schawinski, K., Urry, C. M., Simmons, B. D., Fortson, L., Kaviraj, S., Keel, W. C., Lintott, C. J., Masters, K. L., Nichol, R. C., Sarzi, M., Skibba, R., Treister, E., Willett, K. W., Wong, O. I., & Yi, S. K. 2014, MNRAS, 440, 889

Skibba, R. A., Bamford, S. P., Nichol, R. C., Lintott, C. J., Andreescu, D., Edmondson, E. M., Murray, P., Raddick, M. J., Schawinski, K., Slosar, A., Szalay, A. S., Thomas, D., & Vandenberg, J. 2009, MNRAS, 399, 966

van den Bosch, F. C., Jiang, F., Campbell, D., & Behroozi, P. 2016, MNRAS, 455, 158

van den Bosch, F. C., Pasquali, A., Yang, X., Mo, H. J., Weinmann, S., McIntosh, D. H., & Aquino, D. 2008, ArXiv e-prints

von der Linden, A., Wild, V., Kauffmann, G., White, S. D. M., & Weinmann, S. 2010, MNRAS, 404, 1231

Vulcani, B., Poggianti, B. M., Oemler, A., Dressler, A., Aragón-Salamanca, A., De Lucia, G., Moretti, A., Gladders, M., Abramson, L., & Halliday, C. 2013, A&A, 550, A58

Wang, L., Yang, X., Shen, S., Mo, H. J., van den Bosch, F. C., Luo, W., Wang, Y., Lau, E. T., Wang, Q. D., Kang, X., & Li, R. 2014, MNRAS, 439, 611

Weisz, D. R., Dolphin, A. E., Skillman, E. D., Holtzman, J., Gilbert, K. M., Dalcanton, J. J., & Williams, B. F. 2015, ApJ, 804, 136

Wetzel, A. R., Tinker, J. L., & Conroy, C. 2012, MNRAS, 424, 232

Wetzel, A. R., Tinker, J. L., Conroy, C., & van den Bosch, F. C. 2013, MNRAS, 432, 336

Wetzel, A. R., Tollerud, E. J., & Weisz, D. R. 2015, ApJ, 808, L27

Wheeler, C., Phillips, J. I., Cooper, M. C., Boylan-Kolchin, M., & Bullock, J. S. 2014, MNRAS, 442, 1396

Yang, X., Mo, H. J., van den Bosch, F. C., & Jing, Y. P. 2005, MNRAS, 356, 1293

Yang, X., Mo, H. J., van den Bosch, F. C., Pasquali, A., Li, C., & Barden, M. 2007, ApJ, 671, 153

Ziparo, F., Popesso, P., Biviano, A., Finoguenov, A., Wuyts, S., Wilman, D., Salvato, M., Tanaka, M., Ilbert, O., Nandra, K., Lutz, D., Elbaz, D., Dickinson, M., Altieri, B., Aussel, H., Berta, S., Cimatti, A., Fadda, D., Genzel, R., Le Flo'ch, E., Magnelli, B., Nordon, R., Poglitsch, A., Pozzi, F., Portal, M. S., Tacconi, L., Bauer, F. E., Brandt, W. N., Cappelluti, N., Cooper, M. C., & Mulchaey, J. S. 2013, MNRAS, 434, 3089

This page intentionally left blank.